

e. gy

S  
O  
L  
A  
R

DOE/AL/21557-T1  
(DE85005174)

**ROSA: A COMPUTER MODEL FOR OPTICAL POWER RATIO  
CALCULATIONS**

By  
Ronald M. Anderson  
Wayne T. Ford

July 15, 1984

Work Performed Under Contract AC04-83AL21557

Texas Tech University  
Lubbock, Texas

Technical Information Center  
Office of Scientific and Technical Information  
United States Department of Energy



## DISCLAIMER

This report was prepared as an account of work sponsored by an agency of the United States Government. Neither the United States Government nor any agency thereof, nor any of their employees, makes any warranty, express or implied, or assumes any legal liability or responsibility for the accuracy, completeness, or usefulness of any information, apparatus, product, or process disclosed, or represents that its use would not infringe privately owned rights. Reference herein to any specific commercial product, process, or service by trade name, trademark, manufacturer, or otherwise does not necessarily constitute or imply its endorsement, recommendation, or favoring by the United States Government or any agency thereof. The views and opinions of authors expressed herein do not necessarily state or reflect those of the United States Government or any agency thereof.

This report has been reproduced directly from the best available copy.

Available from the National Technical Information Service, U. S. Department of Commerce, Springfield, Virginia 22161.

Price: Printed Copy A07  
Microfiche A01

Codes are used for pricing all publications. The code is determined by the number of pages in the publication. Information pertaining to the pricing codes can be found in the current issues of the following publications, which are generally available in most libraries: *Energy Research Abstracts (ERA)*; *Government Reports Announcements and Index (GRA and I)*; *Scientific and Technical Abstract Reports (STAR)*; and publication NTIS-PR-360 available from NTIS at the above address.

THE CROSBYTON SOLAR POWER PROJECT

ROSA: A COMPUTER MODEL FOR OPTICAL POWER RATIO CALCULATIONS

Work Performed Under Contract No. DE-AC04-83AL21557

SUBMITTED TO THE

UNITED STATES DEPARTMENT OF ENERGY

BY

TEXAS TECH UNIVERSITY  
LUBBOCK, TEXAS 79409

Ronald M. Anderson and Wayne T. Ford, Principal Investigators

Department of Mathematics  
Texas Tech University  
July 15, 1984

## ABSTRACT

The Ratio of Solid Angles (ROSA) computer code was developed as part of the Crosbyton Solar Power Project (CSPP) for calculation of optical power concentrations due to reflection from a spherical segment mirror. It was developed primarily in support of Department of Energy Contracts DE-AC04-76ET20255 and DE-AC04-83AL21557. This report provides technical information about the ROSA code.

The CSPP is concerned with the development of a technology for producing electric power from steam generated by reflection of the sun's rays from a fixed-mirror solar bowl onto a tracking receiver. In this system, the receiver is cantilevered and pivots about the center of curvature of the mirror. The ROSA code gives optical power concentration ratio profiles at points along the receiver surface.

The ROSA code is written for a spherical segment mirror and the rim angle of the mirror is an input variable. Orientation of the axis of symmetry of the bowl is specified in terms of a vertical-east-north coordinate system. Location of the sun relative to this coordinate system is also an input variable. Shading and rim cutoff effects are automatically included in the computation.

The code permits any convex surface of revolution as a receiver. Normally a cylinder or a cone would be used. For optimum energy capture, the axis of the receiver should lie along the from the center of the sun through the center of the bowl. However, tracking errors can cause misalignment of the receiver axis with this line. The code handles such misalignment in terms of misalignment angle input parameters.

This report consists of two parts, a technical reference manual and a user's guide. The reference manual provides the background material and derivations necessary for the implementation of the code. Computer listings for ROSA are also included in the reference manual.

The user's guide contains an explanation of the input data for the program, special user supplied subroutine requirements, a discussion of the output data, sample output and graphs of sample concentration profiles. Sample BOILER subroutines are given for a right circular cone and a right circular cylinder boiler. A sample RIM subroutine is given for an alternate rim shape.

THE CROSBYTON SOLAR POWER PROJECT

ROSA: A COMPUTER MODEL FOR OPTICAL POWER RATIO CALCULATIONS

PART 1: Technical Description and Fortran Listing

TABLE OF CONTENTS

ABSTRACT. . . . . i

TITLE PAGE - PART I . . . . . iii

LIST OF FIGURES . . . . . v

LIST OF TABLES. . . . . vi

STAFF . . . . . vii

ROSA TECHNICAL DESCRIPTION - Introduction . . . . . 1

1. THE RATIO OF SOLID ANGLES FORMULATION. . . . . 4

2. OPTICAL POWER CONCENTRATION FOR SPHERICAL MIRRORS. . . . .14

3. THE SUN-RECEIVER-COLLECTOR GEOMETRY. . . . .40

4. SOLUTION OF STRUCTURE RELATIONS. . . . .50

5. ROSA PROGRAM STRUCTURE . . . . .59

6. OPTICAL CONCENTRATION PROFILES . . . . .63

7. ALTERNATE RIM SHAPES . . . . .73

REFERENCES. . . . .80

APPENDIX A: ROSA COMPUTER LISTING. . . . .81

## LIST OF FIGURES

### Figure

I-1	Element of Area $dA$ on Sun Illuminates Element of area $dA$ on the earth. . . . .	6
I-2	Section of Generalized Mirror Illuminates Field Point. . . . .	11
II-1	Mirror and Receiver Shape. . . . .	16
II-2	The Solid Angle Parameters $\beta$ and $\omega$ . . . . .	18
II-3	The Sun Cone . . . . .	23
II-4	The Geometrical Dependence of $\beta$ on $\psi$ and $\theta$ . . . . .	24
II-5	Intersection of Constant $\omega$ Plane with the Sun Cone . . . . .	28
II-6	Spherical Triangle Geometry . . . . .	30
II-7	The Ranges in $\beta_i$ Determined by Range in $\psi$ . . . . .	31
II-8	Intersection of Constant $\omega$ Plane with Rim of Dish. . . . .	34
II-9	Effective Rim Angle for Front Rim Cut-off Effect . . . . .	35
II-10	Effective Rim Angle for Front Rim Shadowing Effect . . . . .	36
II-11	Effective Rein Angle for Back-side Rein Effects. . . . .	38
III-1	Relationship Between SEV and DMA Coordinate Systems. . . . .	43
III-2	Relationship Between SEV and $FGe_s$ Coordinate Systems . . . . .	43
III-3	Relationship Between $FGe_s$ and $x_{RYRZ_R}$ Systems . . . . .	45
III-4	Relationship Between $FGe_s$ and $xyz$ Coordinate Systems . . . . .	45
IV-1	$\psi$ - $\beta$ Curve for $n=1$ ( $q=0.55-0.95, 0.99$ ) . . . . .	51
IV-2	$\psi$ - $\beta$ Curve for $n=2$ ( $q=0.90-0.99$ ). . . . .	52
IV-3	$\psi$ - $\beta$ Curve for $n=4$ ( $q=0.95-0.995$ ) . . . . .	53
IV-4	Ranges of $\beta$ Determined by Range of $\psi$ . . . . .	54
VI-1a	Optical Power Profile: Cylinder ( $I=0$ ) . . . . .	65a
VI-1b	Optical Power Profile: Cone ( $I=0$ ) . . . . .	65b
VI-2a	Optical Power Profile: Cylinder ( $I=0, \Delta\psi=.5, PHIR=0$ ). . . . .	67a
VI-2b	Optical Power Profile: Cone ( $I=0, \Delta\psi=.5, PHIR=0$ ). . . . .	67b
VI-3a	Optical Power Profile: Cylinder ( $I=0, \Delta\psi=.5, PHIR=90$ ) . . . . .	68a
VI-3b	Optical Power Profile: Cone ( $I=0, \Delta\psi=.5, PHIR=90$ ) . . . . .	68b
VI-4a	Optical Power Profile: Cylinder ( $I=0, \Delta\psi=.5, PHIR=180$ ) . . . . .	69a
VI-4b	Optical Power Profile: Cone ( $I=0, \Delta\psi=.5, PHIR=180$ ). . . . .	69b
VI-5a	Optical Power Profile: Cylinder ( $I=15, PHIR=0$ ) . . . . .	70a
VI-5b	Optical Power Profile: Cone ( $I=15, PHIR=0$ ) . . . . .	70b
VI-6a	Optical Power Profile: Cylinder ( $I=15, PHIR=90$ ). . . . .	71a
VI-6b	Optical Power Profile: Cone ( $I=15, PHIR=90$ ). . . . .	71b

VI-7a Optical Power Profile: Cylinder(I=15,PHIR=180) . . . . .	72a
VI-7b Optical Power Profile: Cone(I=15,PHIR=180) . . . . .	72b
VII-1 Optical Power Profile: Sliced Dish(I=0,PHIR=0) . . . . .	77
VII-2 Optical Power Profile: Sliced Dish(I=0,PHIR=90). . . . .	78
VII-3 Optical Power Profile: Sliced Dish(I=0,PHIR=180) . . . . .	79

LIST OF TABLES

Table

V.1 ROSA SUBROUTINE SUMMARY. . . . .	62
--------------------------------------	----

STAFF

Ronald M. Anderson and Wayne T. Ford  
Principal Investigators

John T. White  
Research Associate

Clint Dawson, Cathy Norwood, and Read Johnston  
Research Assistants

Department of Mathematics  
Texas Tech University  
Lubbock, Texas 79409

## ROSA TECHNICAL DESCRIPTION

### Introduction

The Ratio of Solid Angles (ROSA) computer code was developed as part of the Crosbyton Solar Power Project (CSPP) for calculation of optical power concentrations due to reflection from a spherical segment mirror. It was developed primarily in support of Department of Energy Contracts DE-AC04-76ET20255 and DE-AC04-83AL21557. This report provides technical information about the ROSA code.

This report consists of two parts, a technical reference manual and a user's guide. The reference manual provides the background material and derivations necessary for the implementation of the code. Computer listings ROSA for the code are also included in the reference manual. The user's guide contains an explanation of the input data for the program, requirements for BOILER and RIM subroutines, a discussion of the output data and sample output. Sample BOILER subroutines are given for a right circular cone and a right circular cylinder boiler. A sample RIM subroutine is given for an alternate rim shape.

In the CSPP solar bowl concept, incident solar energy is focused onto a tracking receiver by the spherical segment mirror. The solar focal region of a spherical segment receiver is the frustrum of a cone. The vertex of the cone is at the center of curvature of the mirror. The axis of the cone lies along the line through the center of curvature of the mirror and center of the sun. The vertex angle of the cone is equal to the angular diameter of the sun. The frustrum is one-half the sphere radius in length, extending from the mirror surface half way to the cone vertex.

The tracking receiver is cantilevered and pivots about the center of curvature of the mirror. It is perfectly aligned when its symmetry axis points directly toward the center of the solar disk. For a perfect spherical mirror, the optimal receiver shape would be the frustrum of a cone, with vertex angle equal to the angular diameter of the sun. However, for imperfect mirrors, a cylindrical receiver is nearly as effective and is cheaper to manufacture. Maximum solar energy is captured at noon and, because the mirror is fixed, the power entering the bowl aperture decreases according to the cosine of the inclination angle of the sun (angle between the sun and the bowl symmetry axis) at other times during the day.

In order to fully describe the optical power concentration profile along a receiver, it is necessary to consider several geometrical and physical factors. The size of the bowl aperture determines the maximum amount of incident energy available to the system. However, as the inclination angle of the sun increases, shading and vignetting effects are seen on the receiver. In addition, misalignment of the receiver effects the optical power profile. Finally, the shape of the receiver itself must be considered. All of the above complications are effectively handled in the ROSA computer code.

The Ratio of Solid Angles formulation yields an analytical formula for the solar concentration ratio at a field point,  $Q$ , on a receiver surface. The result is in the form of a sum of integrals, where the region of integration for each integral is described by a solid angle. Rays strike the receiver after reflecting one or more times from a mirror surface, and the integration regions can be described as the collection of all directions from which reflected rays strike the receiver at  $Q$ . This formulation is applicable to concentration calculations for general reflecting surfaces and general receiver shapes.

However, for the solar bowl technology associated with the CSPP, it is sufficient to consider a spherical segment reflecting surface and a receiver/boiler that is a convex surface of revolution. The ROSA code is implemented for such shapes.

The technical reference manual portion of this report consists of several chapters. The first chapter gives a derivation of the model. The results are due to Reichert and Brock [1,2] and yield an integral expression for the concentration ratio at a receiver point due to reflection from an arbitrary reflecting surface. Chapter 2 is devoted to deriving the necessary formulas for evaluation of this concentration ratio integral for the case where the reflecting surface is a segment of a sphere. Multiple reflections, rim cutoff and rim shadowing effects are also accounted for in these derivations. Several coordinate systems are introduced in Chapter 3 in order to account for the geometrical relationships between the sun, collector, and receiver. Chapter 4 discusses the numerical solution of a family of "structure relations" that must be solved in order to evaluate the concentration integral. A description of the ROSA code is presented in Chapter 5 and a complete listing of the code is given in Appendix A. Alternate rim shapes are discussed in Chapter 6.

## 1. THE RATIO OF SOLID ANGLES FORMULATION

### Introduction

The original formulation of the Ratio of Solid Angles Method was due to Reichert [1]. A very complete discussion of the model was given by Brock in his dissertation [2]. The material appearing in this chapter follows his presentation very closely and is included in this report for the sake of completeness.

### The Solar Model

When viewed from earth, the sun appears as a disc with some distribution of light across its face. The effects of its spherical geometry can be lumped into the intensity distribution over the apparent flat disc. In describing the light from the solar disc, it is useful to take advantage of some of the terminology and concepts of the metrologies of photometry and radiometry. Terms will be defined as used.

Consider a spherical source viewed from a point O as illustrated in Figure I-1. The radiant exitance,  $M$  (emitted power per unit area) of the source will be considered to be uniform,

$$M = \frac{P_T}{A_T} \quad (I-1)$$

where  $P_T$  is the total power emitted from the source and  $A_T$  is the total surface area of the source. The radiance vector,  $\vec{L}$ , (radiance is power per unit area per steradian), is

$$\vec{L} = M B(\Omega, \theta_S, \psi_S) \vec{n}_S \quad (I-2)$$

where  $B(\Omega, \theta_S, \psi_S)$  is the radiant brightness distribution which in general depends of the position  $(\theta_S, \psi_S)$  on the sun and the solid

angle  $\Omega$ . The usual radiance that occurs in radiometry is

$$L = \vec{L} \cdot \vec{e}_{\Omega E} \quad (I-3)$$

where  $\vec{e}_{\Omega E}$  is the unit vector in the direction of the observer. If the solid angle emission characteristic is uniform everywhere on the source (isotropic) then

$$L = \frac{P_T}{A_T} B(\Omega) \cos \alpha . \quad (I-4)$$

The radiant brightness distribution,  $B(\Omega)$ , is normalized so that

$$\int \int B(\Omega) \cos \alpha \, d\Omega = 1 \quad (I-5)$$

If the radiant brightness  $B(\Omega)$  is constant for all  $\Omega$ , then

$$B(\Omega) = 1/\pi \quad (I-6)$$

and the source is a Lambertian radiator. The radiance  $L$  is then proportional to the cosine of the angle,  $\alpha$ , between the direction to the observer and the surface normal to the source surface. This is known as Lambert's Law (cosine law) and the source is said to have uniform brightness.

The quantity of interest is actually the power per unit area per unit solid angle (irradiance per steradian) that passes through an element of area on the earth. This element of area is oriented so that its normal lies along the direction to the sun,  $\vec{e}_s$ . An element of area on the sun  $dA$  illuminates an element of area  $dA$  at the earth which subtends the solid angle

$$d\Omega = \frac{dA}{r^2} \vec{e}_s \cdot \vec{e}_{\Omega s} = \frac{dA}{r^2} \cos \tilde{\psi} \quad (I-7)$$

when viewed from the sun along direction  $\vec{e}_{\Omega E}$  as illustrated in

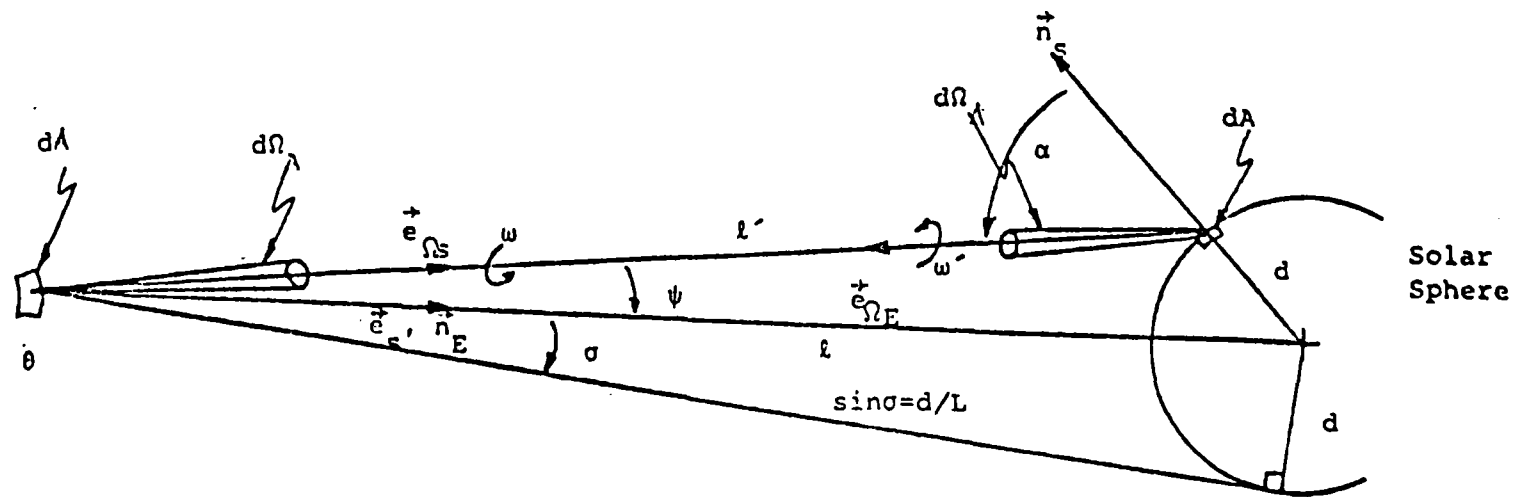


Figure I-1. Element of Area  $dA$  on Sun Illuminates Element of Area  $dA$  on the earth.

Figure I-1. The power received at  $dA$  is

$$dP_o = \vec{L} \cdot \vec{e}_{\Omega E} d\Omega_A dA \quad (I-8)$$

$$= \left( \frac{P_T}{A_T} B(\Omega) \cos \alpha \right) \left( \frac{dA}{r'^2} \cos \psi \right) dA$$

The area on the sun  $dA$  subtends a solid angle

$$d\Omega_A = \frac{dA}{r'^2} \vec{n}_s \cdot \vec{e}_{\Omega E} \quad (I-9)$$

$$= \frac{dA}{r'^2} \cos \alpha$$

when viewed from the earth. The power passing through  $dA$  becomes

$$dP_o = \left( \frac{P_T}{A_T} B(\Omega) \cos \psi \right) \left( \frac{dA}{r'^2} \cos \alpha \right) dA \quad (I-10)$$

$$= \vec{L}_E \cdot \vec{e}_s d\Omega_A dA$$

where

$$\vec{L}_E = (\vec{L} \cdot \vec{n}_s) \vec{e}_{\Omega s} \quad (I-11)$$

is the received radiance vector at the earth. The irradiance at  $dA$  from solid angle  $d\Omega_A$  is

$$\frac{dP_o}{dA} = \vec{L}_E \cdot \vec{e}_s d\Omega_A \quad (I-12)$$

The total irradiance from the entire sun is

$$I_o = \int \int_{\Omega_s} \vec{L}_E \cdot \vec{e}_s d\Omega_A \quad (I-13)$$

$$= \int_0^\sigma \int_0^{2\pi} \frac{P_T}{A_T} B(\omega, \psi) \cos \psi \sin \psi \, d\omega \, d\psi$$

For an isotropic Lambertian source,  $B(\Omega) = 1/\pi$  and

$$I_0 = \frac{P_T}{A_T} \sin^2 \sigma \quad (\text{I-14})$$

The incident radiance  $I$  (irradiance per solid angle) can be written as

$$I = \frac{I_0}{\pi \sin^2 \sigma} \cos \psi \quad (\text{I-15})$$

where

$$0 \leq \tilde{\psi} \leq \sigma$$

The radiance of the source in this case is

$$L = \frac{I_0}{\pi \sin^2 \sigma} \cos \alpha \quad (\text{I-16})$$

It is interesting to note that when the source is Lambertian (follows the cosine law) it produces an incident radiance vector  $\underline{L}_E$  which produces an incident radiance that follows a cosine law at the point of incidence. Emission and reception are isotropic in the same sense.

Few sources are truly Lambertian and the sun is no exception. At optical wavelengths, the sun appears slightly less bright at the limbs, an effect called limb-darkening. (It is interesting to note that at much longer wavelengths, this effect is reversed and limb-brightening occurs.) In such a case, the incident radiance  $I$  becomes

$$I = \frac{I_0 B(\tilde{\psi}) \cos \tilde{\psi}}{2\pi \int_0^\sigma B(\tilde{\psi}) \cos \tilde{\psi} \sin \tilde{\psi} \, d\tilde{\psi}} \quad (\text{I-17})$$

since  $B(\Omega)$  depends only on  $\tilde{\Psi}$  for limb-darkening effects.

However, the limb-darkening effects are slight, so considering the sun to be a Lambertian source is a useful model. Since the sun is so far away,  $\sigma$  is small ( $\sigma \approx 0.267^\circ$ ) so that

$$\cos \tilde{\Psi} = 1 - \frac{1}{2} \sin^2 \tilde{\Psi} > 1 - \frac{1}{2} \sigma^2 \approx 1 \quad (\text{I-18})$$

In this case, the incident radiance can be modeled as

$$I = \frac{I_0}{\Omega_S} \quad (\text{I-19})$$

where

$$\begin{aligned} \Omega_S &= \int_0^\sigma \int_0^{2\pi} \sin \tilde{\Psi} \, d\omega \, d\tilde{\Psi} \\ &= 4\pi \sin^2(\sigma/2) \end{aligned} \quad (\text{I-20})$$

Eq. I-19 is the constant irradiance for solid angle model for the sun.

The solar model for the radiance given by Eq. (I-19) will now be used to obtain the general expression for the optical power concentration. However, it is only used for convenience and it will be shown how it can be replaced by the general model of Eq. (I-17). The results displayed in Chapter II are based on the model of Eq. (I-19) simply because the limb-darkening effects are so small.

## Generalized Optical Power Concentration

The optical power concentration,  $C$ , at a point on a receiver in a collector system is defined to be the ratio of the total optical power per unit area (irradiance) received at that point to the direct irradiance at that point. The direct irradiance is that optical power per unit area (normal to the earth-sun line) received by the collector aperture. If an area  $\Delta A_R$  at a receiver point is illuminated by the area  $\Delta A_A$  in the aperture plane then the total power received at  $\Delta A_R$  is

$$I_0 \Delta A_A$$

where  $I_0$  is the direct irradiance in the aperture plane. The total irradiance at the receiver point is

$$I_0 \Delta A_A / \Delta A_R ,$$

so that the concentration is

$$C = \frac{I_0 \Delta A_A / \Delta A_R}{I_0} = \frac{\Delta A_A}{\Delta A_R} \quad (I-21)$$

The concentration is simply a ratio of areas, but  $\Delta A_R$  depends not only on  $\Delta A_A$  and the location of the receiver point, but also on the shape of the collector mirror. To carry this method of analysis further requires specification of the collector shape, but this approach serves to illustrate the definition of concentration.

Consider an element  $dA$  of receiver area with local "outward" surface normal,  $\vec{\delta}$ , located at  $\vec{q}$  in the neighborhood of a mirror surface as indicated in Fig. I-2. Light from the sun reflected to  $dA$  through the differential of solid angle  $d\Omega$  may be considered to come from a patch of area  $dS$  in a plane tangent to the mirror. The image of the entire sun in the same tangent plane subtends the solid angle  $\Omega_s$  parametrized above. The differential of irradiance at  $dA$  through  $d\Omega$  is, therefore,

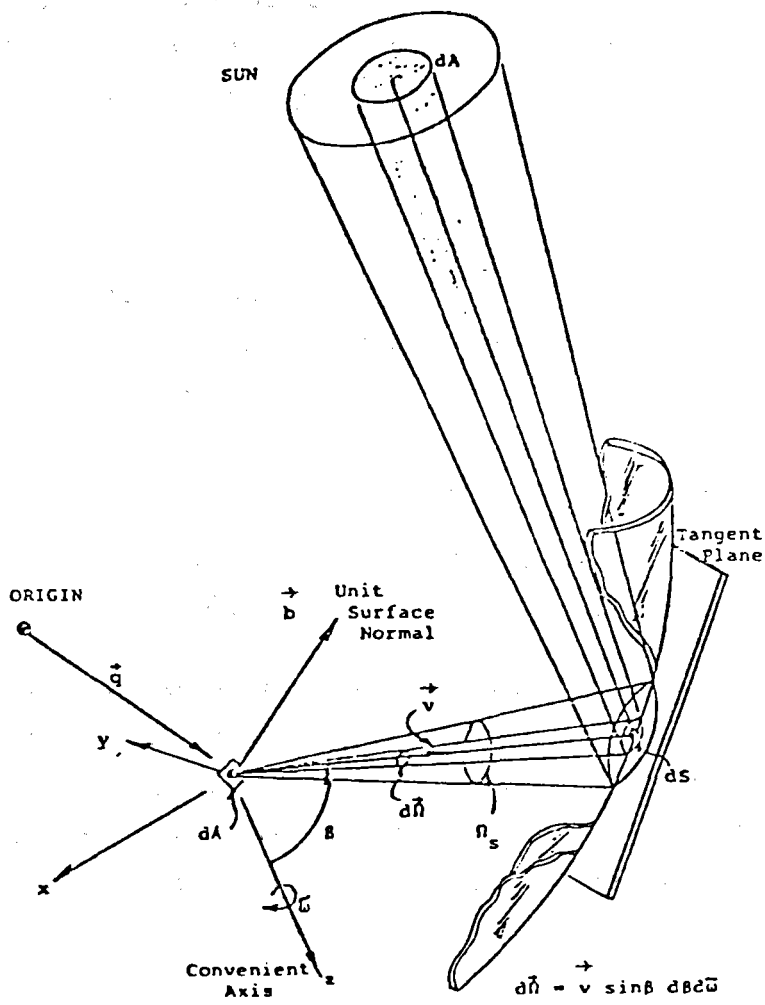


Figure I-2 Section of Generalized Mirror Illuminates Field Point.

$$dI = I d\vec{\Omega} \cdot \vec{b} = \frac{I_0}{\Omega_S} d\vec{\Omega} \cdot \vec{b} \quad (I-22)$$

with the requirement that  $d\vec{\Omega} \cdot \vec{b} > 0$  for illumination only on the outward side of  $dA$ . The differential of optical concentration at  $dA$  is the differential irradiance divided by the input solar intensity,  $I_0$ :

$$dC = \frac{\vec{b} \cdot d\vec{\Omega}}{\Omega_S} \quad (I-23)$$

The optical concentration, then, at  $dA$  is

$$C(\vec{q}, \vec{b}) = \frac{1}{\Omega_S} \int \int_{\Omega_M} \vec{b} \cdot d\vec{\Omega}, \quad \text{for } \vec{b} \cdot d\vec{\Omega} > 0 \text{ only,} \quad (I-24)$$

where  $\Omega_M$  is the apparent solid angle of the entire sun as viewed in the mirror. For a concentrating mirror, one finds  $\Omega_M > \Omega_S$ .

Light in a differential of solid angle will always consider the reflector to be locally flat; i.e., will reflect repeatedly as if from the local tangent planes. Thus the expression Eq. I-24 may be used in the presence of multiple reflections in the mirror by separating and adding the contributions from light that has reflected  $n$  times:

$$C(\vec{q}, \vec{b}) = \sum_n R^n C_n(\vec{q}, \vec{b}) = \frac{1}{\Omega_S} \sum_n R^n \int \int_{Mn} \vec{b} \cdot d\vec{\Omega}_M \quad (I-25)$$

The solid angle  $\Omega_{Mn}$  is the apparent size of the sun as viewed in the mirror with radiation that has reflected  $n$  times. A reflection coefficient  $R$  has been included in Eq. I-25 to account for reflective losses. The factor  $R$  must be kept inside the integral if one wishes to include angle of incidence effects. Similarly, if the wavelength dependence of the reflectivity is of interest, one must add an integral over  $W(\lambda)d\lambda$  to the form shown in Eq. I-25, where  $W(\lambda)$  is a spectral density weight.

If one wishes to use an effective sun size  $\sigma_n$  that depends upon the number of reflections, then  $\Omega_s$  should be expressed:

$$\Omega_{sn} \equiv 4\pi \sin^2(\sigma_n/2) , \quad (I-26)$$

and included inside the summation shown in Eq. I-25. Policies for selecting  $\sigma_n$  are discussed in [2].

The next few chapters of this report will be devoted to evaluation of the concentration ratio integral given in Eq. I-25. The discussion will be limited to spherical collectors and receivers which can be described as surfaces of revolution.

## 2. OPTICAL POWER CONCENTRATION FOR SPHERICAL SEGMENT MIRRORS

### Introduction

The optical power concentration,  $C$ , at a point on a receiver is defined to be the total normally directed optical power per unit area received at that point. In the ROSA code,  $C$  is normalized by dividing by the direct normal insolation incident upon the receiver. The resulting dimensionless quantity becomes a concentration ratio expressed as "number of suns."

The ROSA method deals directly with a finite sun. The sun's size is expressed in terms of an angular radius,  $\sigma$ . Direct sunlight received at a point is viewed as a collection of rays lying inside a right circular cone with vertex at the receiver point  $Q$  and vertex angle  $2\sigma$ .

The ROSA formula for the concentration ratio,  $C$ , at a receiver point,  $Q$ , due to reflection from a mirror surface is given by the integral

$$C(\vec{q}, \vec{b}) = \sum_{\Omega_{Sn}} \frac{R^n}{\Omega_{Sn}} \int \int_{\Omega_{Mn}} \vec{b} \cdot d\vec{\Omega}, \text{ for } \vec{b} \cdot d\vec{\Omega} > 0, \quad (\text{II-1})$$

where,

- $\vec{q}$  = the vector locating a field point  $Q$  on the receiver with respect to a convenient coordinate system;
- $\vec{b}$  = the unit outward normal to the receiver at  $Q$ ;
- $n$  = the number of times a ray has been reflected on the mirror before striking the receiver at  $Q$ ;

$\Omega_{sn} = 4\pi \sin^2(\sigma_n/2)$ , the effective solid angle of the sun as viewed directly from the field point Q;

$\sigma_n$  = the effective angular radius of the sun to be used for light which reflects  $n$  times on the mirror (for a perfect mirror  $\sigma_n = \sigma$ );

$\Omega_{Mn}$  = the apparent solid angle of the sun as viewed in the mirror from the field point Q from light which has reflected exactly  $n$  times;

$R$  = the reflection coefficient of the mirror surface;  
 $0 \leq R \leq 1$ ;

and,

$d\hat{\Omega}$  = differential solid angle directed toward the apparent position of the sun as viewed in the mirror; i. e., the oriented element of surface area on the unit sphere, with unit outward normal.

In order to apply Eq. II-1, a convenient parameterization of the solid angle is required. Thus, the receiver and mirror shapes must be specified. As illustrated in Fig. II-1, the mirror to be studied is a concave hemispherical segment of radius  $R_s$  and rim angle  $\theta_R$ . The center of curvature of the mirror is at C and the axis of symmetry of the spherical segment is along the direction  $\vec{A}$ . The unit vector  $\vec{A}$  is directed from C away from the mirror. The rim angle  $\theta_R$  is the zenith angle (measured from the  $-\vec{A}$  direction) of the circular aperture rim of the mirror. The aperture radius is  $R_A = R_s \sin \theta_R$ , in units of  $R_s$ . In the discussion to follow, it is convenient to normalize all units by dividing by the radius of the spherical segment mirror. Thus, the mirror will always be taken to have unit radius of curvature.

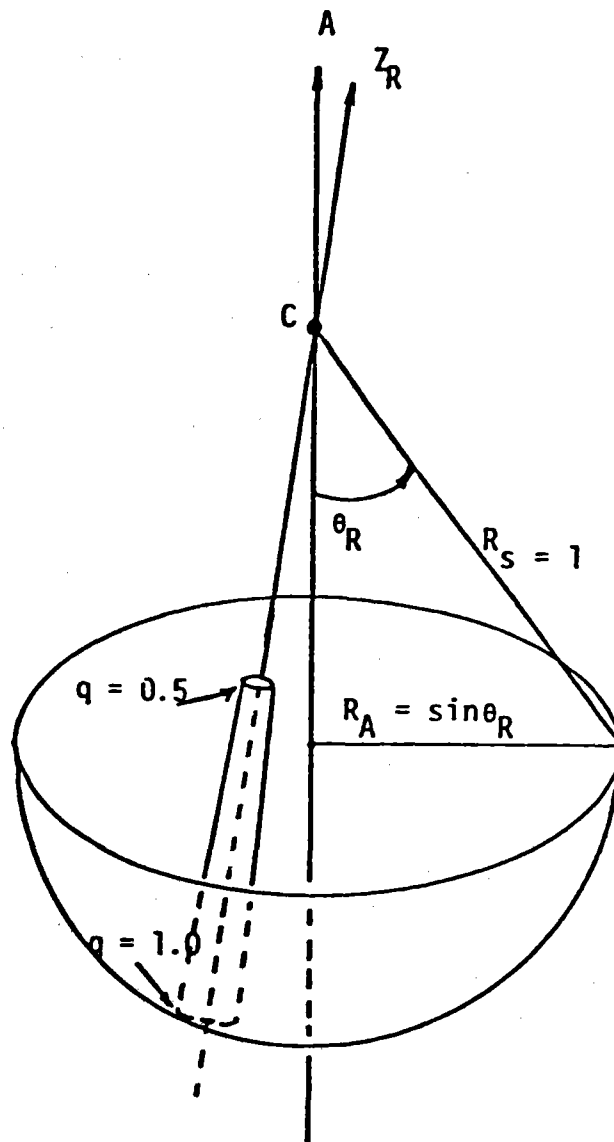


Figure II-1 Mirror and Receiver Shape

The receiver to be studied is assumed to be a convex surface of revolution. The symmetry axis of the receiver lies along the unit vector  $\vec{z}_R$ . The vector  $\vec{q}$ , locating a field point Q on the receiver surface, has origin at C. The unit outward normal to the surface is denoted by  $\vec{v}$  and originates at Q. The receiver

is suspended from C and hangs down into the mirror surface. The mirror-receiver geometry is illustrated in Fig. II-2.

A parameterization for the integral given by Eq. II-1 is obtained by introducing a local x, y, z coordinate system with origin at the field point Q. As shown in Fig. II-2, the z axis lies along the line segment CQ and the positive z direction is directed downward. The directions of x and y will be specified later. The integration is to be carried out over the solid angle  $\Omega_{Mn}$ . Using spherical coordinates, Eq. II-1 can be parameterized in terms of a zenith angle  $\beta$  measured from the positive z axis and an azimuth  $\omega$  measured from the positive x axis, so that,  $0 \leq \beta \leq \pi$  and  $0 \leq \omega \leq 2\pi$ . Then

$$d\Omega = \vec{v} d\Omega = \vec{v} \sin \beta d\beta d\omega.$$

Thus, Eq. II-1 can be written

$$C(\vec{q}, \vec{b}) = \sum_n \frac{B_n}{\Omega_{Sn}} \int \int_{\Omega_{Mn}} (\vec{b} \cdot \vec{v}) \sin \beta d\beta d\omega, \quad \vec{b} \cdot \vec{v} > 0. \quad (\text{II-2})$$

The unit vector  $\vec{v}$  designates the direction of a ray which reaches Q after n reflections from the mirror. The vector  $\vec{v}$  can be expressed in terms of its components in the xyz coordinate system as

$$\vec{v} = (\sin \beta \cos \omega, \sin \beta \sin \omega, \cos \beta).$$

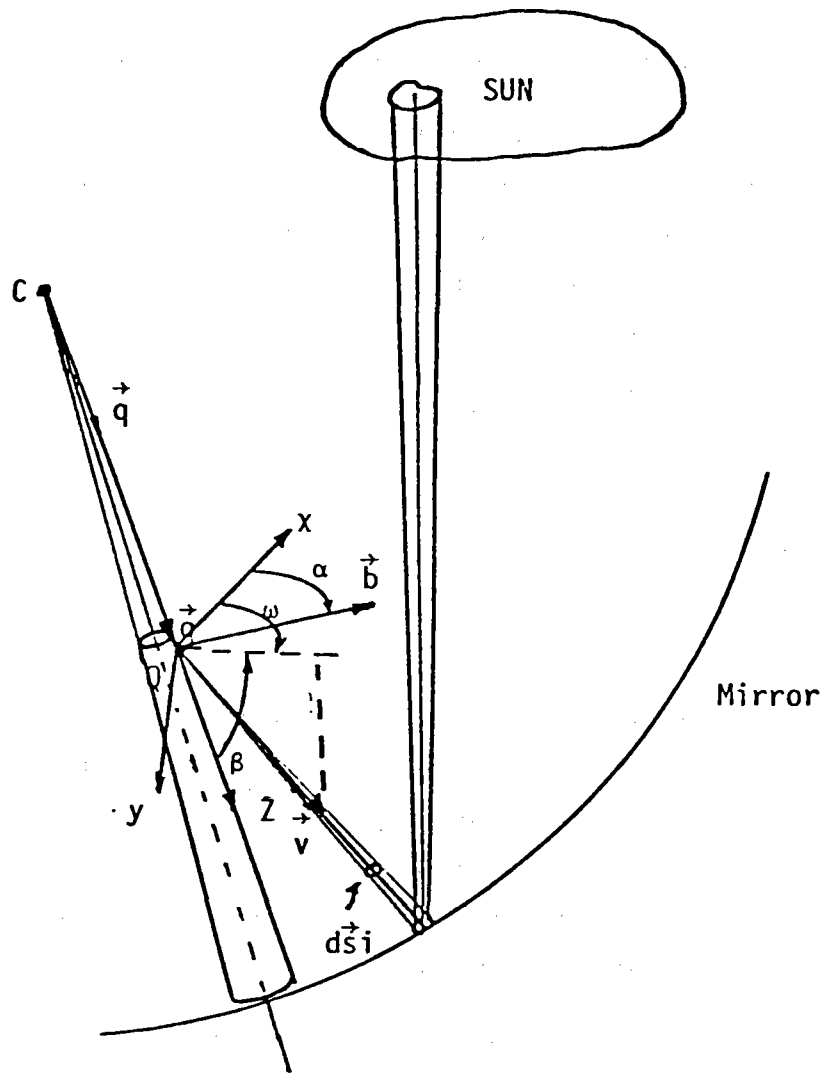


Figure II-2 The Solid Angle Parameters  $\beta$  and  $\omega$

The unit surface normal to the receiver will have components of the form

$$\vec{b} = (b_x, b_y, b_z)$$

so that

$$\vec{b} \cdot \vec{v} = (b_x \cos \omega + b_y \sin \omega) \sin \beta + b_z \cos \beta \quad . \quad (\text{II-3})$$

Substitution of Eq. II-3 into the integral in Eq. II-2 allows the integral to be expressed as an iterated integral. From a computational standpoint, it is convenient to carry out the integration by first integrating on  $\beta$ , followed by integration on  $\omega$ . The concentration formula then becomes

$$C(\vec{q}, \vec{b}) = \sum_{\Omega_{sn}} \frac{R^n}{\Omega_{sn}} C_n(\vec{q}, \vec{b}) \quad ,$$

where,

$$C_n(\vec{q}, \vec{b}) = \int_{\omega} \int_{\beta(\omega)} \{(b_x \cos \omega + b_y \sin \omega) \sin^2 \beta + b_z \cos \beta \sin \beta\} d\beta d\omega \quad . \quad (\text{II-4})$$

The above integral gives a very simple formula for the concentration ratio at a receiver point. The difficult part of the integration arises in determining the region of integration, i.e. describing the solid angle consisting of all directions from which reflected light reaches the field point Q from the mirror. The complications for a given order of light (fixed n) arise from

- (1) the limitations on  $\beta$  and  $\omega$  necessary to insure that  $\vec{b} \cdot \vec{v} > 0$ ;
- (2) the finite size of the sun;
- (3) aperture cut-off effects: vignetting and shading.

The next several sections of this report will be devoted to handling these difficulties.

THE CONDITION  $\vec{b} \cdot \vec{v} > 0$ .

In this section we derive the conditions on  $\omega$  and  $\beta$  that insure  $\vec{b} \cdot \vec{v} > 0$ . Using Eq. II-3, this condition can be written as

$$(b_x \cos \omega + b_y \sin \omega) \sin \beta + b_z \cos \beta > 0. \quad (\text{II-5})$$

There are three cases that must be considered.

Case 1 :  $b_z = 0$ .

In this case, the tangent plane to the surface at the field point Q contains the z axis of the local coordinate system. Eq. II-5 then can be written in the form

$$\cos(\omega - \alpha) > 0, \quad (\text{II-6})$$

where  $\cos \alpha = b_x$  and  $\sin \alpha = b_y$ , and  $\omega \in [0, 2\pi]$ .

Case 2 :  $0 < |b_z| < 1$ .

It is convenient to set  $b_{xy}^2 = b_x^2 + b_y^2$ . Then

$$b_x \cos \omega + b_y \sin \omega = b_{xy} \cos(\omega - \alpha)$$

where,  $\alpha$  is defined by the conditions that  $b_x = b_{xy} \cos \alpha$ , and  $b_y = b_{xy} \sin \alpha$ . Eq. II-5 then becomes

$$b_{xy} \cos(\omega - \alpha) \sin \beta + b_z \cos \beta > 0,$$

or,

$$D(\omega) \cos(\beta - \xi) > 0, \quad (\text{II-7})$$

where,

$$D^2(\omega) = b_{xy}^2 \cos^2(\omega - \alpha) + b_z^2, \quad \omega \in [0, 2\pi],$$

and,  $\xi$  is defined by the conditions

$$D(\omega) \cos \xi = b_z, \quad D(\omega) \sin \xi = b_{xy} \cos(\omega - \alpha).$$

Case 3 :  $|b_z| = 1$ .

Eq. II-5 becomes  $b_z \cos \beta > 0$ . If  $b_z = 1$ , then this condition requires that  $0 \leq \beta \leq \pi/2$ , while if  $b_z = -1$ , then  $\pi/2 \leq \beta \leq \pi$ . If we set  $\xi = 0$  when  $b_z = 1$  and  $\xi = \pi$  when  $b_z = -1$ , then Eq II-7 still applies provided we set  $\alpha = 0$ .

## The Structure Relations

The location of the sun is determined by a unit vector,  $\vec{e}_S$ , pointing from C to the geometrical center of the sun. Because the sun is very far away, light from a region on the solar disk very near the center may be considered to come to the dish aperture as a uniform distribution of rays moving in the direction,  $-\vec{e}_S$ . Other locations on the solar disk may be specified by a family of unit vectors  $\vec{e}_S'$ , pointing from C toward the solar disk, as illustrated in Fig. II-3. This family of "sun directions" forms a cone with vertex at C with semivertex angle,  $\sigma$ , equal to the angular radius of the sun.

The extension of these directions through toward the mirror defines a cone called the "sun cone." The sun cone is a family of directions locating distant differential sources of solar input power. The direction  $\vec{e}_S$  is called the axis of the sun cone. The  $x'$  and  $y'$  axes shown in the figure are parallel to  $x$  and  $y$ , respectively, but pass through C as origin instead of Q. These axes will be of use later.

For any one of the directions  $\vec{e}_S'$  in the sun cone, the angle,  $\beta$ , of the light received at Q may be determined as a function of the angles  $\psi$  and  $\theta$  illustrated in Fig. II-4. This figure illustrates the ray plane for light that can reach Q from sun direction  $\vec{e}_S'$ ; i.e. C, Q, and the differential source on the sun located by  $\vec{e}_S'$  are coplanar and the ray lies in the plane determined by these three points.

The angle  $\theta$  is called the "impact zenith" of a ray that first strikes the mirror at a point of impact P and eventually reaches the receiver surface at Q. Note that  $\theta$  is measured from  $\vec{e}_S'$  and that both the value of and the orientation of the ray plane

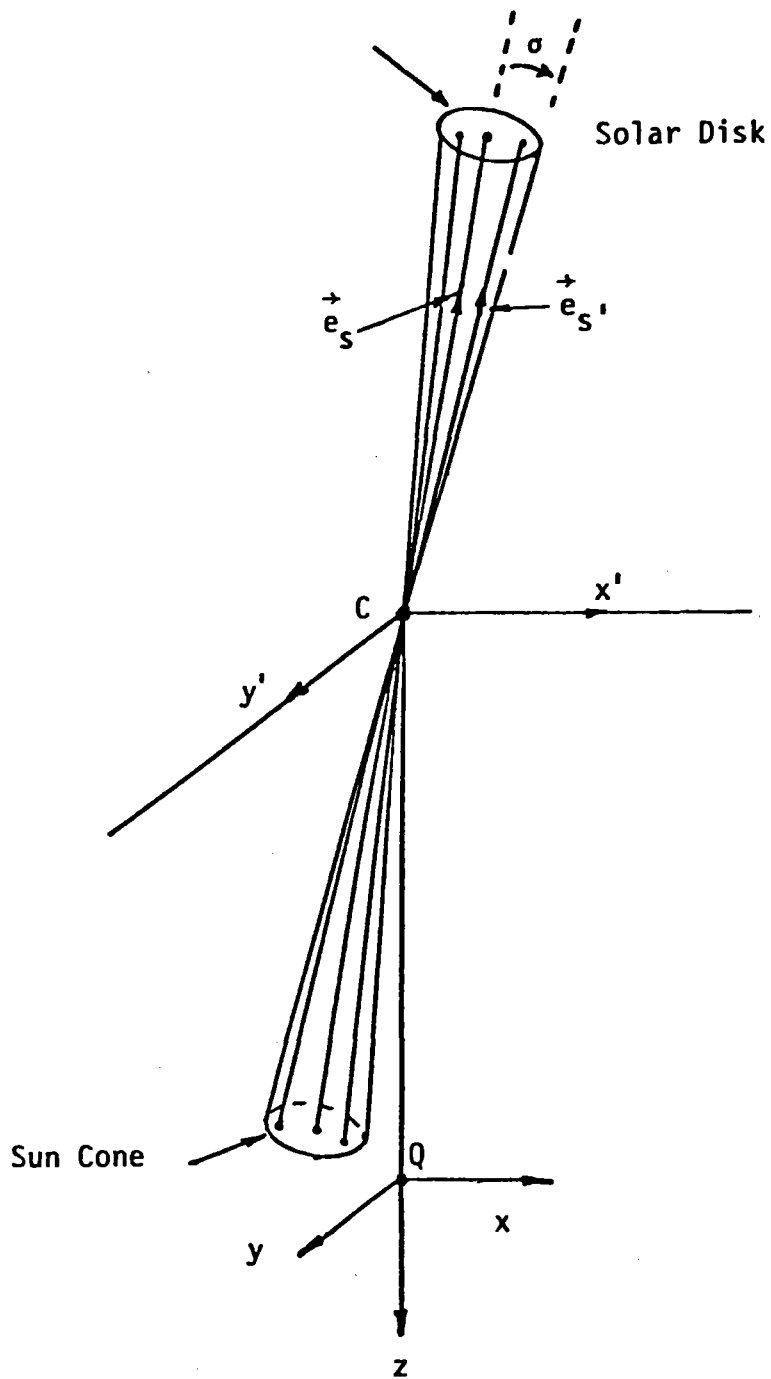


Figure II-3 The Sun Cone

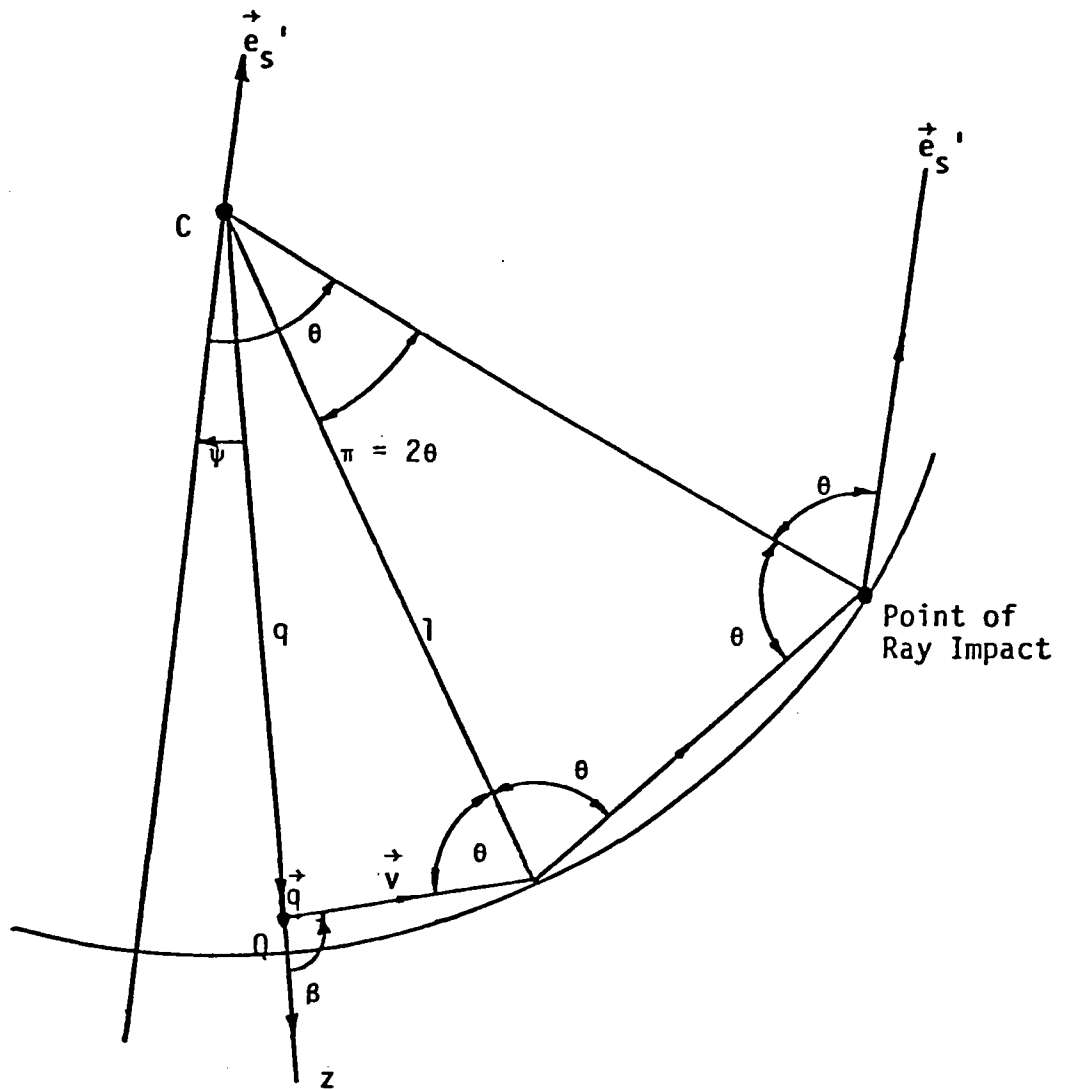


Figure II-4 The Geometrical Dependence of  $\beta$  on  $\psi$  and  $\theta$ , shown for  $n = 2$

depend upon the orientation of  $\vec{e}_S'$  in the sun cone.

The angle  $\psi$  is a zenith angle for  $-\vec{e}_S'$  as measured from the z axis through Q. The zenith of the sun cone axis, the angle between z and  $(-\vec{e}_S')$ , is designated  $\psi_0$ . The value of  $\psi$  in the ray plane depends upon the orientation of  $\vec{e}_S'$  in the sun cone. The parameters  $\psi$  and  $\theta$  are the mechanism for describing the shape of the receiver and the shape of the mirror. The values of  $\psi$  at various q determine the shape and location of the receiver surface. The corresponding values of  $\theta$  are essential to the description of the mirror shape and location. The relationship between these shape parameters and  $\beta$  is given by the "structure relations":

$$\beta = 2n\theta - \psi - (n-1)\pi \quad (\text{II-8a})$$

and

$$\sin\theta = q \sin\beta \quad (\text{II-8b})$$

The structure relations are easily deduced from Fig. II-4, drawn for  $n = 2$ . They are obtained by considering the triangle CQP<sub>1</sub>. Eq. II-8a is the measure of the angle at the vertex C for this triangle and Eq. II-8b follows from an application of the law of sines to this triangle. As a convention, if, for any reason, Q and the point of ray impact P lie on opposite sides of the axis  $\vec{e}_S$ , then the angle  $\psi$  from q to  $(-\vec{e}_S')$  is assigned a negative sign. One may easily verify that  $\theta$  and  $\beta$  remain positive and that Eqs. II-8 are still valid in this situation.

The impact zenith can be eliminated from Eqs. II-8 to produce

$$\beta = 2n \sin^{-1}(q \sin\beta) - \psi - (n-1)\pi \quad (\text{II-9})$$

This equation plays a central role in determining the limits of integration in the integral appearing in Eq. II-4. A detailed discussion of the solutions of this equation will be given in a later section. Graphs of  $\psi$  versus  $\beta$  for various values of q will

also be given. It will be shown that for given values of  $n$  and  $\psi$ , Eq. II-9 may have more than one solution,  $\beta$ . With some ray tracing, one finds that, typically, there are two values of  $\theta$  (and, hence, two values of  $\beta$ ) that contribute light at  $Q$  when  $\psi > 0$ , but only one value of  $\theta$  (and, hence, one value of  $\beta$ ) that contributes when  $\psi < 0$ . A subscript  $i = 1, 2$  will be attached to  $\beta$  to distinguish the various solutions of Eq. II-9 for given values of  $\psi$  and  $n$ . Thus, if there are two solutions,  $\beta_1$  will denote the smaller and  $\beta_2$  will denote the larger.

### Effects of Finite Sun Size.

It should be clear from the discussion above that contributions at Q come from a range of values of  $\theta$  and  $\psi$  produced by moving the vector  $\vec{e}_S'$  throughout the sun cone. Due to this effect, for each  $\omega$  in Eq. II-4, one may find a range of values of  $\psi$  locating sun axes,  $\vec{e}_S'$ , lying in the plane of constant  $\omega$ . Such a range of values for  $\psi$ , when used in Eq. II-9 determines ranges of values for the  $\beta$ . The set union of these ranges of values of the  $\beta_i$  is, for the specified  $\omega$ , the range of  $\beta$  integration required in Eq. II-4 to account for finite sun size. As will be described later, this range of integration may be reduced because of "rim effects."

The range of values of  $\psi$  mentioned above is, of course, non-existent if the constant  $\omega$  plane does not intersect the sun cone. If it does intersect, then the algebraically smallest and largest values of permitted  $\psi$  are designated  $\psi_-$  and  $\psi_+$ , respectively. Fig. II-5 illustrates a case in which Q lies inside the sun cone. As may be seen in Fig. II-2, by definition, the points C and Q lie on the plane of constant  $\omega$  (because  $\omega$  is measured about the CQ line, i.e., about the z axis). Thus, the dashed lines marked by  $\psi_-$  and  $\psi_+$  are coplanar with CQ and a ray plane is defined whose contributions will be received at Q as it is located (as in Fig. II-4) by a range of values of  $\psi$  from  $\psi_-$  to  $\psi_+$ .

$\psi_{\pm}$  are always measured from the z axis. The positive direction is taken to be opposite that of  $\vec{v}$ . Thus, in Fig. II-5,  $\psi_- < 0$  and  $\psi_+ > 0$ . This will always be the case when the field point Q lies inside the sun cone. If the field point Q lies outside the sun cone and the  $\omega$  plane intersects the sun cone,  $\psi_+$  and  $\psi_-$  will have the same sign. In particular, if  $\vec{v}$  is directed away from the sun cone, then both will be positive, while if  $\vec{v}$  is directed towards the sun cone, both will be negative.

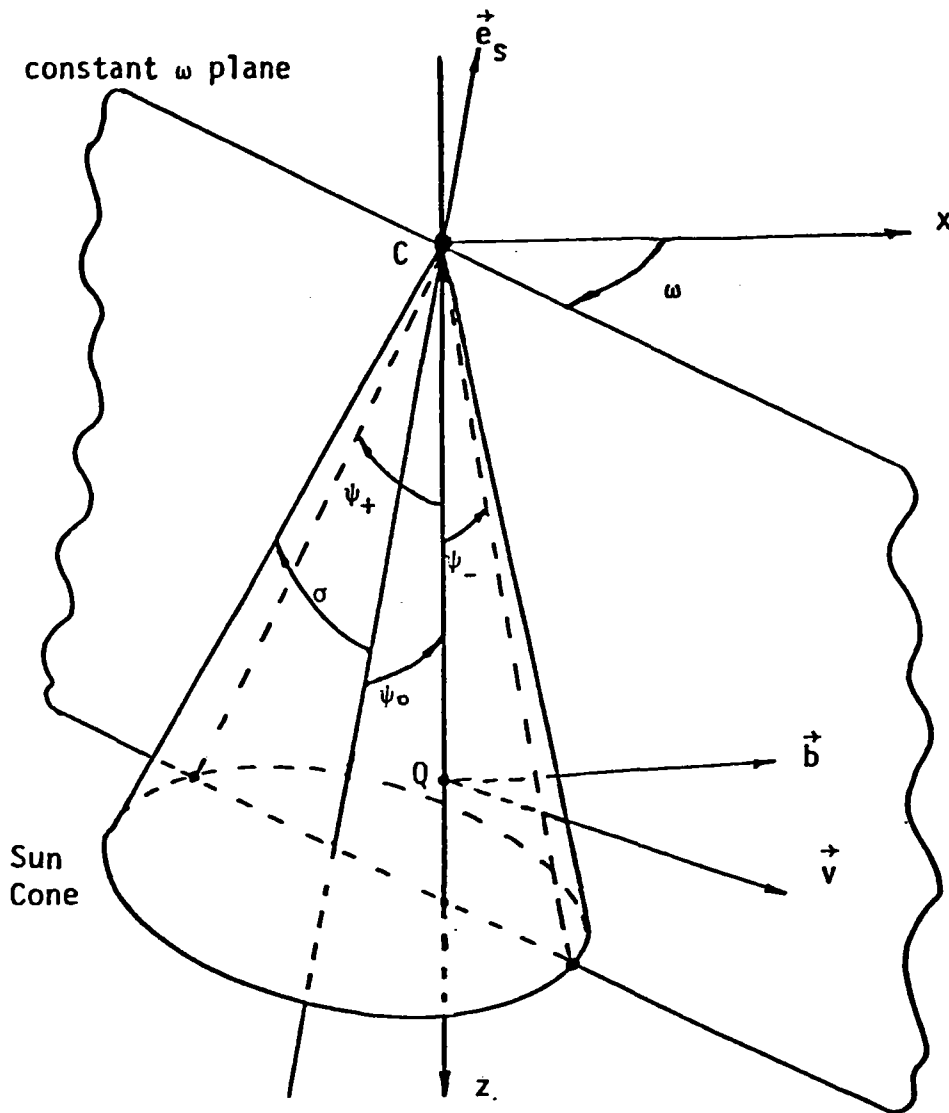


Figure II-5 The Intersection of a Constant  $\omega$  Plane with the Sun Cone

The formulas for  $\psi_+$  and  $\psi_-$  can be obtained from a detailed consideration of the geometry for the  $\omega$  plane-sun cone intersection. The analysis is carried out using spherical trigonometry. The appropriate spherical triangle is shown in Fig. II-6. The law of cosines for spherical triangles gives

$$\cos \sigma_n = \cos \psi_0 \cos \psi_+ + \sin \psi_0 \sin \psi_+ \cos \omega. \quad (\text{II-10})$$

Setting

$$D = \sqrt{\cos^2 \psi_0 + \sin^2 \psi_0 \cos^2 \omega},$$

Eq. II-10 can be rewritten as

$$\cos(\psi_{\pm} + \eta) = \pm [\cos \sigma_n] / D$$

where,

$$\eta = \tan^{-1}(\tan \psi_0 \cos \omega), \quad \eta \in [-\frac{\pi}{2}, \frac{\pi}{2}].$$

These results are to be used for all cases with  $\omega$  for which

$$(\vec{b} \cdot \vec{v}) > 0.$$

For any  $\omega$ , once the range  $\psi_-(\omega)$  to  $\psi_+(\omega)$  has been determined, then the corresponding ranges of  $\beta_1$  may be determined from Eq. II-9, as mentioned earlier. The nature of the ranges in  $\beta_1$  is illustrated in Fig. II-7. For the positive values illustrated for  $\psi_-$  and  $\psi_+$ , two ranges are indicated:

$$\begin{aligned} \text{range for } \beta_1: & [\beta_{10}(\psi_-), \beta_{11}(\psi_+)] \\ \text{range for } \beta_2: & [\beta_{20}(\psi_+), \beta_{21}(\psi_-)]. \end{aligned} \quad (\text{II-11})$$

Two additional quantities are illustrated in the figure:  $\beta_{\min}$  and  $\beta_{\max}$ . These are constraints on the range of  $\beta$  integration imposed by mirror rim effects to be discussed later.

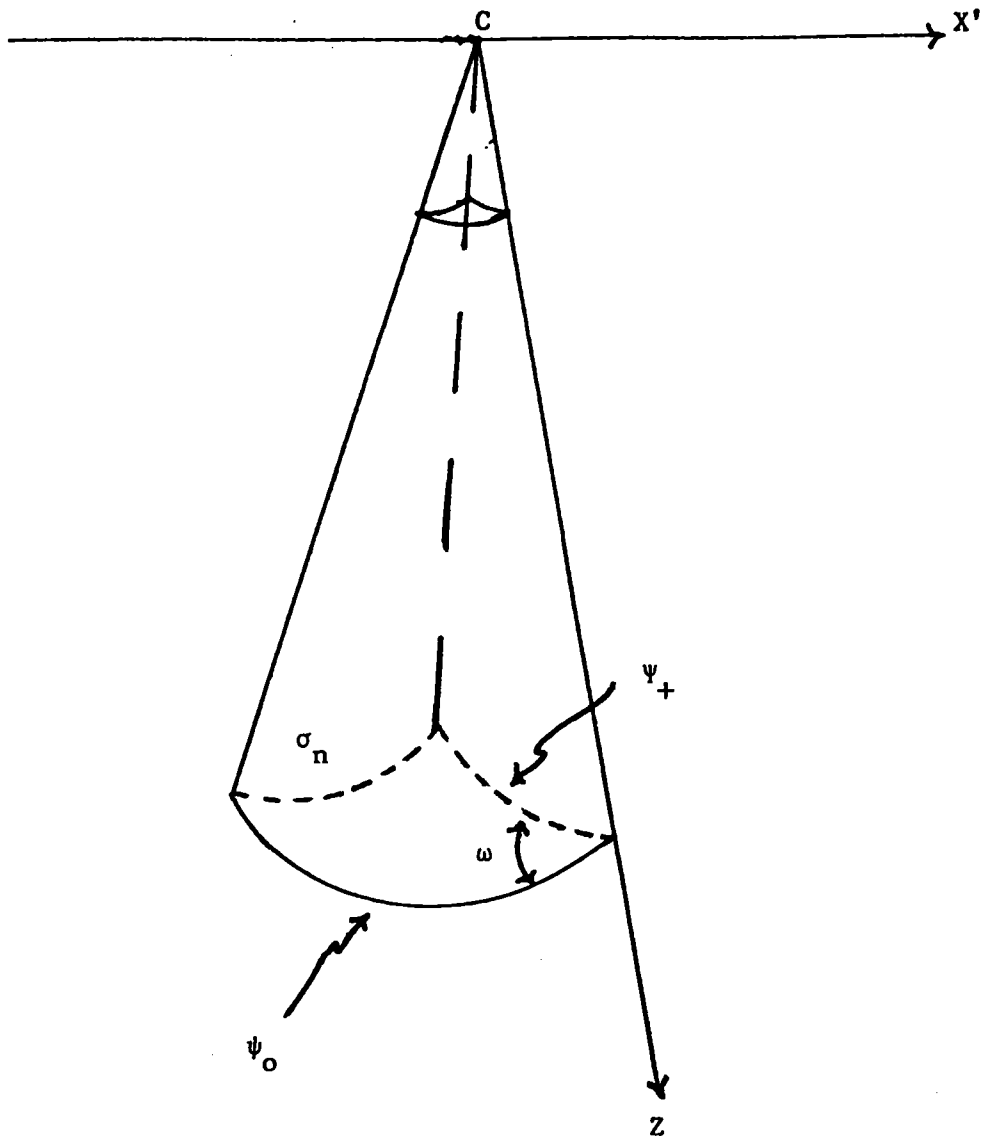


Figure II-6 Spherical Triangle Geometry

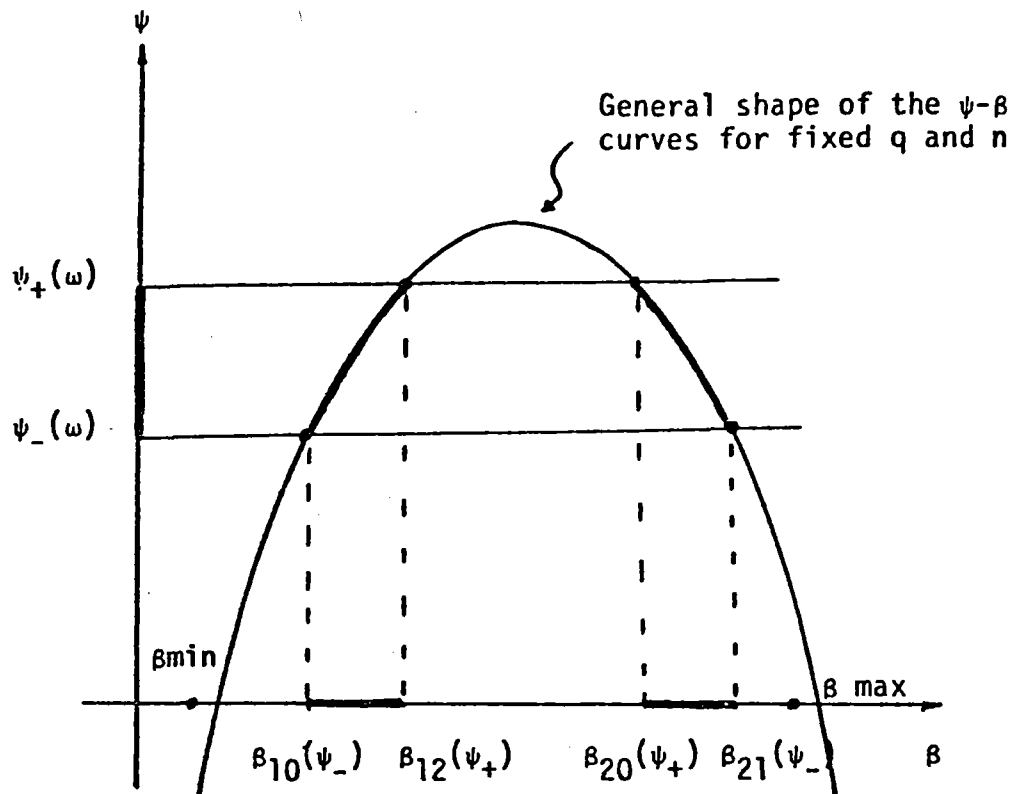


Figure II-7 The Ranges in  $\beta_i$  Determined by Range in  $\psi$

If one defines the quantities:

$$\begin{aligned} \beta_{Li} &= \text{Max} \{ \beta_{\text{min}}(\omega), \beta_{i0}(\psi_{\pm}) \} \\ \beta_{Ui} &= \text{Min} \{ \beta_{\text{max}}(\omega), \beta_{i1}(\psi_{\pm}) \} \end{aligned} \quad (\text{II-12})$$

where the top subscript on  $\psi$  is intended for  $i = 1$  and the lower is intended when  $i = 2$ , then Eq. II-4 can be brought to the form:

$$C_n(\vec{q}, \vec{b}) = \frac{1}{2} \int_i \sum [ (b_x \cos \omega + b_x \sin \omega) (\beta - \frac{1}{2} \sin 2\beta) + b_z \sin^2 \beta ] \Big|_{\beta_{Li}}^{\beta_{Ui}} d\omega \quad (\text{II-13})$$

where the  $i^{\text{th}}$  term is to be kept only if  $\beta_{Ui} > \beta_{Li}$ .

The problem has now been reduced to the numerical work required to evaluate the quantities  $\beta_{Li}$  and  $\beta_{Ui}$  and, subsequently, to evaluate the integral over  $\omega$ . Further progress requires determination of the range of  $\omega$  integration.

If the field point  $Q$  lies inside the sun cone; i.e.,  $\sigma \geq \psi_0$ , then there is no restriction on  $\omega$  in addition to that shown in Eq. II-13. On the other hand, if  $\sigma < \psi_0$ , the field point  $Q$  lies outside the sun cone and the  $\omega$  plane may not intersect the sun cone. Since contributions to  $C_n(\vec{q}, \vec{b})$  in Eq. II-13 only arise if the  $\omega$  plane intersects the sun cone, it is possible to limit the required range of  $\omega$  even more. If  $Q$  is outside the sun cone, intersection with the sun cone is possible if and only if  $D \geq \cos \sigma_n$ , where  $D$  is defined above. Solving this equation for  $\omega$  yields

$$\cos^2 \omega = \frac{\cos^2 \sigma_n - \cos^2 \psi_0}{\sin^2 \psi_0} \quad (\text{II-14})$$

This relation determines regions in  $\omega$  for which the intersection occurs. The set intersection of the set union of these regions with the region defined in Eq. II-12 is the required region of intergration.

### Rim Angle Effects.

The effect of the dish rim will now be considered. It determines the availability of the mirror support for contributions at the field point Q. This support may be missing due to either cut-off or shading. The constant  $\omega$  plane, containing the incoming ray  $\vec{v}$ , cuts the rim of the dish as shown in Fig. II-8. The dish rim angle in the  $\omega$  plane can best be expressed as the front-side rim angle,  $\theta_z^+$ , and the back-side rim angle,  $\theta_z^-$ . Both  $\theta_z^+$  and  $\theta_z^-$  are zeniths from the z axis, measured positive in the direction of  $\vec{v}$ . When  $\theta_z^+ \leq 0$ , the dish is not seen in the  $\vec{v}$  direction and, thus, there is no contribution.

When  $0 < \theta_z^+ + \psi \leq \pi/2$  there is a rim cut-off; part of the mirror support is not present. As shown in Fig. II-9, the effective rim angle,  $\theta_{z,eff}$ , describes the "illuminated" region of the dish. The angle  $\psi$  shown in Fig. II-9 is measured negative in the direction of  $\vec{v}$ , so  $\theta_z^+ + \psi$  is less than  $\theta_z^+$ . This is the edge of the region from which light of order n reflects for the last time and leaves the mirror to strike Q. From the geometry in the figure, it is clear that the effective rim angle for rim cut-off is

$$\theta_{z,eff} = \theta_z^+ - (n-1)(\pi - 2\theta_z^+ - 2\psi) \quad . \quad (II-15)$$

For a finite sun, the incoming rays arrive in a band between  $\psi_- \leq \psi \leq \psi_+$ . There is a portion of the dish that will be partially cut-off as illustrated in Fig. II-9. This partially cut-off region is small enough that  $\psi$  can be approximated as  $(\psi_+ + \psi_-)/2$  and Eq. II-15 becomes

$$\theta_{z,eff} = \theta_z^+ - (n-1)(\pi - 2\theta_z^+ - \psi_+ - \psi_-) \quad . \quad (II-16)$$

When  $\pi/2 < \theta_z^+ + \psi \leq \pi$ , a portion of the mirror is shaded. This effect is called rim shadowing. As shown in Fig. II-10,  $\theta_{z,eff}$

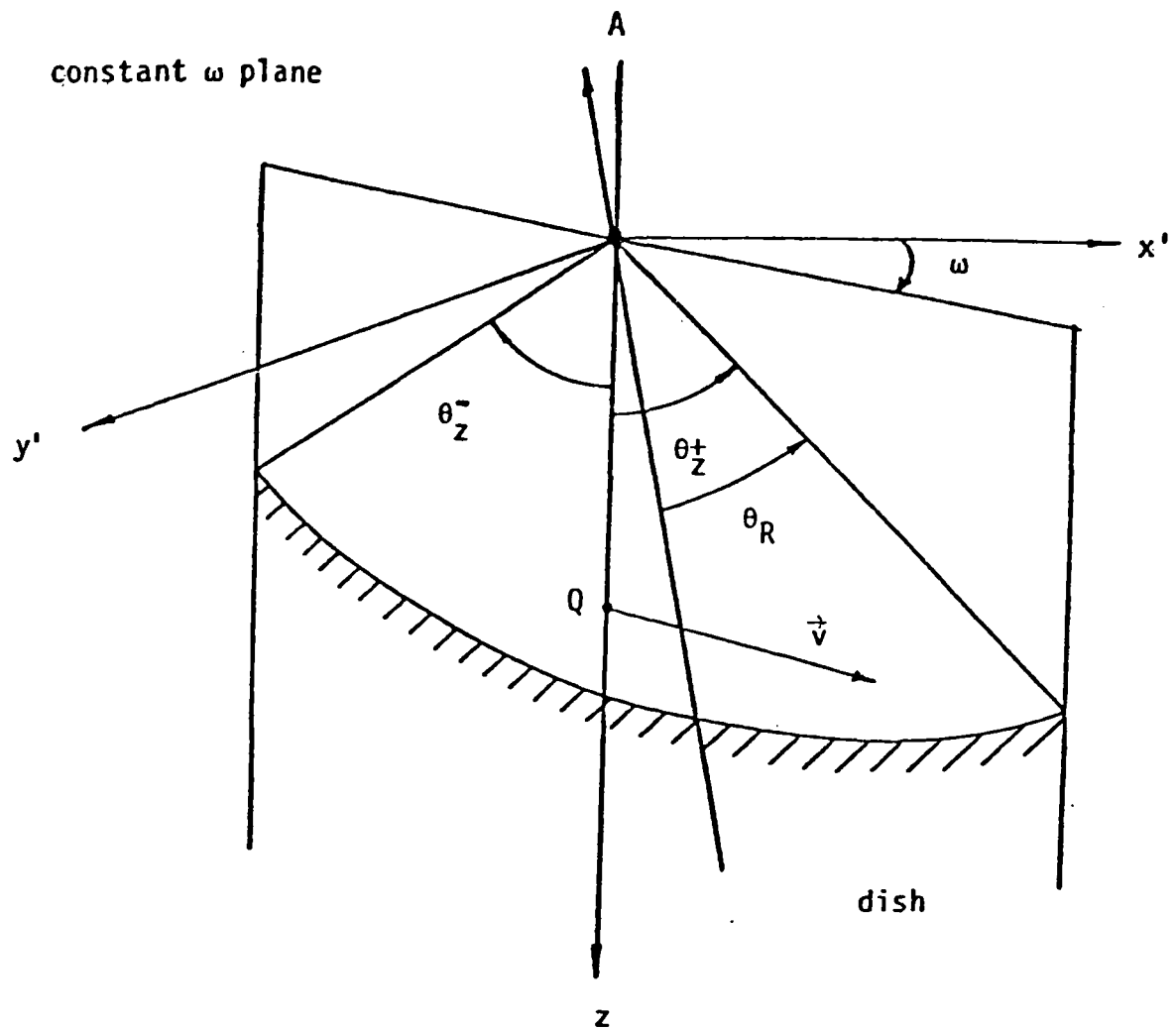


Figure II-8 The Intersection of a Constant  $\omega$  Plane with the Rim of the Dish

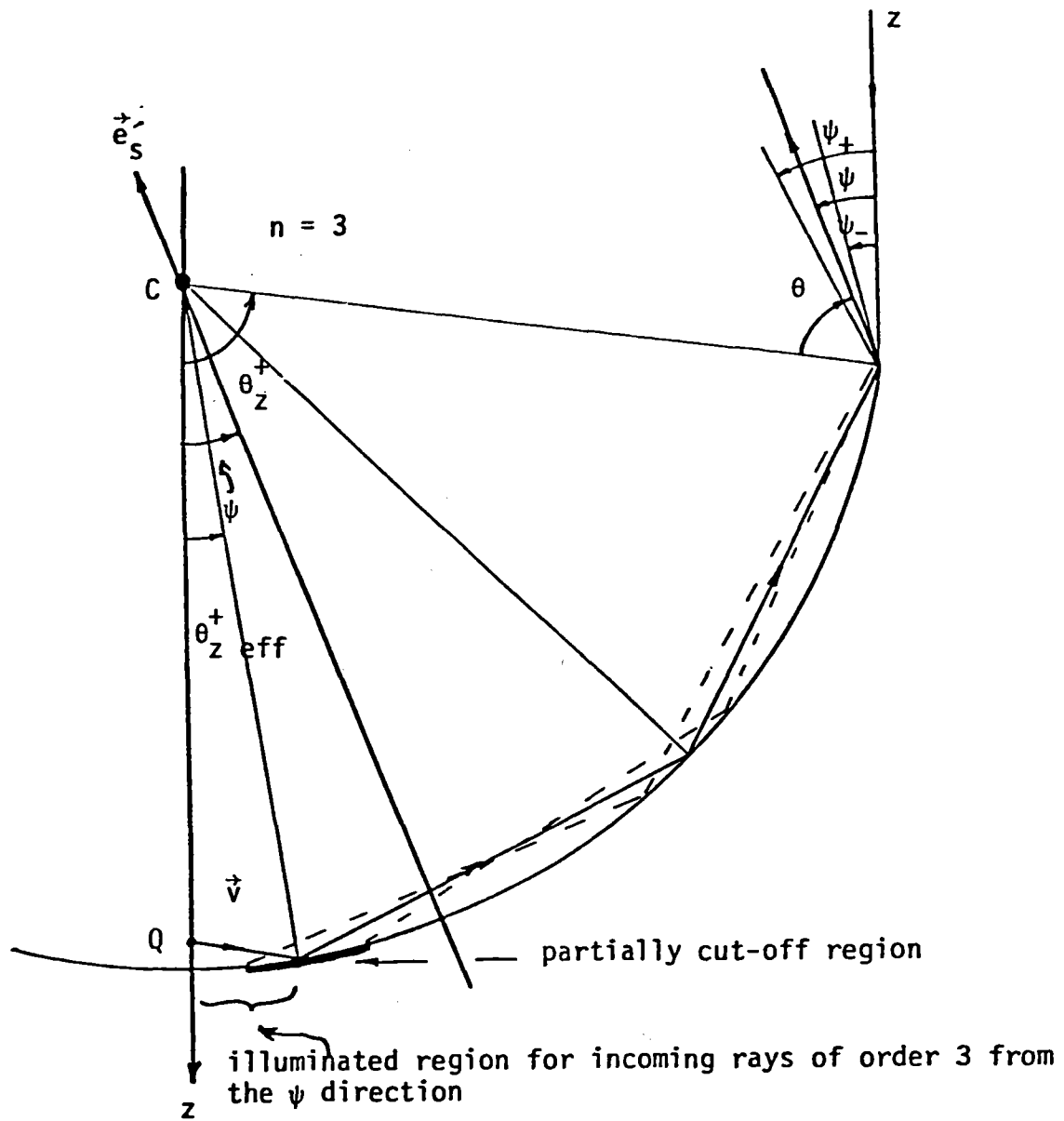


Figure II-9 The Effective Rim Angle for the Front Rim Cut-off Effect

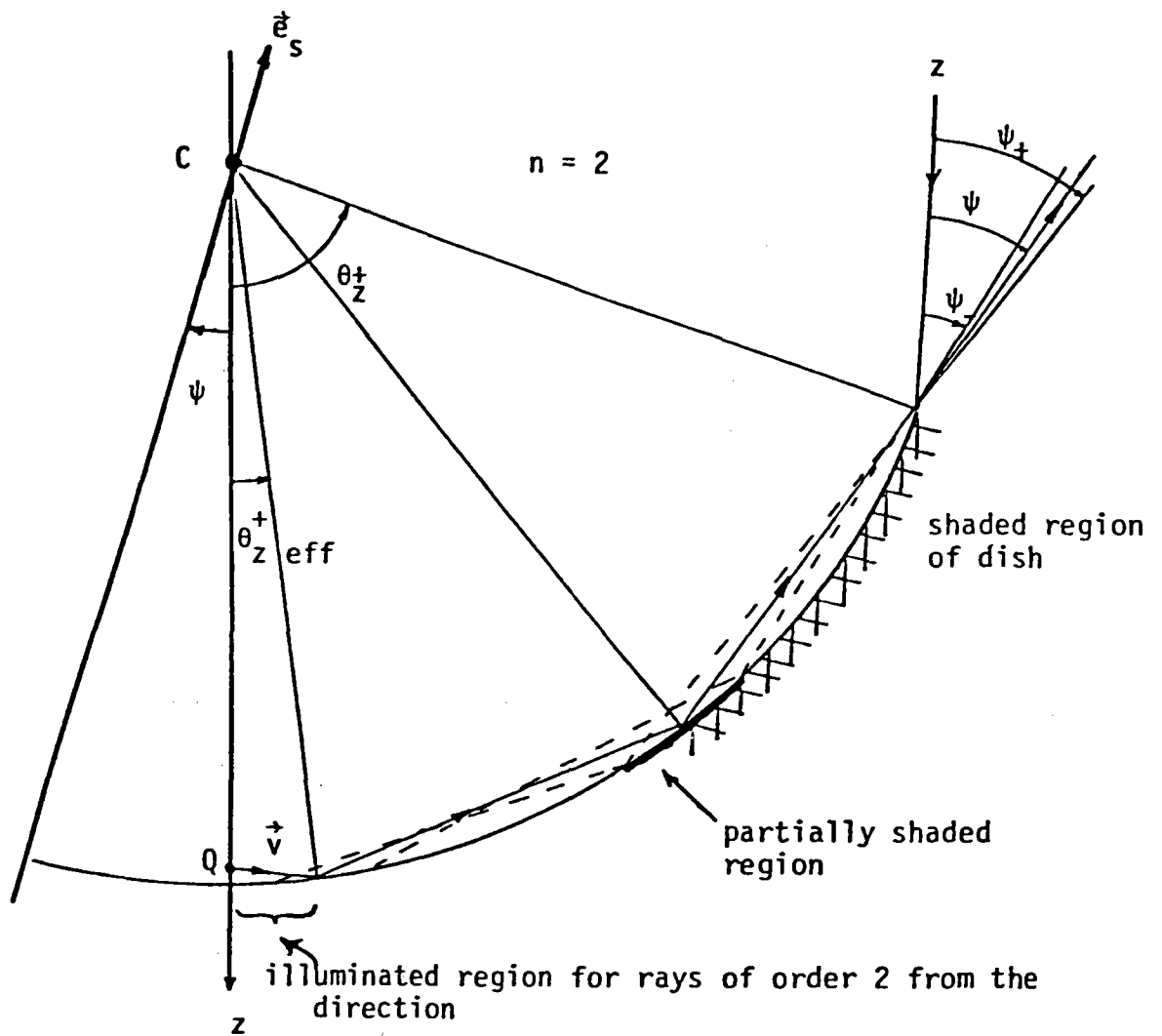


Figure II-10 The Effective Rim Angle for the Front Rim Shadowing Effect

describes the "illuminated" region. Again, there is a portion of the dish that will be partially shaded as illustrated in Fig. II-10. With the same approximation, the effective rim angle for rim shadowing is

$$\theta_{z,eff}^+ = \theta_z^+ + n(\pi - 2\theta_z^+ - \psi_+ - \psi_-) . \quad (II-17)$$

The front-side rim effect comes from either the cut-off or the shadowing. Always, the smaller of the values determined by Eqs. II-16 and 17 must be used. The overall front-side effective rim angle is

$$\theta_{z,eff}^+ = \text{Min} [ \theta_z^+ - (n-1)K, \theta_z^+ + K ] \quad (II-18)$$

where 
$$K = \pi - 2\theta_z^+ - \psi_+ - \psi_- .$$

The back-side rim angle effect is simpler. If  $-\pi \leq \theta_z^- \leq 0$ , the back-side rim angle does not affect the contribution, because light from this region cannot reach Q. If  $0 \leq \theta_z^- \leq \pi/2$ , the receiver field point Q is outside the dish and some of the reflected rays will be lost. If  $\theta_z^- \leq -\pi$ , a portion of the dish will be shaded, as shown in Fig. II-11. The overall result for the back-side becomes

$$\theta_{z,eff}^- = \text{Max} [ 0, \theta_z^-, -\theta_z^- - \pi + \psi_+ - \psi_- ] . \quad (II-19)$$

The front-side and back-side rim angle effects place restrictions on the values of  $\beta$ . If  $\theta_{z,eff}^+ \leq \theta_{z,eff}^-$ , there is no limits of  $\beta$  must satisfy

$$\sin(\pi - \beta_{max}) = \frac{\sin(\beta_{max} - \theta_{z,eff}^+)}{q} \quad (II-20)$$

and

$$\sin(\pi - \beta_{min}) = \frac{\sin(\beta_{min} - \theta_{z,eff}^-)}{q} . \quad (II-21)$$

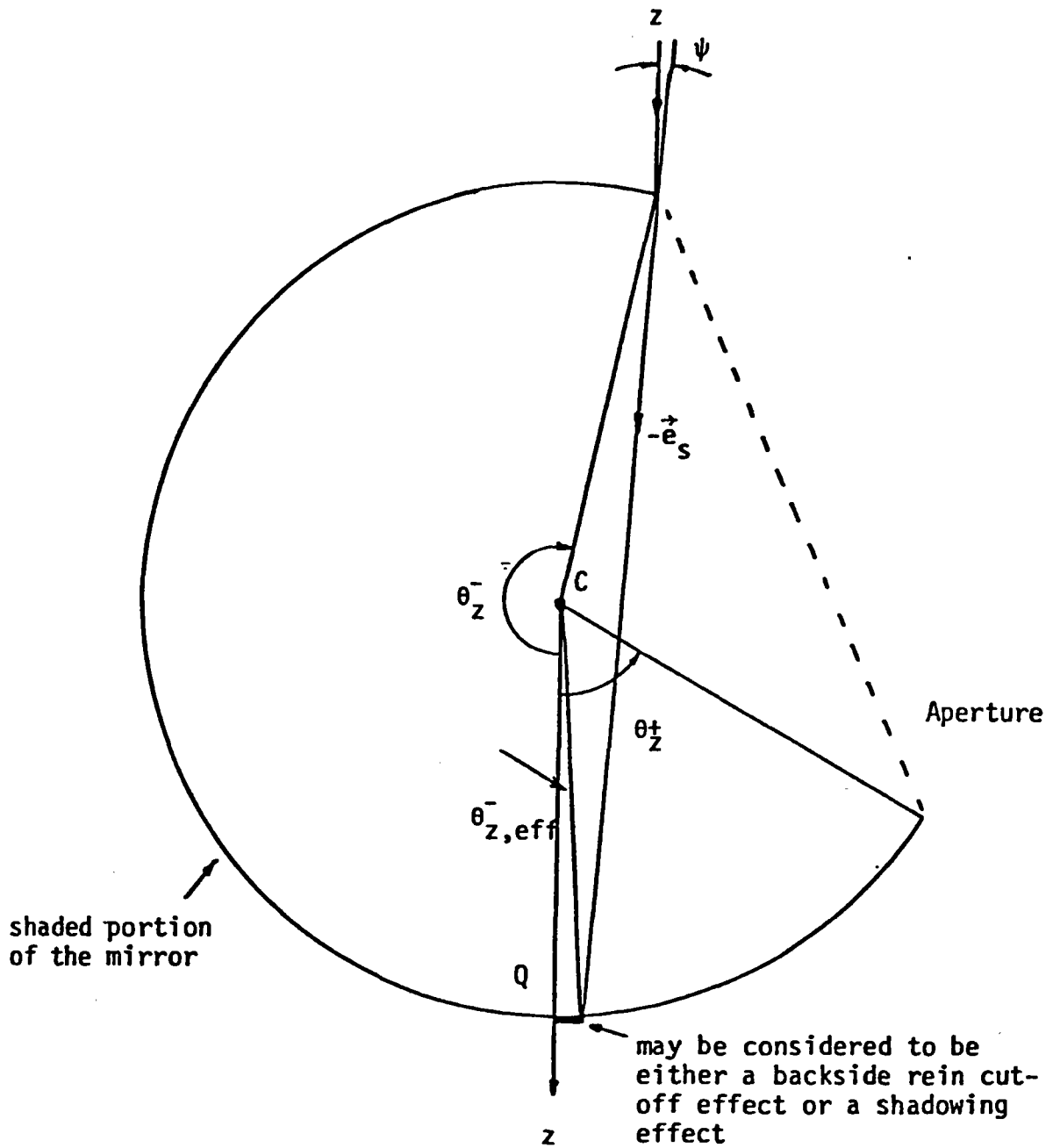


Figure II-11 The Effective Rein Angle for the Back-side Rein Effects

Solving Eqs. II-20 and 21 for  $\beta$ , one obtains:

$$\beta_{\max}(\omega) = \text{Tan}^{-1} \left\{ \frac{\sin \theta_{z,\text{eff}}^+}{\cos \theta_{z,\text{eff}}^+ - q} \right\} \quad (\text{II-22})$$

and

$$\beta_{\min}(\omega) = \text{Tan}^{-1} \left\{ \frac{\sin \theta_{z,\text{eff}}^-}{\cos \theta_{z,\text{eff}}^- - q} \right\} . \quad (\text{II-23})$$

These are the quantities required in Eq. II-12 to determine the limits of the  $\beta$  integral,  $\beta_{Lj}$  and  $\beta_{Uj}$ . These complete the constraints on the  $\beta$  and  $\omega$  in Eq. II-13 and the power concentration is obtained by evaluating the integral.

### 3. THE SUN-RECEIVER-COLLECTOR GEOMETRY

#### Introduction

The previous sections developed formulas for finding the limits of integration for the ROSA integral given by Eq. II-4. The integration is accomplished by introducing a local xyz coordinate system at the field point Q and using spherical coordinates in this system. The limits of integration are then found by intersecting planes  $\omega = \text{constant}$  with the sun cone which corresponds to light of order n (light which has reflected n times before striking the field point).

The location of the sun cone relative to the point Q depends upon several factors. These include the position of the sun, the size and orientation of the collector, and the shape and position of the receiver. It is therefore necessary to define additional coordinate systems in order to describe the geometrical relationship between these factors.

The next few sections will be used to define appropriate coordinate systems for describing the sun-collector-receiver geometry. The location of a field point, Q, on the receiver can be described in terms of these coordinate systems. In this way, the concentration calculations can be associated with specified locations on a receiver surface.

### The Earth-fixed Coordinate System

This coordinate system is a South-East-Vertical coordinate system. The axes are called S, E, and V, respectively. The origin of this coordinate system is taken to be at C, the center of curvature of the spherical segment mirror.

### The Bowl Symmetry Coordinate System

This collector fixed coordinate system has origin at C, and the axes are called D, M, and A. The standard collector is taken to be a segment of a sphere, and the A axis is the symmetry axis of the collector, pointing away from the bowl (see Fig. II-2). D is oriented such that the lowest point (with respect to the vertical) on the rim of the mirror lies in the VD plane and has positive D component. If A coincides with the V axis, then D is taken to lie along S. The M axis is chosen so that the DMA system forms a right hand coordinate system.

The parameters  $\gamma$  (the tilt angle) and  $\phi_D$  (the dip azimuth) serve to define this system with respect to the SEV coordinate system as shown in Fig. III-1. The M axis lies in the SE plane. The transition matrix from the SEV system to the DMA system is given by :

$$[p]_{DMA} = \begin{bmatrix} \cos \gamma \cos \phi_D & \cos \gamma \sin \phi_D & -\sin \gamma \\ -\sin \phi_D & \cos \phi_D & 0 \\ \sin \gamma \cos \phi_D & \sin \gamma \sin \phi_D & \cos \gamma \end{bmatrix} [p]_{SEV} \quad (III-1)$$

The DMA and SEV coordinate systems are identical when  $\gamma = 0$  and  $\phi_D = 0$  (The above matrix reduces to the identity.)

This coordinate system will also be used in describing alternate rim shapes. The standard bowl of unit radius is defined as the segment of the unit sphere lying below the plane  $A = -\sin \theta_R$ , where  $\theta_R$  is the rim angle of the bowl.

## The Sun Tracking Coordinate System

The sun tracking coordinate system also has its origin at C. Its axes are denoted by F, G, and  $e_s$ . The positive  $e_s$  axis points to the center of the sun. The F axis lies in the plane determined by V and  $e_s$ . The positive F axis is chosen so that the projection of the positive V axis onto the F axis is negative (if the V and  $e_s$  axis coincide, then F and S are taken to be coincident). G lies in the SE plane. Fig III-2 shows the relationship between these systems in terms of the solar elevation  $E_s$  and the solar azimuth  $A_s$ . The alternate azimuth  $A'_s = \pi - A_s$  is also used on occasion. The transition matrix between the two systems is given by:

$$[p]_{FGe_s} = \begin{bmatrix} \sin E_s \cos A_s & \sin E_s \sin A_s & -\cos E_s \\ -\sin A_s & \cos A_s & 0 \\ \cos E_s \cos A_s & \cos E_s \sin A_s & \sin E_s \end{bmatrix} [p]_{SEV} \quad (\text{III-2})$$

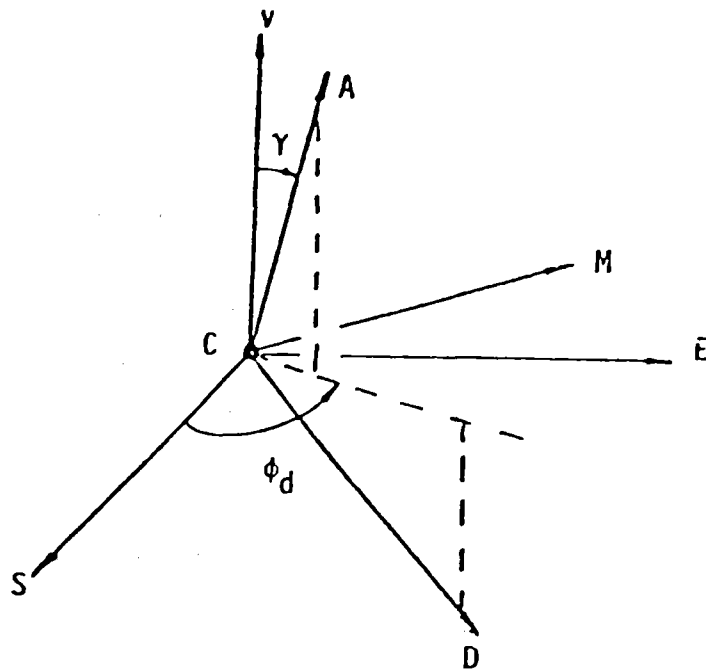


Figure III-1 The Relationship Between the SEV and DMA Coordinate Systems

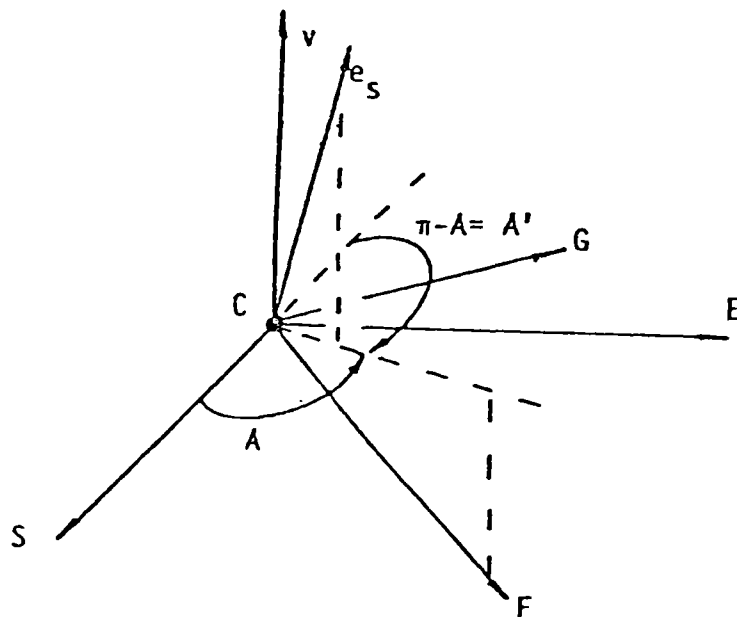


Figure III-2 The Relationship Between the SEV and  $FGe_s$  Coordinate Systems

### Receiver Location and Orientation

In order to locate a field point  $Q$  on the surface of the receiver and determine the limits  $\beta_{\min}(\omega)$  and  $\beta_{\max}(\omega)$ , it is necessary to discuss the alignment of the receiver. An  $x_R y_R z_R$  coordinate system is fixed in the receiver, and locations on the surface of the receiver are determined by  $z_R$  and an azimuth  $\phi_R$ , measured about the  $z_R$  axis, positive from  $x_R$  toward  $y_R$ . The azimuth  $\phi_R = 0$  locates the  $x_R$  axis and, for a perfectly aligned receiver,  $x_R$  is chosen to coincide with the  $F$  axis of the  $FGe_s$  coordinate system and the  $z_R$  axis coincides with the  $e_s$  axis direction. For a perfectly aligned receiver, the receiver surface generator at  $\phi_R = 0$  is the one closest to the  $-V$  direction, the negative vertical, so that  $\phi_R = 0$  denotes the bottom (or lowest) side of the receiver. This is only true for perfectly aligned receivers.

Receiver misalignment is described by the rotation angles  $\Delta\phi$  and  $\Delta\psi$ . The rotation is described by a rotation through an angle  $\Delta\phi$  about the  $e_s$  axis, followed by a rotation through an angle  $\Delta\psi$  about the new  $y_R$  axis. The relationship between the  $FGe_s$  and  $x_R y_R z_R$  coordinate systems is shown in Fig. III-3. The transition matrix between the two systems is given by:

$$[p]_{x_R y_R z_R} = \begin{bmatrix} \cos\Delta\psi \cos\Delta\phi & \cos\Delta\psi \sin\Delta\phi & -\sin\Delta\psi \\ -\sin\Delta\phi & \cos\Delta\phi & 0 \\ \sin\Delta\psi \cos\Delta\phi & \sin\Delta\psi \sin\Delta\phi & \cos\Delta\psi \end{bmatrix} [p]_{FGe_s} \quad (\text{III-3})$$

The coordinates of a point  $Q$  on the receiver can be found in the sun tracking coordinate system by application of the above transition matrices. In order to relate these coordinates to the local  $xyz$  coordinate system, it is convenient to introduce two additional parameters  $\phi_0$  and  $\psi_0$ . The angle  $\phi_0$  is the azimuth of  $\vec{q}$  (the vector locating  $Q$  from  $C$ ) measured positive from  $F$  toward  $G$ . The angle  $\psi_0$  is the angle between  $\vec{q}$  and the negative  $e_s$  axis. The relationship between the  $xyz$  and  $FGe_s$  coordinate

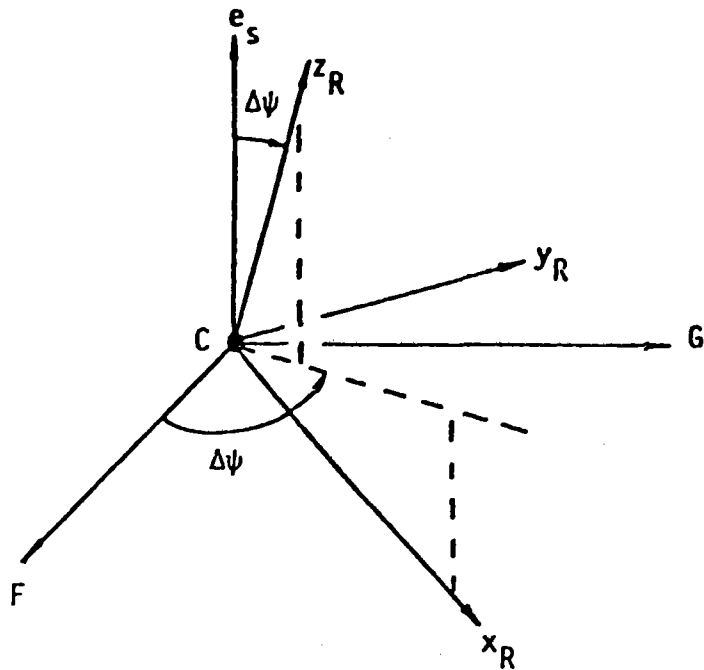


Figure III-3 The Relationship Between the  $FGe_s$  and  $x_R y_R z_R$  coordinate systems

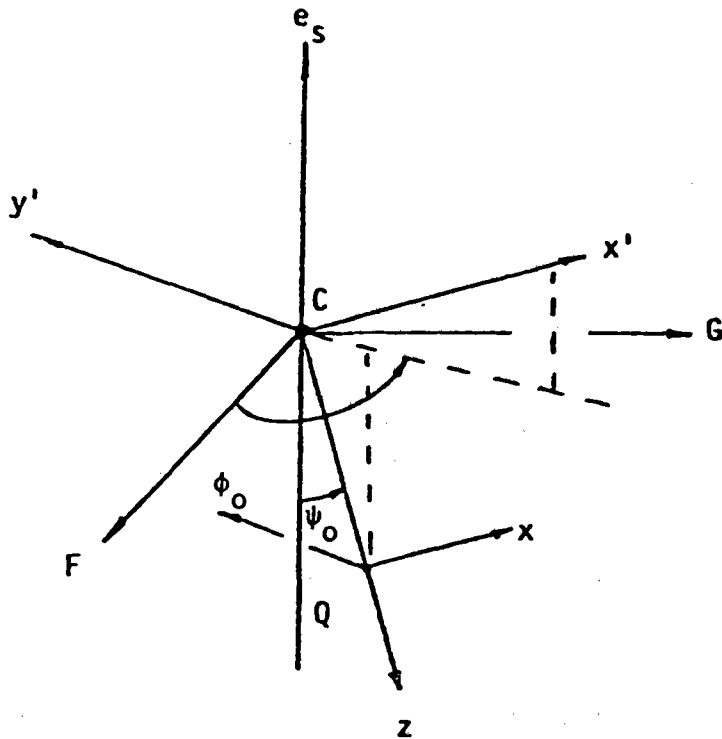


Figure III-4 The Relationship Between the  $FGe_s$  and X-Y-Z coordinate systems

coordinate systems is shown in Fig. III-4. The transition matrix between the two systems is given by

$$[p]_{xyz} = \begin{bmatrix} \cos\psi_0 \cos\phi_0 & \cos\psi_0 \sin\phi_0 & \sin\psi_0 \\ \sin\phi_0 & -\cos\phi_0 & 0 \\ \sin\psi_0 \cos\phi_0 & \sin\psi_0 \sin\phi_0 & -\cos\psi_0 \end{bmatrix} [p]_{FGes} \quad (\text{III-4})$$

### Location of Field Point in the Sun Tracking System .

It is useful to obtain expressions for  $\psi_0$  and  $\phi_0$  in terms of the azimuth,  $\phi_R$ , of the field point Q and the misalignment parameters  $\Delta\psi$  and  $\Delta\phi$ . It is simple to write down the components of  $\vec{q}$  in the  $FGe_S$  system and in the  $xyz$  system:

$$[\vec{q}]_{FGe_S} = q(\sin \psi_0 \cos \phi_0, \sin \psi_0 \sin \phi_0, -\cos \psi_0), \quad (III-5)$$

$$[\vec{q}]_{x_R y_R z_R} = q(\sin \psi_R \sin \phi_R, \sin \psi_R \cos \phi_R, -\cos \psi_R).$$

The coordinate transformation between these systems, given by Eq. III-3, may be applied to obtain a second representation of  $\vec{q}$  in the  $FGe_S$  coordinate system and the two may then be compared. One obtains:

$$\psi_0 = \cos^{-1} \{ \cos \psi_R \cos \Delta\psi + \sin \psi_R \cos \phi_R \sin \Delta\psi \}$$

and (III-6)

$$\sin \psi_0 \sin \phi_0 = \sin \psi_R \cos \phi_R \cos \Delta\psi \sin \Delta\phi + \sin \psi_R \sin \phi_R \cos \Delta\phi - \cos \psi_R \sin \Delta\psi \sin \Delta\phi,$$

$$\sin \psi_0 \cos \phi_0 = \sin \psi_R \cos \phi_R \cos \Delta\psi \cos \Delta\phi - \sin \psi_R \sin \phi_R \sin \Delta\phi - \cos \psi_R \sin \Delta\psi \cos \Delta\phi$$

If  $\sin \psi_0 = 0$  in the above formula, then  $\phi_0$  is assigned the value 0. Otherwise,  $\phi_0$  and  $\psi_0$  are uniquely determined by Eqs. III-6.

### Local Coordinates of the Unit Surface Normal .

The components of the unit surface normal,  $\vec{b}$ , in the xyz coordinate system are obtained by manipulations similar to those of the previous section. Writing  $\vec{b} = (B_1, B_2, B_3)$  in the  $x_R y_R z_R$  coordinate system, and using the rotation matrices given by Eq. III-3 and III-4, we find that:

$$\begin{aligned} b_x = & B_1 [\cos \psi_0 \cos \Delta\psi \cos (\phi_0 - \Delta\phi) - \sin \psi_0 \sin \Delta\psi] \\ & + B_2 \cos \Delta\psi \sin (\phi_0 - \Delta\phi) \\ & + B_3 [\cos \psi_0 \sin \Delta\psi \cos (\phi_0 - \Delta\phi) + \sin \psi_0 \cos \Delta\psi], \end{aligned}$$

$$\begin{aligned} b_y = & B_1 \cos \Delta\psi \sin (\phi_0 - \Delta\phi) - B_2 \cos (\phi_0 - \Delta\phi) \\ & + B_3 \sin \Delta\psi \sin (\phi_0 - \Delta\phi), \end{aligned} \quad (\text{III-7})$$

$$\begin{aligned} b_z = & B_1 [\sin \psi_0 \cos \Delta\psi \cos (\phi_0 - \Delta\phi) + \cos \psi_0 \sin \Delta\psi] \\ & + B_2 \sin \Delta\psi \sin (\phi_0 - \Delta\phi) \\ & + B_3 [\sin \psi_0 \sin \Delta\psi \cos (\phi_0 - \Delta\phi) - \cos \psi_0 \cos \Delta\psi]. \end{aligned}$$

In order to obtain expressions for the components of  $\vec{b}$  in the  $x_R y_R z_R$  coordinate system, we use the assumption that the receiver surface is described as a surface of revolution, with the  $z_R$  axis being the axis of symmetry of the receiver. The surface is then described by an expression of the form

$$r = f(z_R), \quad z_R \leq 0,$$

where  $r$  denotes the perpendicular distance from the  $z_R$  axis to the receiver surface. A straightforward calculation then gives the formula

$$\vec{b}_{[x_R y_R z_R]} = (\cos \phi_R \cos \zeta, \sin \phi_R \cos \zeta, -\sin \zeta), \quad (\text{III-8})$$

where,

$$\tan \xi = f'(z_R) \quad \xi \in (-\pi/2, \pi/2),$$

and  $\phi_R$  denotes the azimuthal angle of the field point in the receiver coordinate system.

#### 4. SOLUTION OF THE STRUCTURE RELATIONS

##### Introduction

The structure relations arise in determining the  $\beta$ -limits on the solar concentration integrals. The structure relations were derived in Chapter II and are given by Eq. II-8a and II-8b and in combined form by Eq. II-9. They are applied to the integral given by Eq. II-13.

The structure relation has the form

$$\psi = 2n \sin^{-1}(q \sin \beta) - \beta - (n-1)\pi, \quad (\text{IV-1})$$

where  $\beta \in [0, \pi]$ ,  $0 < q \leq 1$ , and  $n$  is a positive integer. Fig. IV-1 through IV-3 illustrate the relationship between  $\psi$ ,  $\beta$ , and  $q$  for  $n = 1, 2$ , and  $4$ . The curves show  $\psi$  plotted against  $\beta$  for various values of  $q$ .

In the application of the structure relation IV-1,  $q$ ,  $n$ , and two values of  $\psi$ ,  $\psi_{\pm}$ , are given, where  $-\pi < \psi_{-} < \psi_{+} < \pi$ . The problem is to find  $\beta$ -intervals on  $[0, \pi]$  such that the inequality

$$\psi_{-} < \psi(\beta) < \psi_{+} \quad (\text{IV-2})$$

is satisfied. A case where two  $\beta$ -intervals exist is illustrated in Fig. IV-4. The number of solution intervals depends upon the values of  $\psi_{-}$  and  $\psi_{+}$ . It should be clear from Fig. IV-4 that the possibility exists for no solution to Eq. IV-2, one solution, or two solutions. The remainder of this chapter is devoted to describing a method for finding these limits numerically.

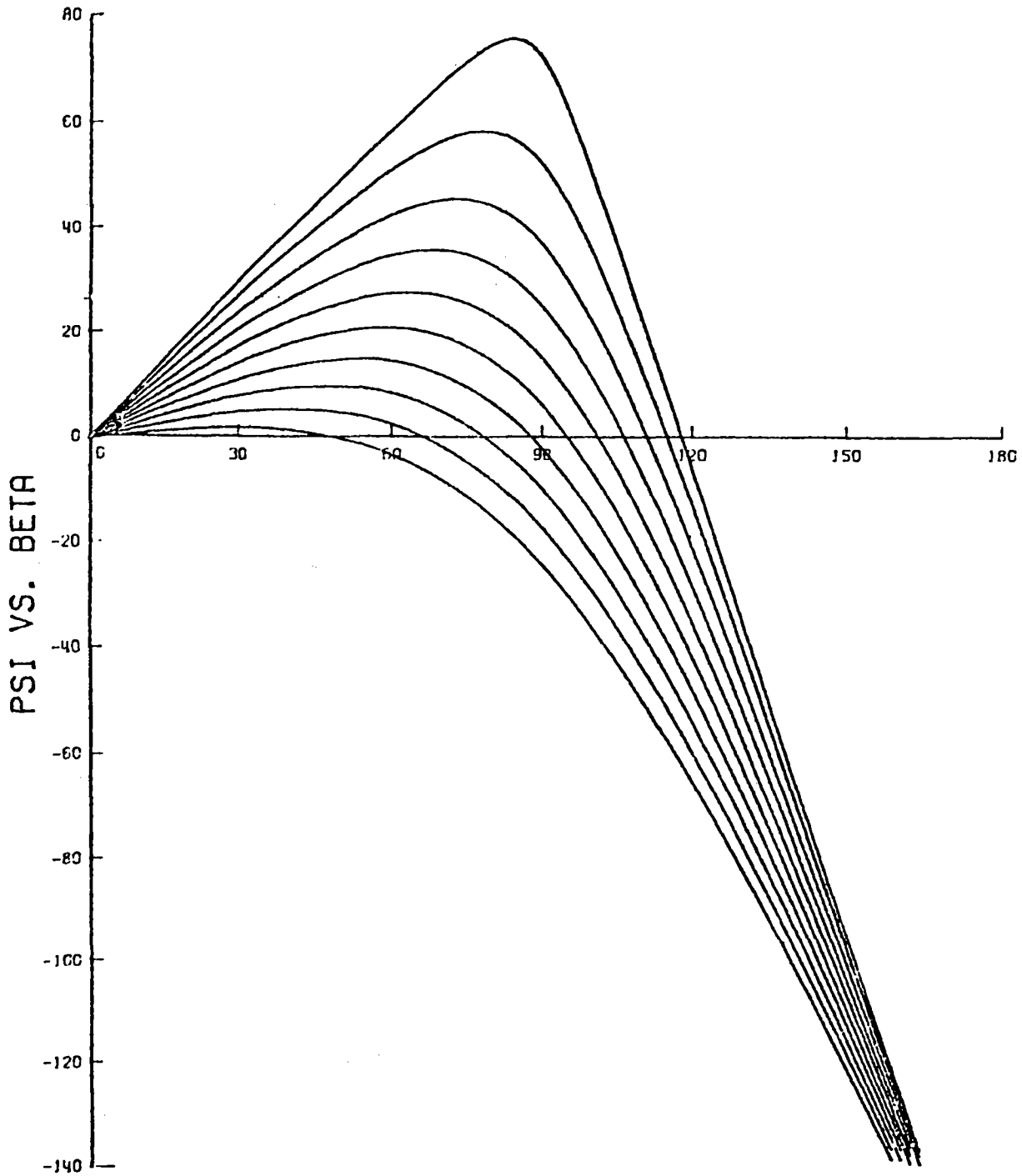


Figure IV-1  $\Psi$ - $\beta$  curve for  $n=1$  ( $q=0.55-0.95, 0.99$ )

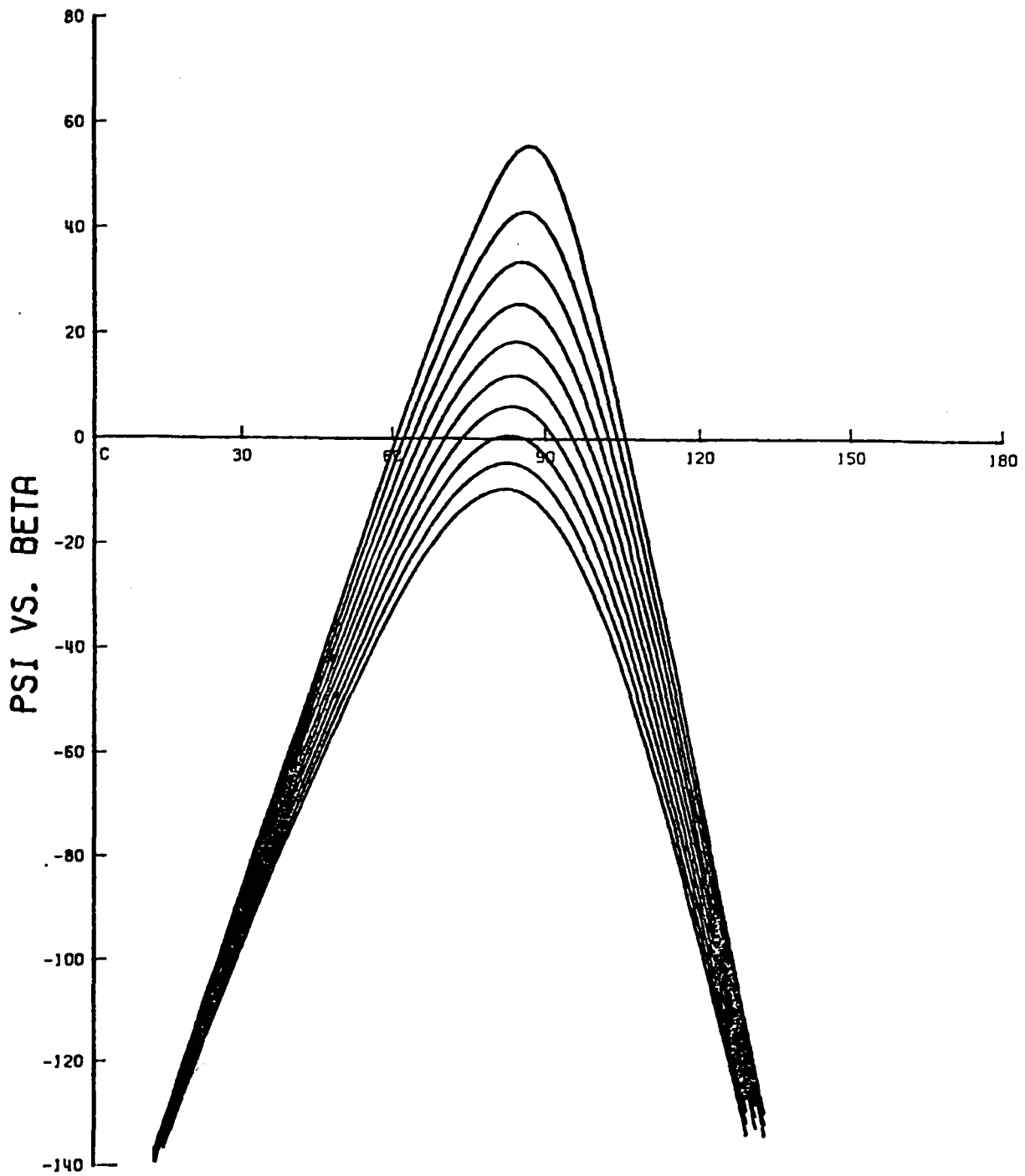


Figure IV-2  $\Psi$ - $\beta$  curve for  $n=2$  ( $q=0.90-0.99$ )

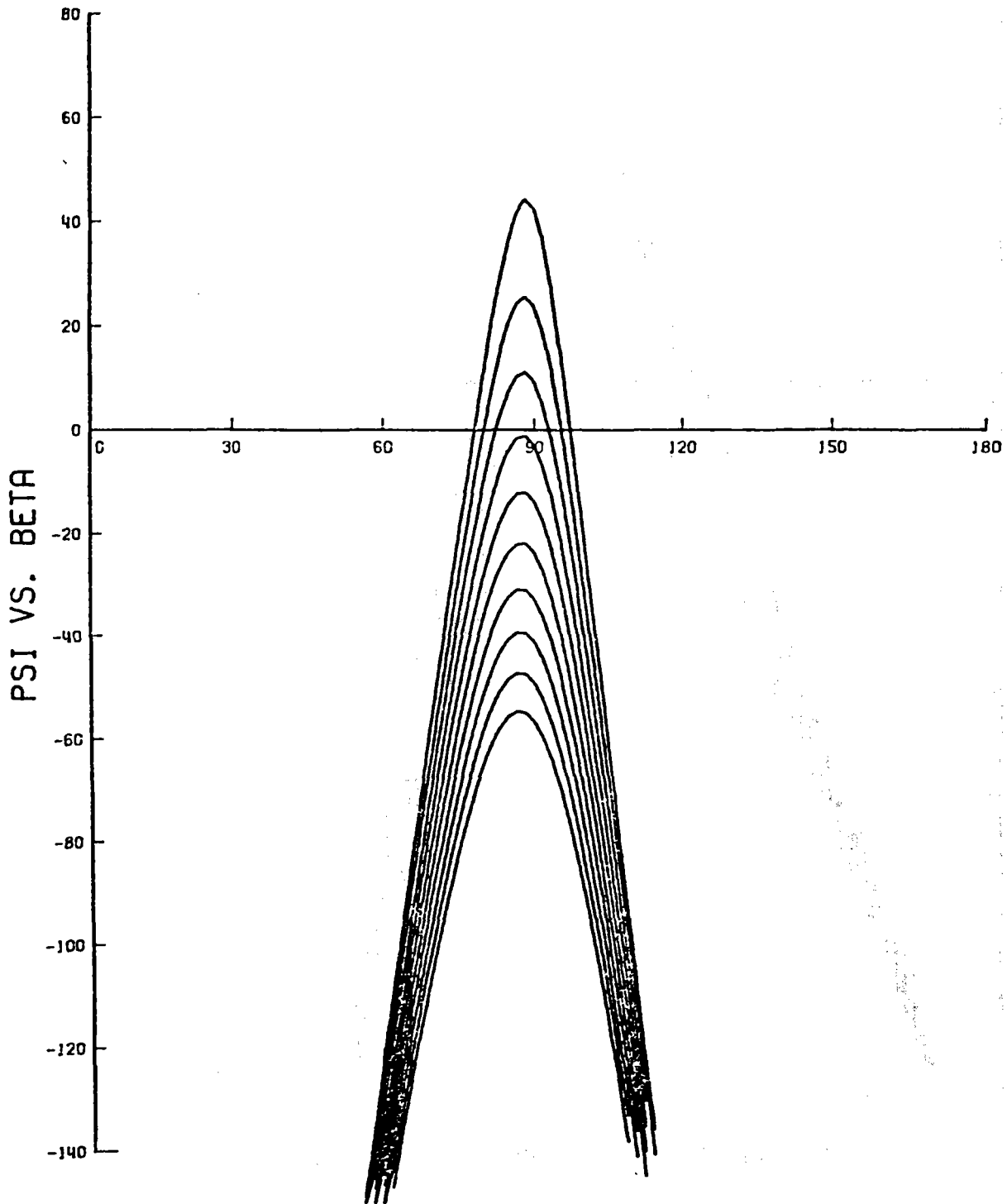


Figure IV-3  $\Psi$ - $\beta$  curve for  $n=4$  ( $q=0.95-0.995$ )

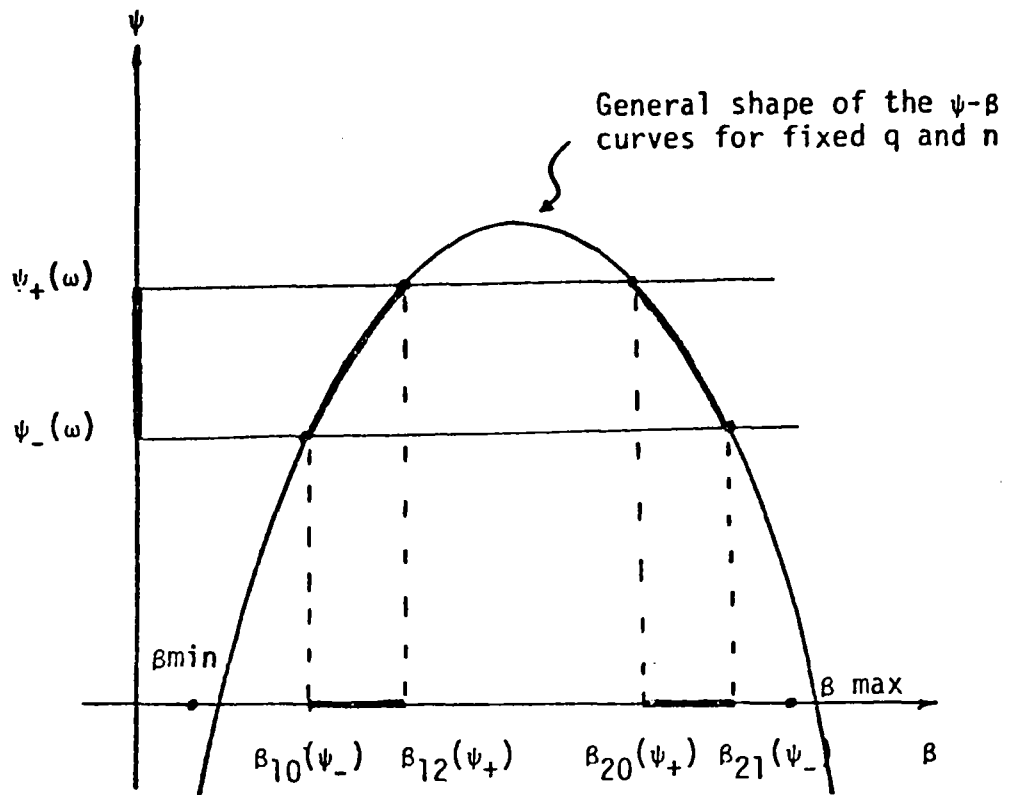


Figure IV-4 The Ranges in  $\beta_i$  Determined by Range in  $\psi$

### Properties of the $\psi$ vs $\beta$ curve

In this section we show analytically that the graphs shown in Figs. IV-1 through IV-3 are representative of the  $\psi$  vs  $\beta$  curves given by Eq. IV-1. Differentiation of Eq. IV-1 with respect to  $\beta$  yields

$$\frac{d\psi}{d\beta} = \frac{2nq\cos\psi}{\sqrt{1-q^2\sin^2\beta}} - 1. \quad (\text{IV-3})$$

We note that at  $\beta = 0$ ,  $d\psi/d\beta = 2nq - 1$ , and hence is positive provided  $q > 1/2n$ , while  $d\psi/d\beta < 0$  for  $\beta > \pi/2$ . Thus, for  $q > 1/2n$ ,  $\psi$  must attain a maximum on the interval  $[0, \pi/2]$ . Moreover,  $d\psi/d\beta$  vanishes only once on the interval  $[0, \pi/2]$  and hence  $\psi(\beta)$  has exactly one maximum and no minimum on this interval. The value of  $\beta$  where this maximum occurs will be denoted by  $\beta_{\text{peak}}$  and is given by the formula

$$\beta_{\text{peak}} = \sin^{-1} \left[ \frac{4n^2q^2 - 1}{(4n^2 - 1)q^2} \right]^{1/2} \quad (\text{IV-4})$$

where  $q$  must satisfy  $1/2n \leq q \leq 1$ . The corresponding maximum value of  $\psi$  is denoted by  $\psi_{\text{peak}}$  and is obtained by substituting  $\beta_{\text{peak}}$  into Eq. IV-1.

## The Solution Strategy

In this section we briefly describe the logic involved in solving the inequality given by Eq. IV-2. We assume that  $\psi_-$  and  $\psi_+$  are given and that  $\psi_{\text{peak}}$  has been calculated from Eq. IV-4. Reference to Fig. IV-4 will be helpful in understanding the various cases. The case when  $n = 1$  differs slightly from the case  $n > 1$ , and will be treated separately (compare Fig. IV-1 and Fig. IV-2).

### 1. Solutions for $n = 1$ .

- a. If  $\psi_- \geq \psi_{\text{peak}}$ , then no solution interval exists.
- b. If  $0 \leq \psi_- < \psi_{\text{peak}} \leq \psi_+$ , then a solution interval of the form  $[\beta_L, \beta_U]$  exists, where  $\beta_L$  and  $\beta_U$  are the two solutions to the transcendental equation

$$2\sin^{-1}(q\sin\beta) - \beta = \psi_- . \quad (\text{IV-5})$$

- c. If  $\psi_- \leq 0 < \psi_{\text{peak}} \leq \psi_+$ , then the solution interval has the form  $[0, \beta_U]$ , where  $\beta_U$  is the positive solution to Eq. IV-5.
- d. If  $0 \leq \psi_- < \psi_+ < \psi_{\text{peak}}$ , then two solution intervals exist of the form  $[\beta_{L1}, \beta_{U1}]$ ,  $[\beta_{L2}, \beta_{U2}]$ , where  $\beta_{L1}$  and  $\beta_{U1}$  are the smaller and larger of the solutions to

$$2\sin^{-1}(q\sin\beta) - \beta = \psi_- \quad (\text{IV-6})$$

and  $\beta_{L2}$  and  $\beta_{U2}$  are the smaller and larger of the solutions to

$$2\sin^{-1}(q\sin\beta) - \beta = \psi_+ . \quad (\text{IV-7})$$

- e. If  $\psi_- < 0 < \psi_+ < \psi_{\text{peak}}$ , two solution intervals exist of the form  $[0, \beta_{U1}]$  and  $[\beta_{L2}, \beta_{U2}]$ .  $\beta_{U2}$  is obtained as the positive solution to Eq. IV-6, while  $\beta_{U1}$  and  $\beta_{L2}$  are the smaller and larger solutions to Eq. IV-7.

- f. If  $\psi_- < \psi_+ < 0$ , then a single solution interval exists of the form  $[\beta_L, \beta_U]$ , where  $\beta_L$  satisfies

$$2\sin^{-1}(q\sin\beta) - \beta = \psi_+ \quad (\text{IV-8})$$

and  $\beta_U$  satisfies

$$2\sin^{-1}(q\sin\beta) - \beta = \psi_- . \quad (\text{IV-9})$$

2. Solutions for  $n > 1$ .

- a. If  $\psi_- \geq \psi_{\text{peak}}$ , then no solution interval exists.  
 b. If  $\psi_- < \psi_{\text{peak}} \leq \psi_+$ , then a solution interval of the form  $[\beta_L, \beta_U]$  exists, where  $\beta_L$  and  $\beta_U$  are the smaller and larger solutions to

$$2n\sin^{-1}(q\sin\beta) - \beta - (n-1)\pi = \psi_- . \quad (\text{IV-10})$$

- c. If  $\psi_- < \psi_+ < \psi_{\text{peak}}$ , then two solution intervals exist of the form  $[\beta_{L1}, \beta_{U1}]$  and  $[\beta_{L2}, \beta_{U2}]$ .  $\beta_{L1}$  and  $\beta_{U2}$  are the smaller and larger of the two solutions to the equation

$$2n\sin^{-1}(q\sin\beta) - \beta - (n-1)\pi = \psi_- \quad (\text{IV-11})$$

while  $\beta_{U2}$  and  $\beta_{L1}$  are the smaller and larger of the two solutions to

$$2n\sin^{-1}(q\sin\beta) - \beta - (n-1)\pi = \psi_+ . \quad (\text{IV-12})$$

## Numerical solutions of the structure equations

Finding solutions to the structure equation involves solving the transcendental equation

$$2n\sin^{-1}(q\sin\beta) - \beta - (n-1)\pi = \psi, \quad (\text{IV-13})$$

where  $q$ ,  $n$ , and  $\psi$  are given and  $\beta$  is to be determined. This equation is readily solved by Newton's method provided a sufficiently accurate guess is made for the starting value of the iteration procedure.

Because of the nature of the curve described by Eq. IV-13, a parabolic approximation is used. The approximating parabola is defined to have its vertex at  $(\beta_{\text{peak}}, \psi_{\text{peak}})$  and contain the point  $(0, (n-1)\pi)$ . The resulting equation for the parabola is

$$\psi = \psi_{\text{peak}} - T(\beta - \beta_{\text{peak}})^2, \quad (\text{IV-14})$$

where

$$T = [(n-1)\pi + \psi_{\text{peak}}] / \beta_{\text{peak}}^2 \quad (\text{IV-15})$$

The starting values for the iteration for finding the smaller and larger solutions to Eq. IV-14 are then given by

$$\beta = \beta_{\text{peak}} \pm [(\psi - \psi_{\text{peak}}) / T]^{1/2} \quad (\text{IV-16})$$

where the + sign is used for the larger solution and the - sign is used for the smaller solution.

## 5. ROSA PROGRAM STRUCTURE

### Introduction

The ROSA code gives the normalized optical power concentration ratio at user specified points on a receiver surface. The calculated values are normalized to units of number of suns. The code also uses normalized dimensions, with the radius of the spherical segment bowl taken to be unity. Physical and geometrical parameters for the program include the solar inclination and size, position of the receiver, receiver alignment, bowl rim angle, and the reflection coefficient the bowl. The receiver shape must be a surface of revolution and must be described in a subroutine named BOILER. Alternate rim shapes can be introduced by providing a RIM subroutine.

Receiver points are specified in terms of a distance,  $z_R$ , measured along the axis of symmetry of the receiver and an azimuthal angle,  $\phi_R$ , measured about this axis. If the concentration ratio is to be computed for several  $(z_R, \phi_R)$  pairs the computation is most efficient if the outer loop is on the  $\phi_R$  variable. The program requires that loop parameters be input for each of these variables.

The program flow for the ROSA code is given in the next section, together with a short table describing the ROSA subroutines. A complete computer listing is given in Appendix A.

## ROSA Calculation Procedure

The calculation procedure which is used by ROSA can be divided into three segments, an initialization segment, a computational segment and an output segment. The procedure is listed below:

### BEGIN INITIALIZATION SEGMENT

1. Read Input Variables
  - A. Boiler title: ITITLE
  - B. Boiler-sun alignment parameters: DPSID,DPHID
  - C. Sun parameters:  
Sun cone half-angle: SIGMAD  
Sun position parameters: elevation (ED), azimuth (AD)
  - D. Dish parameters:  
Dish half-angle: THTARD  
Dish alignment parameters: GAMMAD,PHID
  - E. Reflection coefficient: REFC
  - F. ISTEPS--number of omega integration steps
  - G. STPHIR,SPPHIR,DPHIRD--initial and final values of the receiver azimuthal angle PHIR, and the amount to be incremented each time in the PHIR-loop.
  - H. NZRR--number of receiver axis subintervals to be used. The data in H. below will occur NZRR times.
  - I. NZZ, ZSTART,ZSTOP--the number of times Z will be incremented in the Q loop, and the initial and final values of Z (this line is read NZRR times).
2. Convert angles from degrees to radians
3. Calculate rim angle constants
4. Calculation rotation matrices
5. Initialization of PHIRD--azimuthal angle, and JSTOP--number of times PHIR loop is to be repeated.
6. Echo print all input values.

BEGIN COMPUTATIONAL SEGMENT

Begin PHIR loop

Begin NZRR loop

Initialize Z loop parameters (Z=ZSTART), NQSTOP (number of times Z loop is repeated), and DZ (the Z increment)

Begin Z loop

CALL BOILER--BOILER subroutine gets Z and PHIR and returns Q, PSIR, and XR,YR,and ZR--the components of the outward normal to the receiver in the XR-YR-ZR coordinate system.

Calculate PSIO and PHIO--the rotation angles between the F-G-ES and the X-Y-Z coordinate systems.

Calculate the components of the unit outward normal to the receiver surface in the X-Y-Z coordinate system

Find OMEGAU and OMEGAL--the omega limits and NOMEGA--the number of omega-intervals.

Begin OMEGA integration loop

CALL INTGRL - This subroutine computes the concentration integral for the given omega-interval.

END omega interval loop

END Z loop

END NZRR loop

BEGIN OUTPUT SEGMENT

Begin Z loop

Print Z

Begin NBOUNCE loop

Print contribution from n-th bounce

Add n-th bounce contribution the total concentration

END NBOUNCE loop

Print total concentration

END Z loop

END PHIRD loop

END PROGRAM

Table 5.1: ROSA SUBROUTINE SUMMARY

<u>Subroutine</u>	<u>Purpose</u>
BLIMIT	Performs the logic for computing the beta integral integration ranges.
BOILER	A user supplied routine for computing distance and angle to a point on a receiver surface and the outward normal to the surface at the point.
INTGRL	Computes the solar concentration integral at a point on the receiver surface.
RIM	An optional user supplied routine for handling special rim shapes.
SOLN	Computes a solution to the structure relation equation by Newton's method.

## 6. OPTICAL CONCENTRATION PROFILES

### Introduction

In previous chapters, we have stressed the dependence of the concentration ratio profiles on several geometrical and physical parameters. This chapter gives a few representative profiles, in order to illustrate the nature of the results which are obtained from the ROSA code.

Only a few parameters will be varied in these profiles. Basically, only the solar inclination, position of the receiver, and receiver alignment are varied. The mirror rim angle is set at  $\theta_R = 60$  degrees. The receiver shape is taken to be a right circular cylinder, of radius 0.0066 (this is the normalized radius of the cylindrical receiver being used in the CSPP.) The cylinder extends from  $Z = 0.5$  to  $Z = 1.0$ . The reflectivity of the mirror is set at 0.88, independent of angle of incidence or wave length. Only power reflected by the mirror is counted, direct radiation on the receiver is ignored. The effective sun size is taken to be  $\sigma = 0.5$  degrees for all reflected rays.

Location of the center of the sun is accomplished by using the inclination angle,  $I$ , of the sun relative to the axis of symmetry of the mirror. The optical concentration profiles depend upon  $I$ , which, in turn, depends upon time, latitude, and the tilt of the solar bowl with respect to the vertical. The tilt of the mirror axis with respect to the vertical is described by the tilt angle,  $\gamma$ , and tilt azimuth  $\phi_d$ . The location of the sun is described in terms of an azimuth,  $A$ , and elevation,  $E$ . These parameters are related to  $I$  by the formula

$$\cos I = [\cos \gamma \sin E + \sin \gamma \cos E \cos (A - \phi_d)]. \quad (\text{VI-1})$$

## Results for $I = 0$

The case of a perfectly aligned receiver when the solar inclination is zero is called the "symmetric case" because the concentration profile is symmetrical about the axis of the receiver. The concentration profile for the symmetric case is shown as a function of  $Z$  in Fig. VI-1. The large peak near the top of the receiver is the paraxial peak resulting from rays at small impact angle,  $\theta$ , tending to focus midway between the mirror surface and its center of curvature. The peak concentration is a sensitive function of  $\sigma$  and tends to infinity as  $\sigma$  tends to zero [5].

There are no multiple bounce contributions in the symmetric case because they are cut off by the 60 degree rim angle. Multiple reflections result from impact angles larger than 60 degrees and the required mirror support is not present for  $I = 0$ .

The legend printed in Fig. VI-1 and in subsequent figures may be translated as follows:

PHIR  $\equiv \phi_R$ , the azimuth for locations on the receiver;

SOLAR ELEVATION = 90 degrees -  $I$

SIGMA  $\equiv \sigma$ , effective sun size

DPSI =  $\Delta\psi$ , the zenith misalignment angle

DPHI =  $\Delta\phi$ , the azimuthal misalignment angle

Concentration profiles are also presented for the case where the receiver is the frustrum of a cone. The angular radius,  $\psi_R$ , of the cone (half the vertex angle) is set equal to the angular radius of the sun, i.e.,  $\psi_R = 0.5$ .

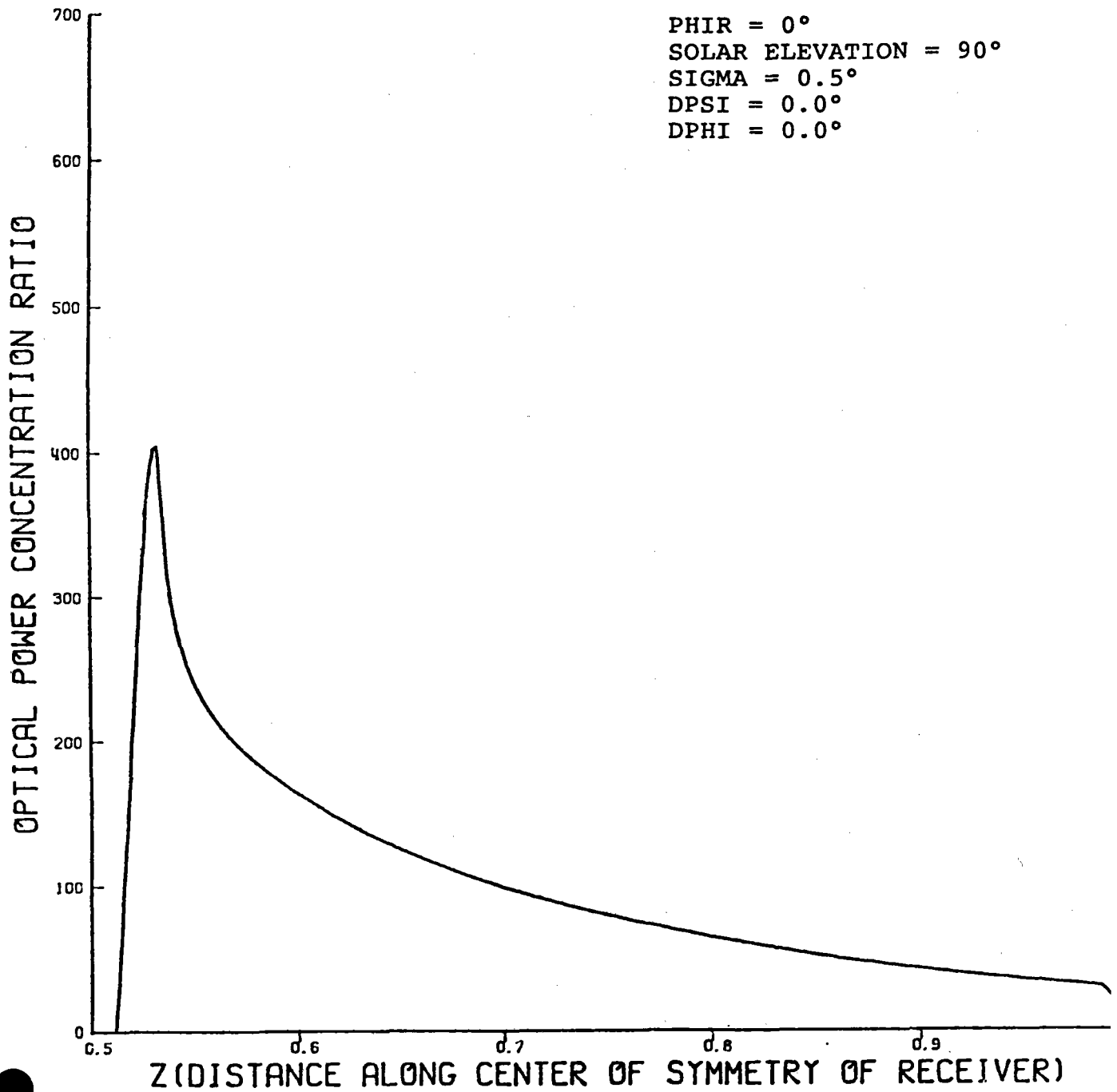


Figure VI - 1a Optical Power Concentration for a Cylindrical Receiver

PHIR = 0°  
SOLAR ELEVATION = 90°  
SIGMA = 0.5°  
DPSI = 0.0°  
DPHI = 0.0°

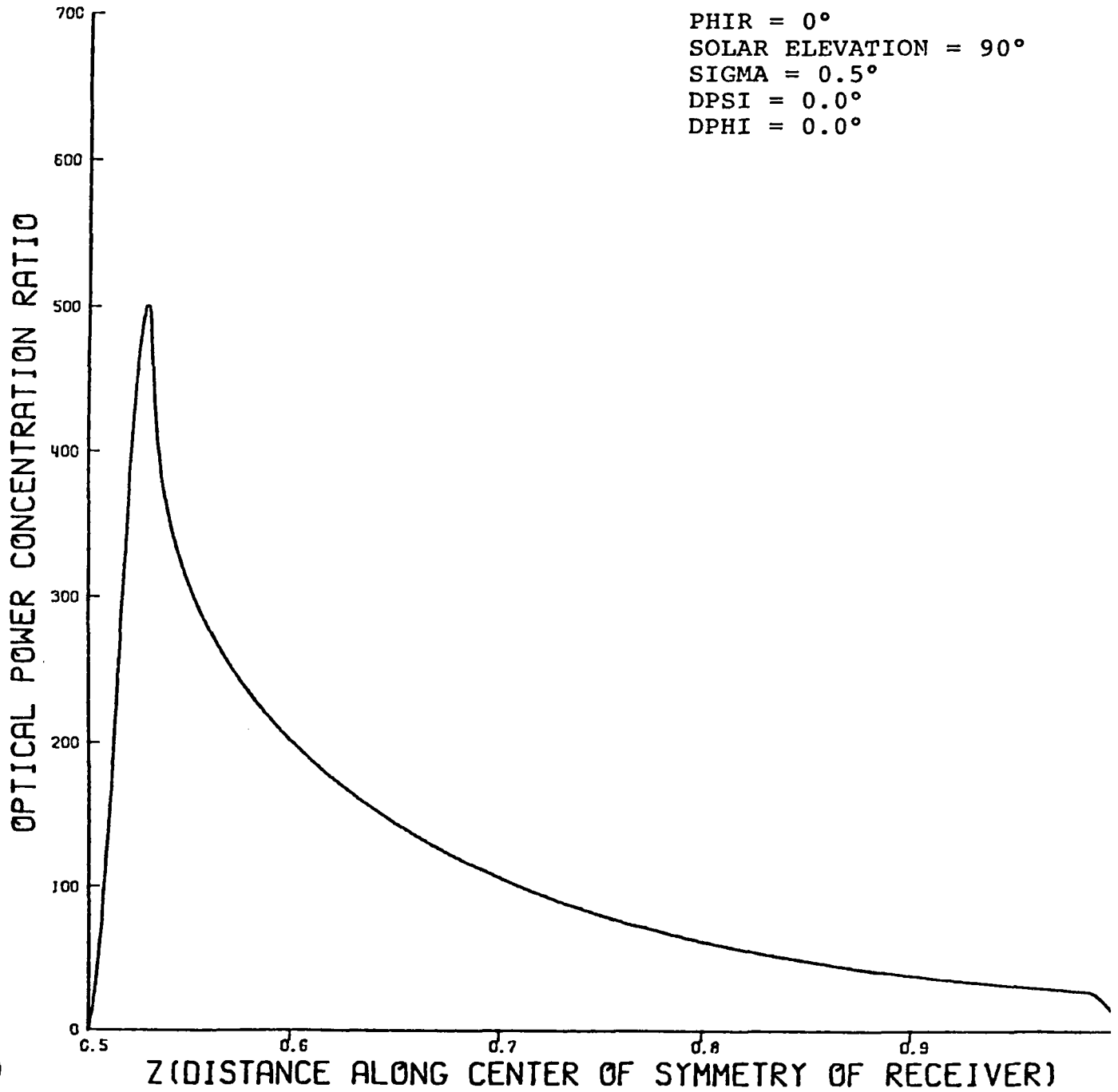


Figure VI - 1b Optical Power Concentration for a Conical Receiver ( $\Psi_R = 0.5^\circ$ )

Concentration profiles on a misaligned receiver for  $I = 0$  and  $\Delta = 0.5$  degrees are shown in Figs. VI-2, 3, and 4. These figures show the profiles along the three slices:

$\phi_R = 0, 90, \text{ and } 180$  degrees, respectively.

#### Results for $I = 15$

Figs. VI-5 through VI-7 illustrate the features of the concentration profile for nonzero inclination angles. Due to loss of symmetry with respect to the aperture rim, there is no azimuthal dependence in the concentration profiles.

For  $I = 15$  degrees the mirror support is 75 degrees at  $\phi_R = 0$ , and peaks due to second and third bounce rays are observed. At  $\phi_R = 180$  degrees, rim cutoff effects occur.

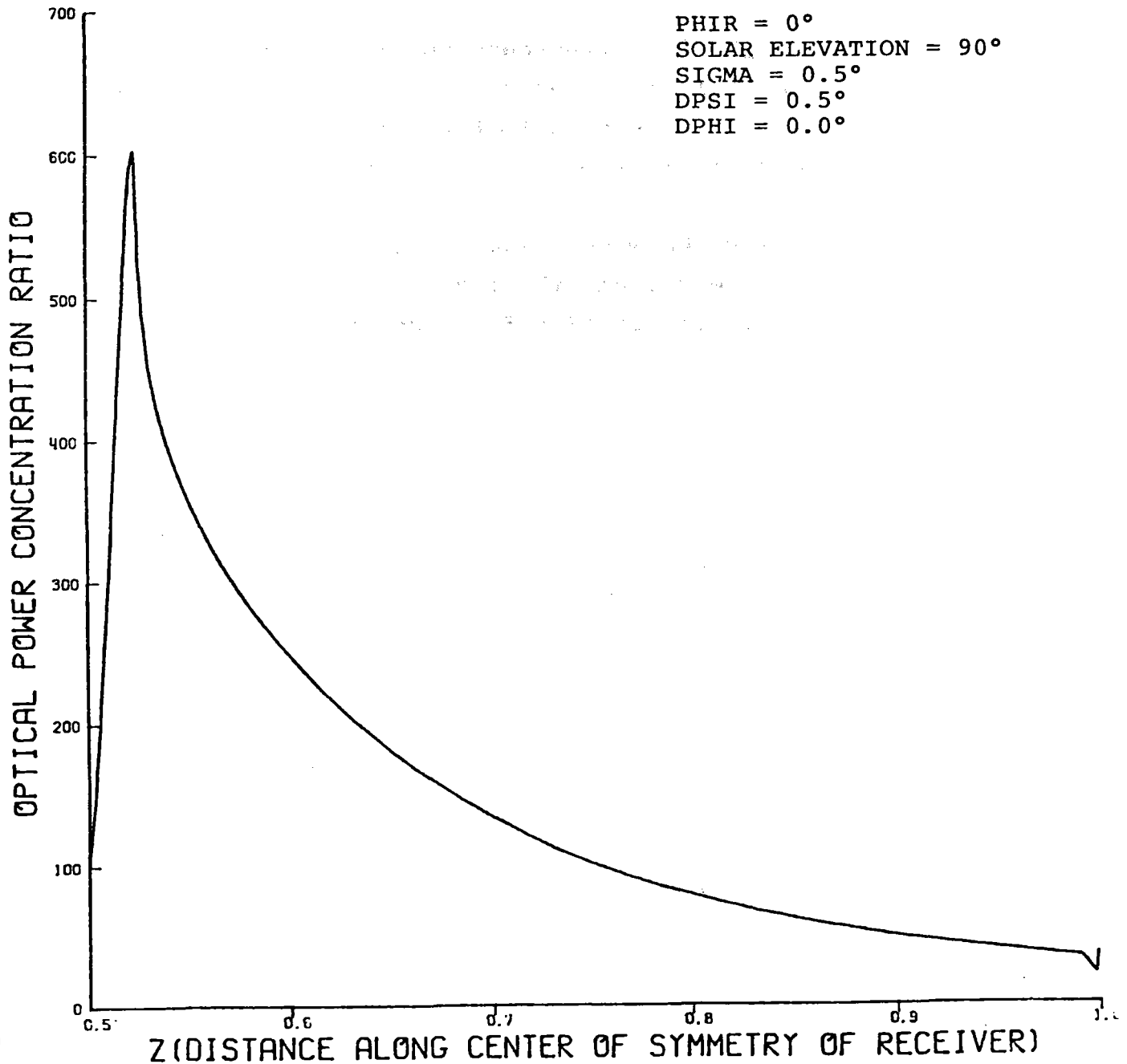


Figure VI - 2a Optical Power Concentration for a Cylindrical Receiver

67-A

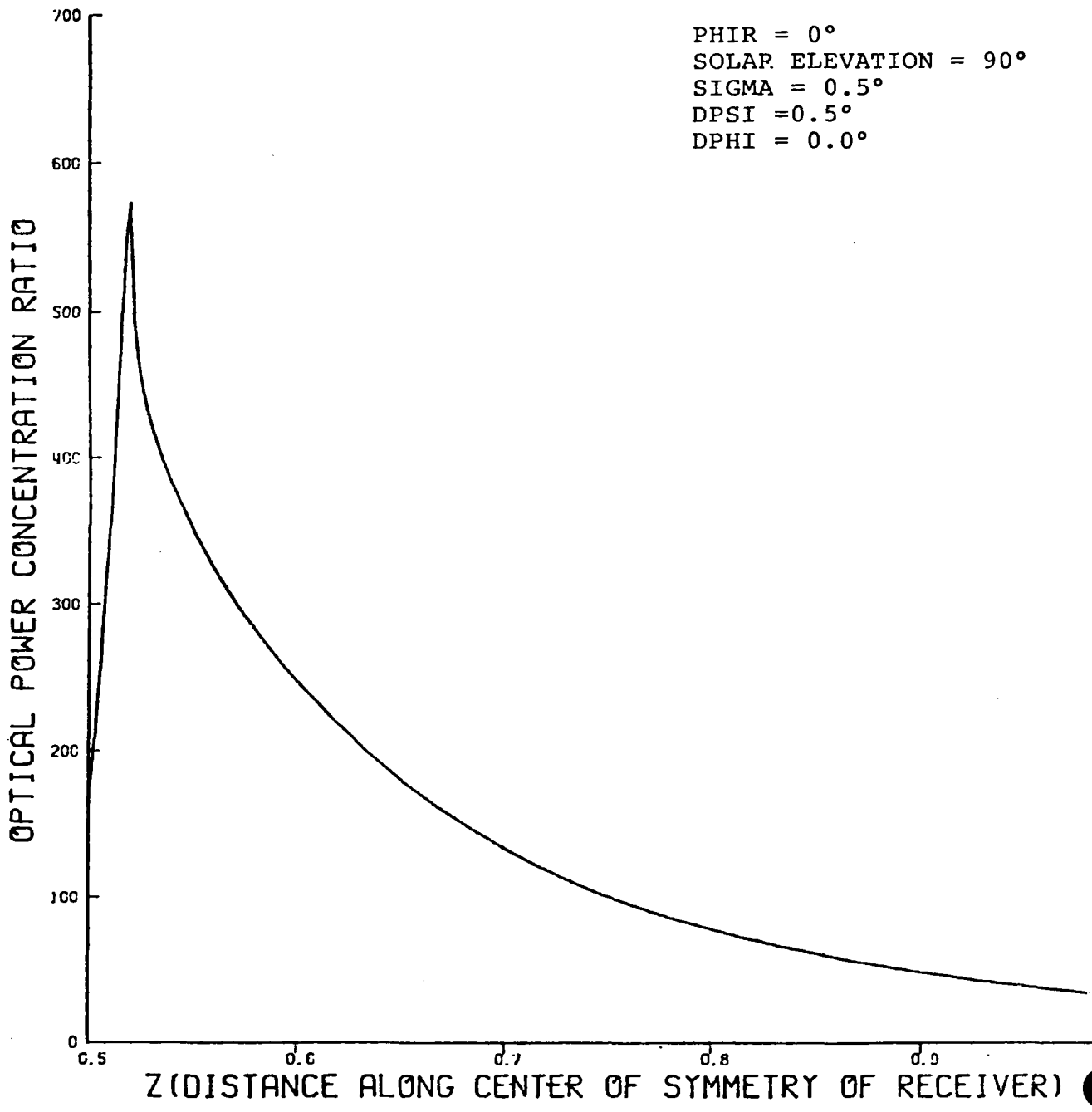


Figure VI - 2b Optical Power Concentration for a Conical Receiver ( $\Psi_R = 0.5^\circ$ )

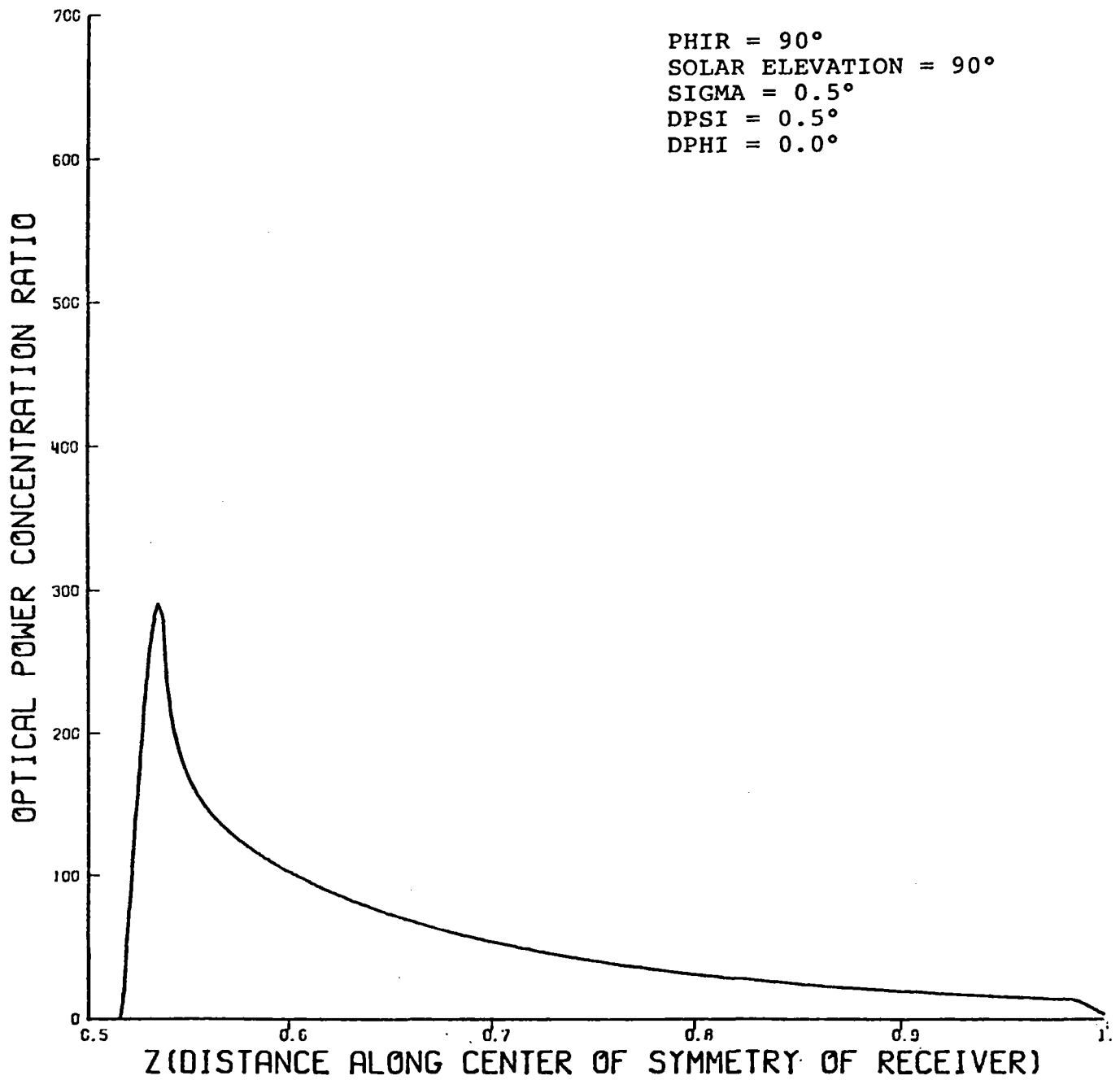


Figure VI -3a Optical Power Concentration for a Cylindrical Receiver

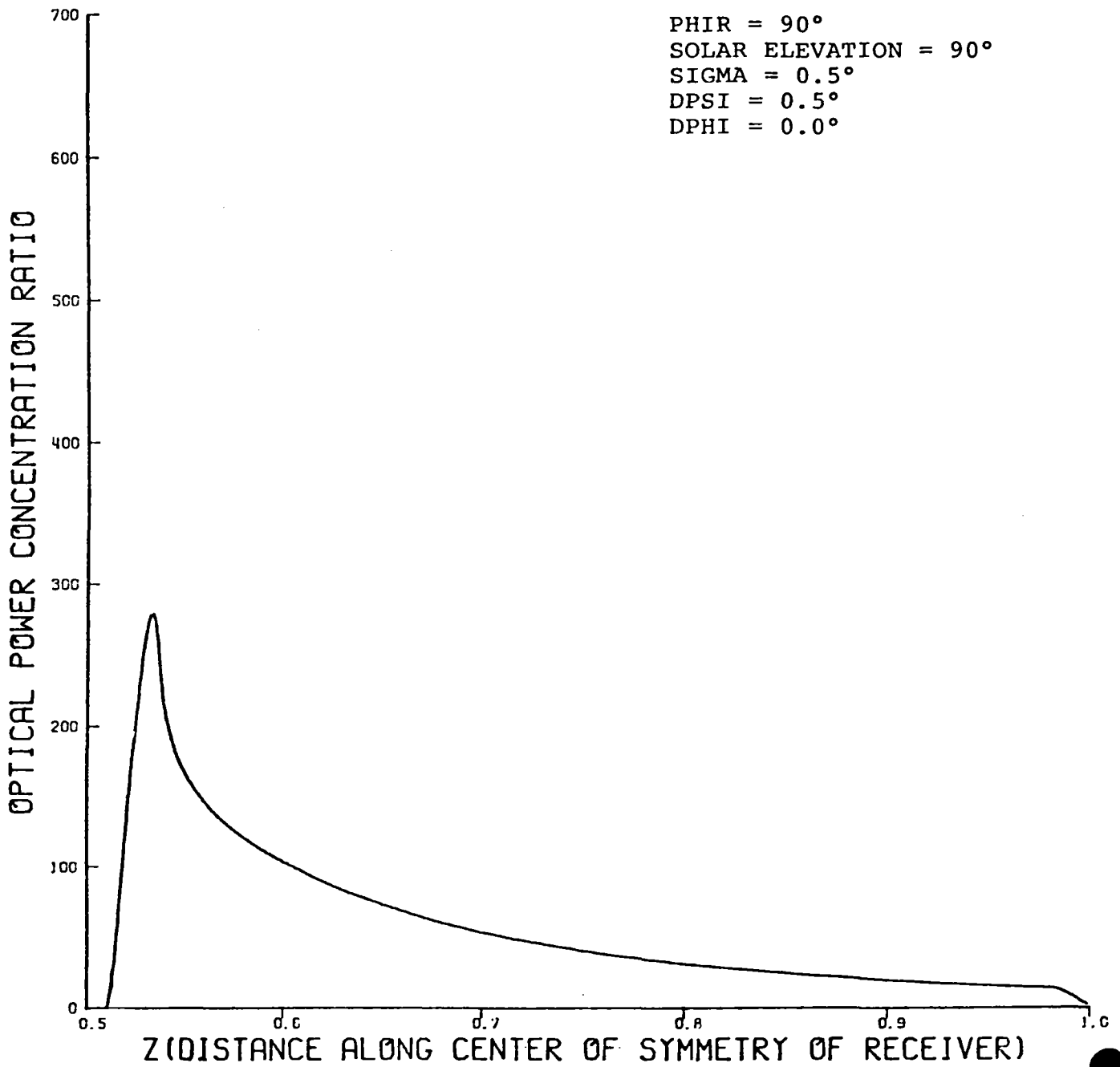


Figure VI - 3b Optical Power Concentration for a Conical Receiver ( $\Psi_R = 0.5^\circ$ )

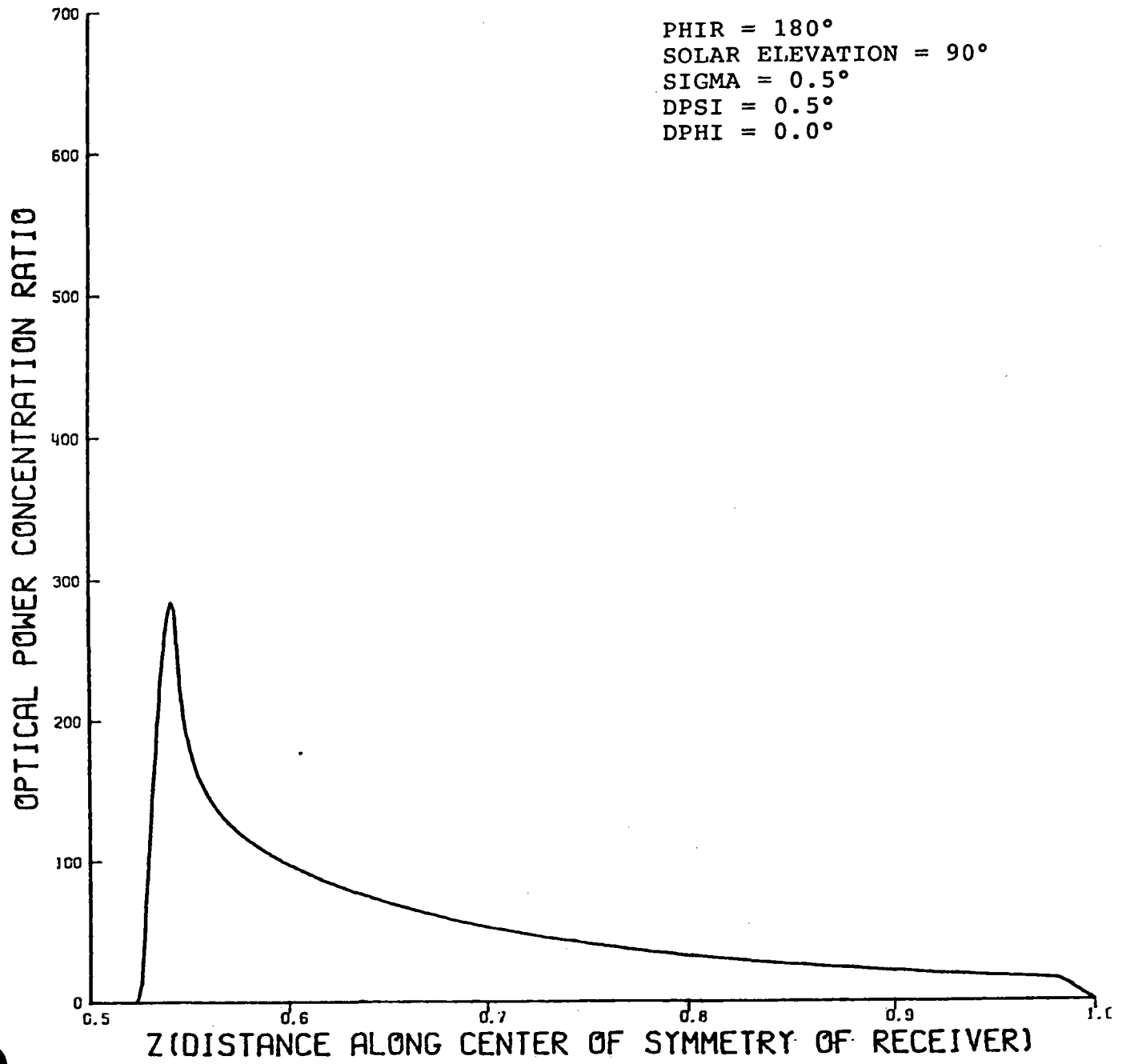


Figure VI - 4a Optical Power Concentration for a Cylindrical Receiver

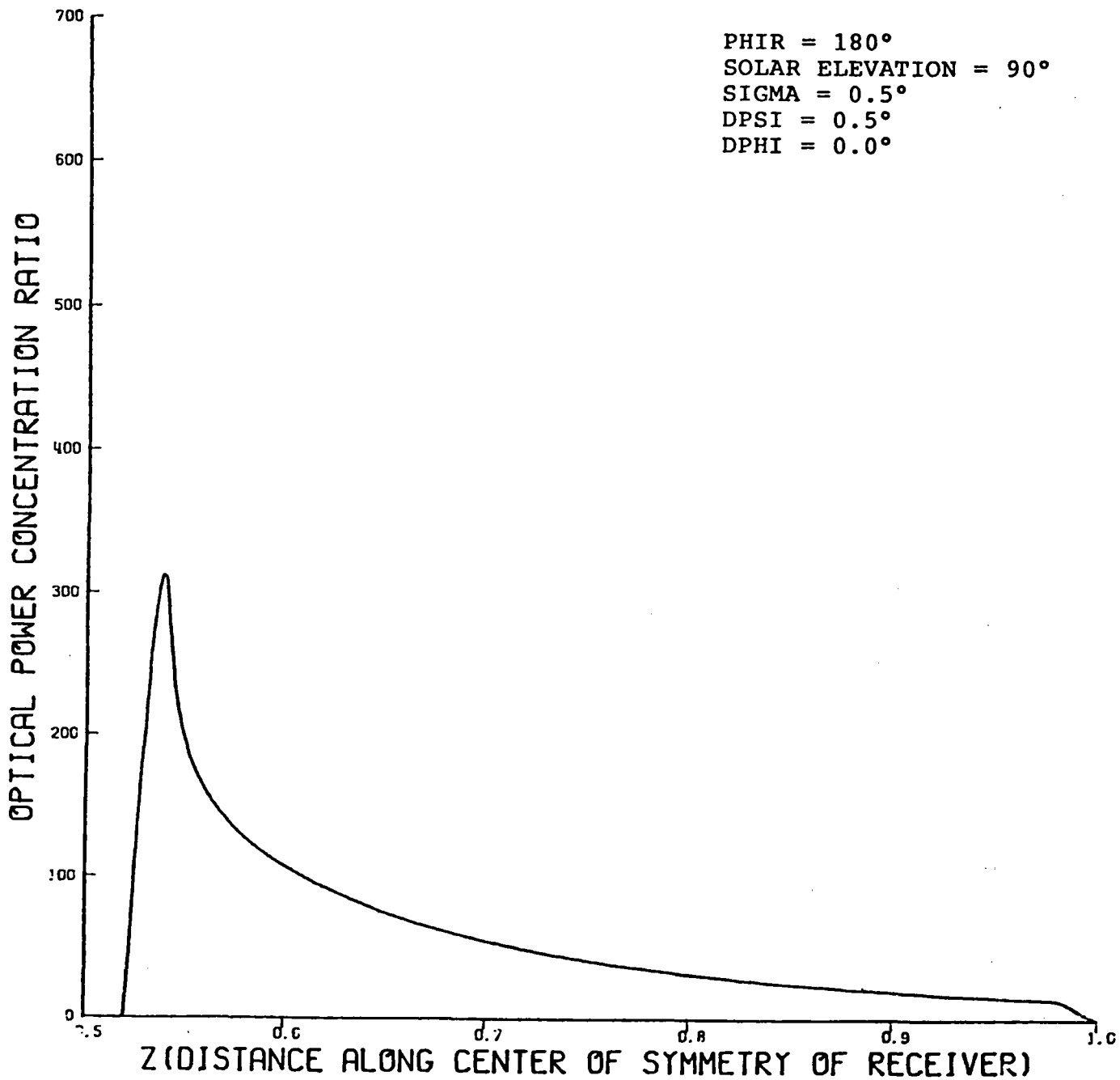


Figure VI - 4b Optical Power Concentration for a Conical Receiver ( $\Psi_R = 0.5^\circ$ )

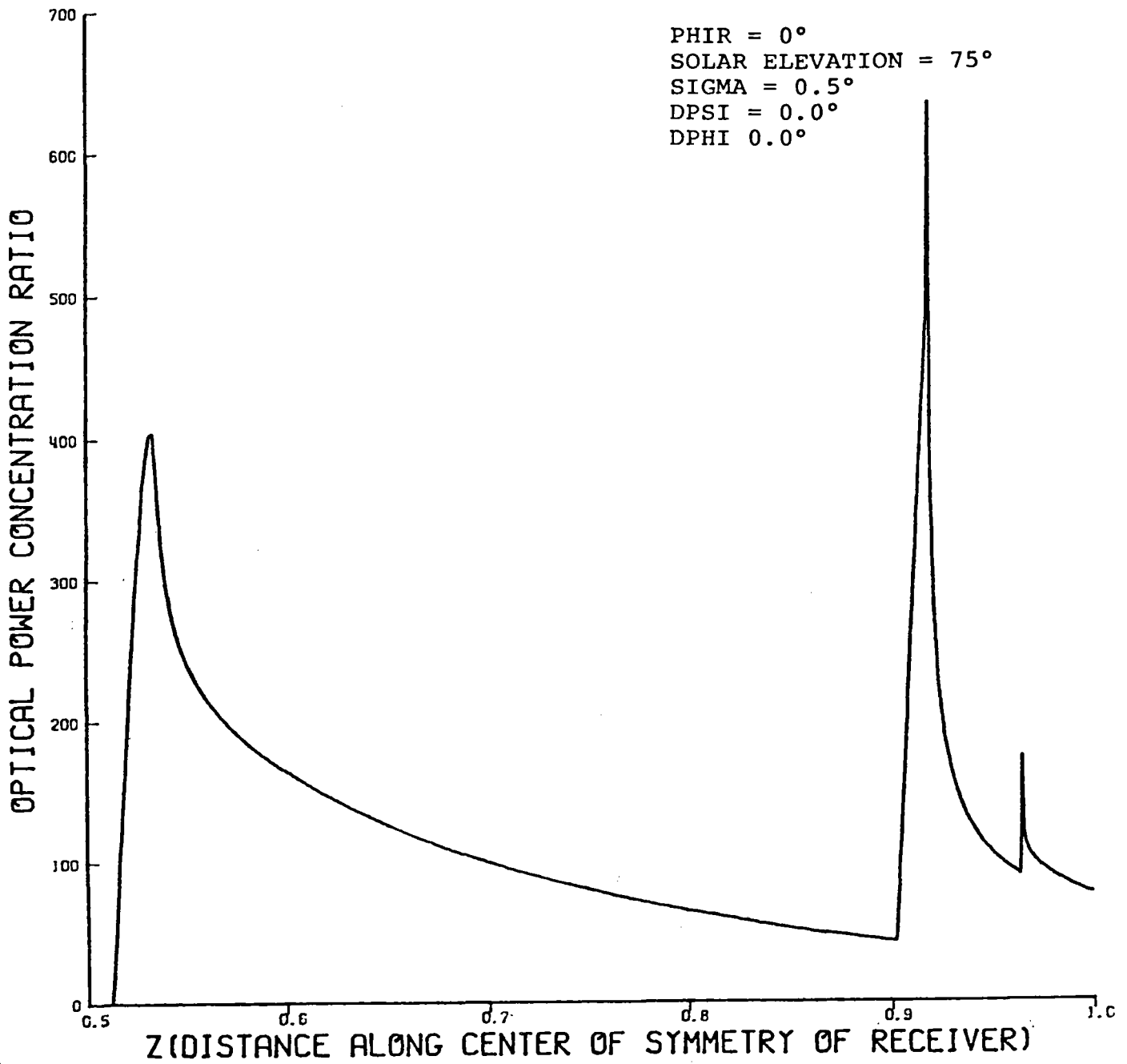


Figure VI - 5a Optical Power Concentration for A Cylindrical Receiver

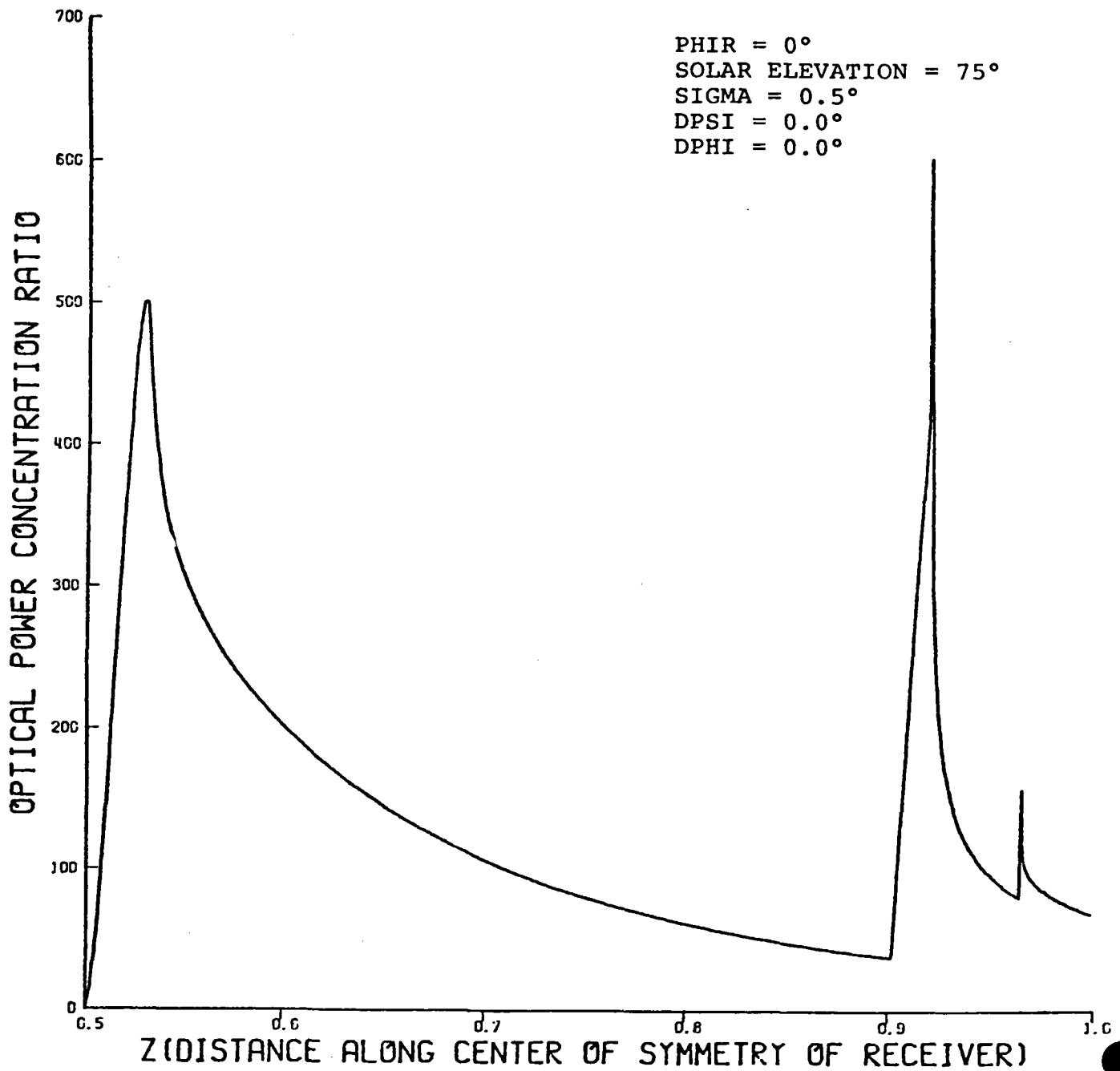


Figure VI - 5b Optical Power Concentration for a Conical Receiver ( $\Psi_R = 0.5^\circ$ )

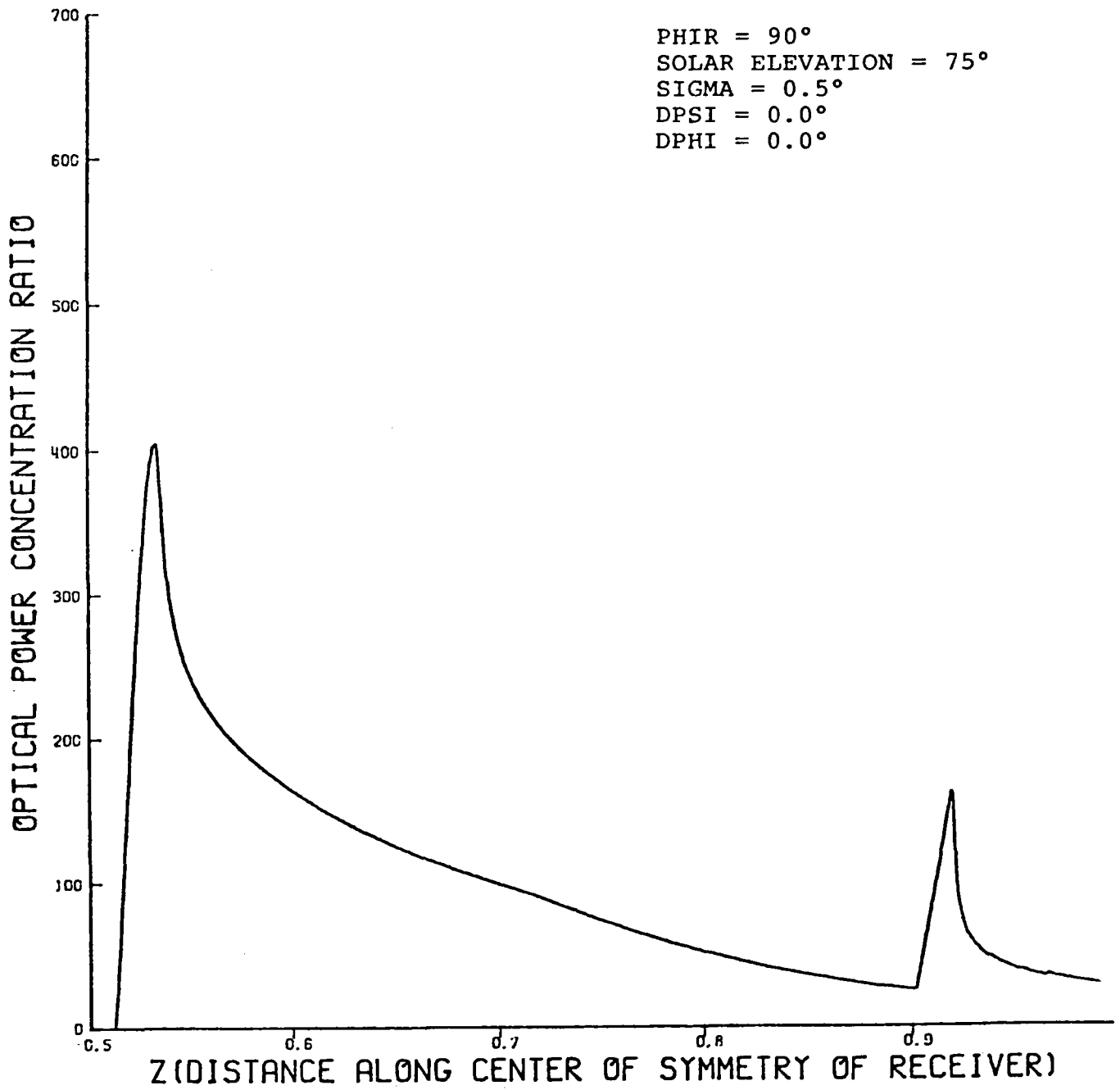


Figure VI - 6a Optical Power Concentration for a Cylindrical Receiver

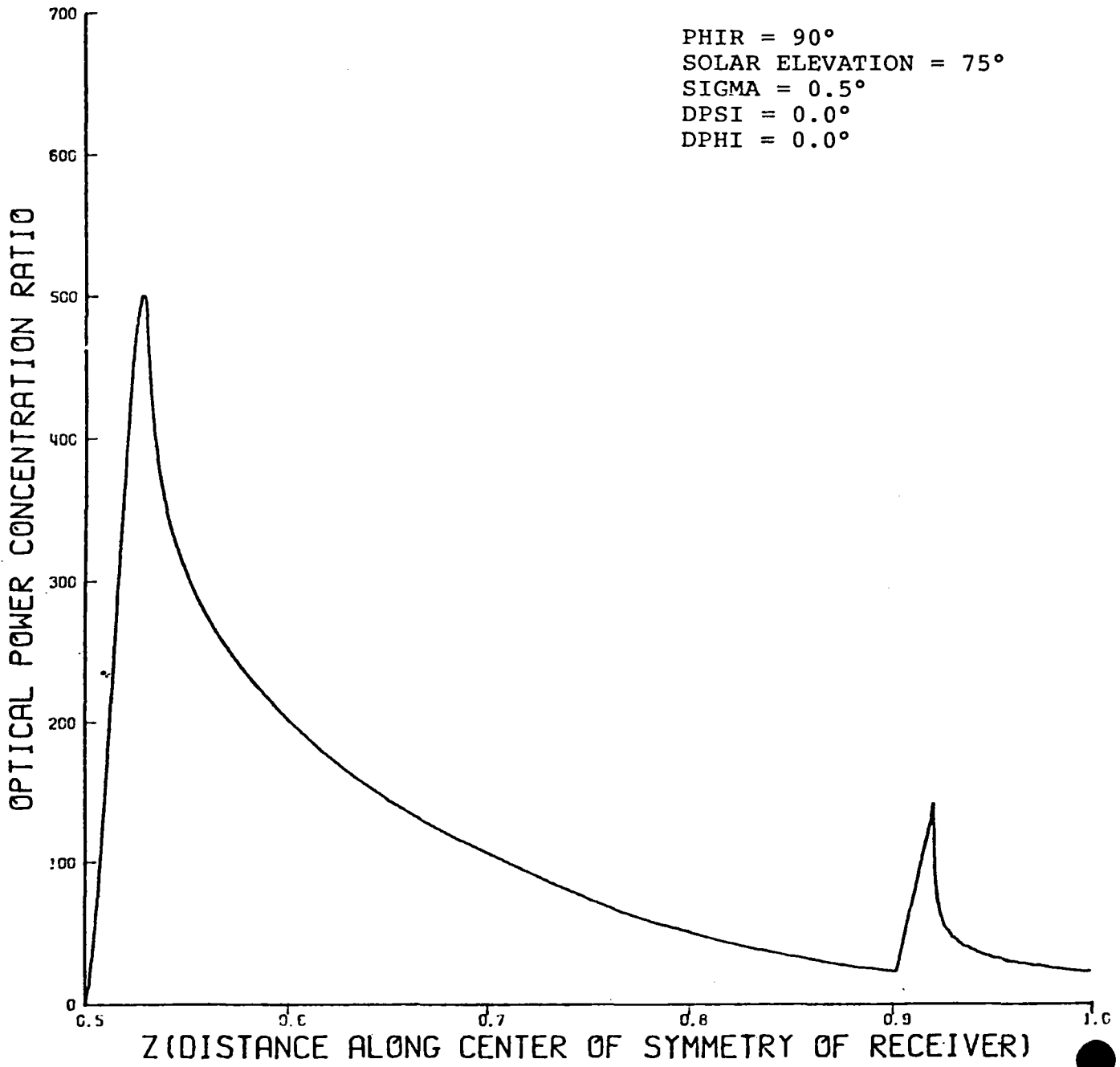


Figure VI - 6b Optical Power Concentration for a Conical Receiver ( $\psi_R = 0.5^\circ$ )

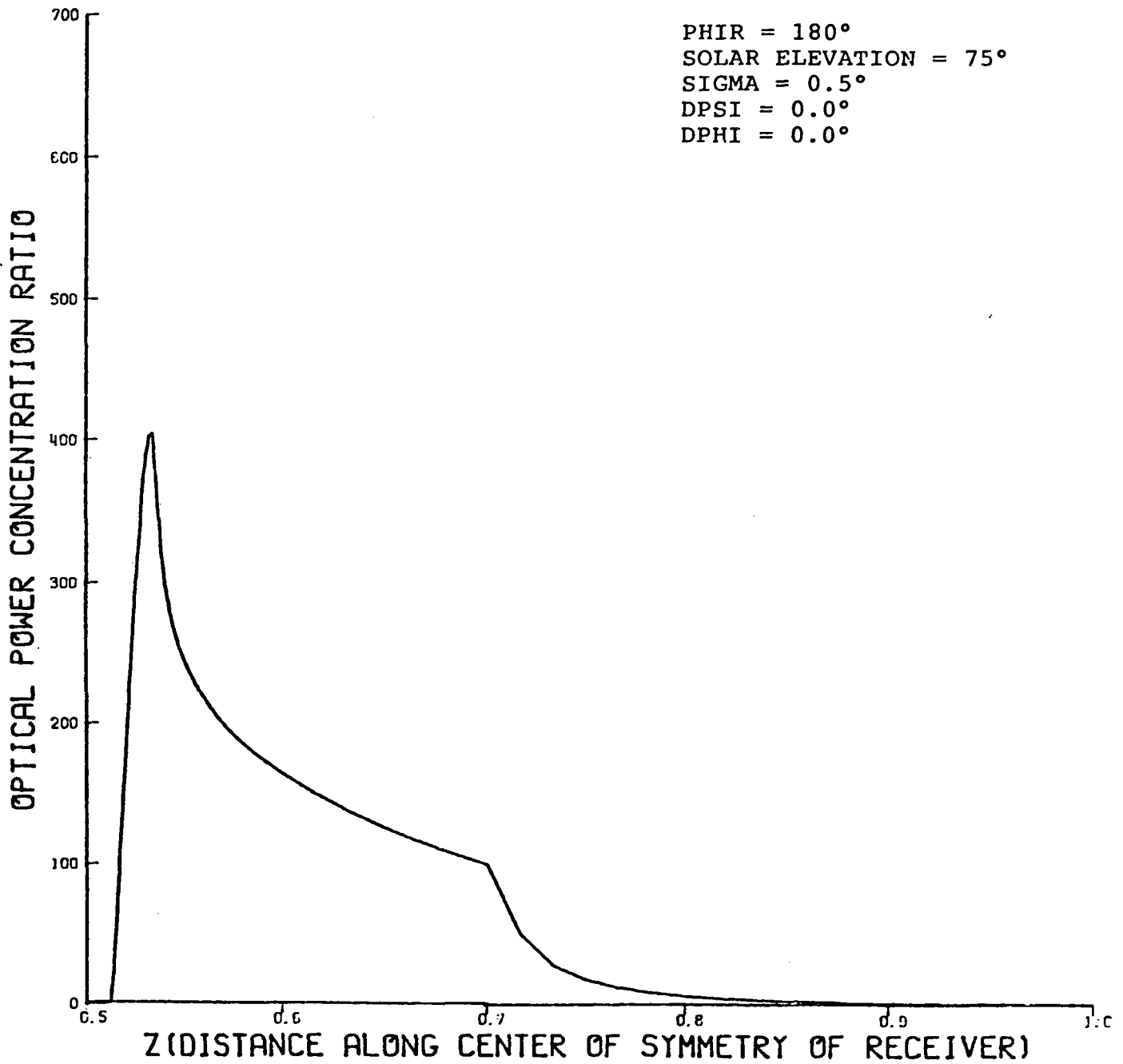


Figure VI - 7a Optical Power Concentration for a Cylindrical Receiver

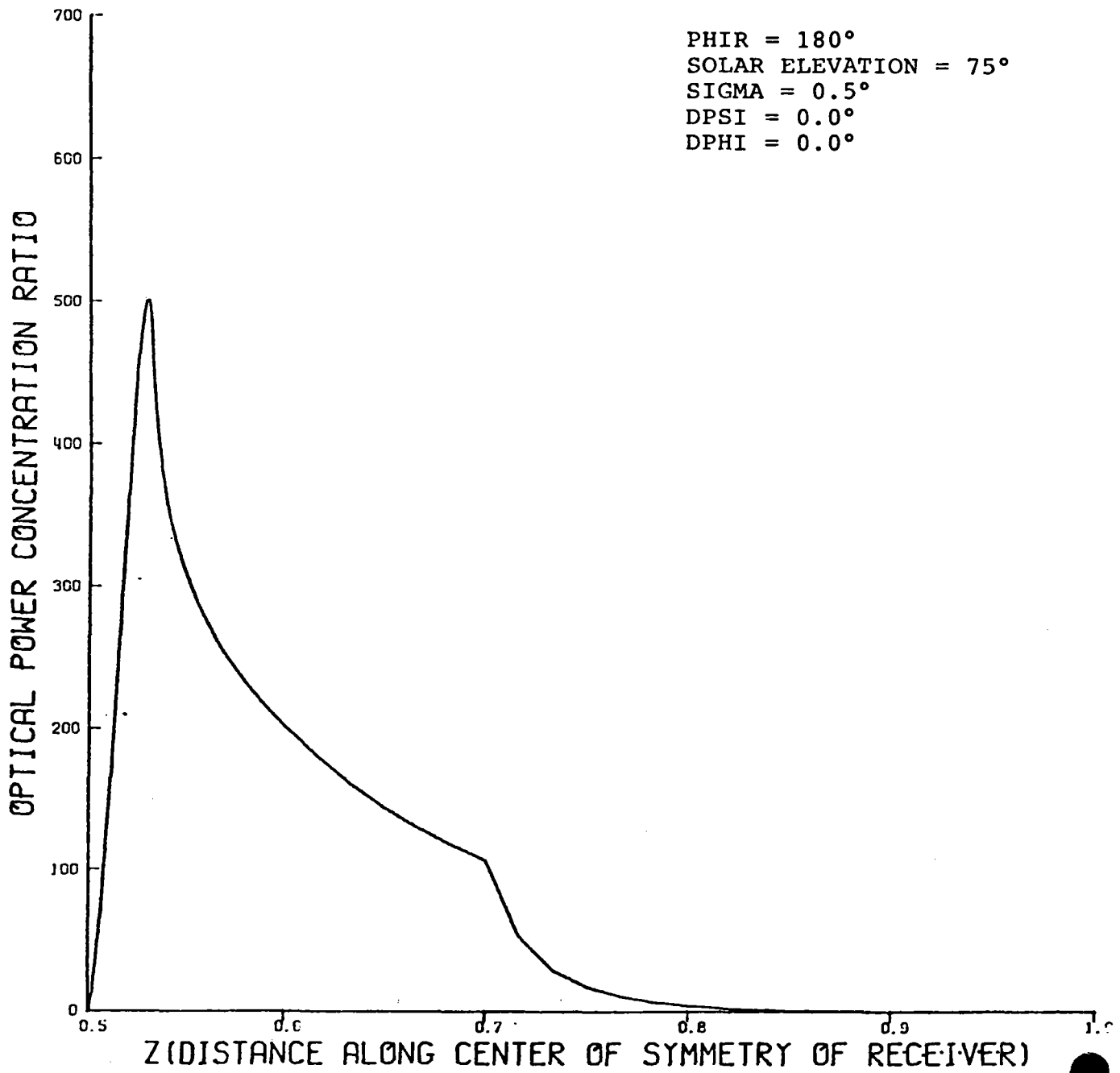


Figure VI - 7b Optical Power Concentration for a Conical Receiver ( $\Psi_R = 0.5^\circ$ )

## 7. ALTERNATE RIM SHAPES

### Introduction

In all previous derivations, we have assumed that the solar collector was a segment of a sphere. In this chapter, an analysis is carried out to extend the ROSA code to more general rim shapes. In this analysis, the rim is assumed to be expressed in the form

$$\theta = f(\phi), \quad (\text{VII-1})$$

where  $\theta$  is the zenith angle of a point on the rim and  $\phi$  is the azimuthal angle of the point on the rim. The angles are expressed in the bowl centered D-M-A coordinate system, where A is perpendicular to the aperture plane of the bowl and is directed upward. The rim angle  $\theta$  is measured from the negative A axis and  $\phi$  is measured from the D axis. As an example,  $\theta = \theta_R = 60$  degrees at the Crosbyton site.

Integration for the calculation of the solar concentration is carried out in the local x-y-z coordinate system and rim angles must be calculated in this coordinate system in order to account for rim cutoff and shading. The D-M-A and x-y-z systems are related by a formula of the form

$$[p]_{xyz} = \Lambda [p]_{DMA} \quad (\text{VII-2})$$

where  $[p]_{DMA}$  represents a point in the D-M-A coordinate system,  $[p]_{xyz}$  represents the same point in the x-y-z coordinate system and  $\Lambda$  is a known rotation matrix ( $\Lambda$  is readily computed using the transition matrices of Chapter III.)  $\Lambda$  depends upon the tilt angle of the bowl, the position of the sun, the shape and orientation of the receiver, the location of a field point on the receiver, and values of the variables of integration in the ROSA code.

Eq. VII-2 can be expressed in component form to yield a system of three equations,

$$\sin \theta_2 \cos \omega = (L_1 \cos \phi + L_2 \sin \phi) \sin \theta - L_3 \cos \theta$$

$$\sin \theta_2 \sin \omega = (M_1 \cos \phi + M_2 \sin \phi) \sin \theta - M_3 \cos \theta \quad (\text{VII-3})$$

$$\cos \theta_2 = (N_1 \cos \phi + N_2 \sin \phi) \sin \theta - N_3 \cos \theta .$$

In these equations,  $\theta$  is the unknown rim angle in the local x-y-z coordinate system,  $\phi$  is an unknown azimuthal angle in the D-M-A coordinate system and  $\theta = f(\phi)$  according to Eq. VII-1.  $\omega$  is an integration variable and  $L_i, M_i, N_i$   $i=1,2,3$  are direction cosines relating the D-M-A and x-y-z coordinate systems.

## A Special Rim Shape

The above formulas will now be applied to the case where the standard bowl shape is sliced by planes  $M = \pm M_0$  (in the D-M-A coordinate system). Eq. VII-1 then takes the form

$$\theta = \theta_0 \text{ for } -\phi_0 \leq \phi \leq \phi_0 \text{ and } \pi - \phi_0 \leq \phi \leq \pi + \phi_0,$$

$$\theta = \text{Arccos} [1 - M_0 \csc \phi] \quad , \text{ elsewhere,} \quad (\text{VII-4})$$

where,  $\sin \phi_0 = M_0 / \sin \theta_0$ .

The equation  $\omega = \text{constant}$  defines a plane in the x-y-z coordinate system with equation  $y = x \tan \omega$ . In the D-M-A coordinate system, this same plane has equation

$$M_1 D + M_2 M + M_3 A = (L_1 D + L_2 M + L_3 A) \tan \omega. \quad (\text{VII-5})$$

This plane will intersect the plane  $M = M_0$  along the line

$$(M_1 - L_1 \tan \omega) D + (M_2 - L_2 \tan \omega) M_0 + (M_3 - L_3 \tan \omega) A = 0. \quad (\text{VII-6})$$

If this line intersects the unit sphere (using normalized units), the additional condition

$$D^2 + M^2 + A^2 = 1, \quad (\text{VII-7})$$

must be satisfied. Simultaneous solution of Eqs. VII-6 and 7 gives

$$A = \frac{-(a_2 a_3 M_0) \pm [(a_1^2 + a_3^2) a_1^2 (1 - M_0^2) - (a_1 a_2^2 M_0)^2]^{1/2}}{(a_1^2 + a_3^2)}. \quad (\text{VII-8})$$

where,

$$a_i = M_i - L_i \tan \omega, \quad i=1,2,3.$$

D is then calculated from Eq. VII-6.

There are three cases to consider.

1. If the quantity under the radical sign in Eq. VII-8 is negative, then the line of intersection of the  $\omega$ -plane and the plane  $M = M_0$  does not intersect the unit sphere and the rim angle in the D-M-A system is given by  $\theta = \theta_0$ .

If A is real in Eq. VII-8, then let  $\theta_1 = \text{Arccos } A$ .

2. If  $\theta \leq \theta_0$ , then  $\theta = \theta_0$ .

3. if  $\theta < \theta_0$ , then  $\theta = \theta_0$ .

In each of the above cases,  $\theta_2$  can be computed from  $\theta$  using formulas that were developed previously for a dish with a constant rim angle.

The formulas for the plane  $M = -M_0$  can be obtained from the above formulas by simply replacing  $M_0$  by  $-M$ .

Sample concentration profiles are given in Figs. VII-1 through VII-3.

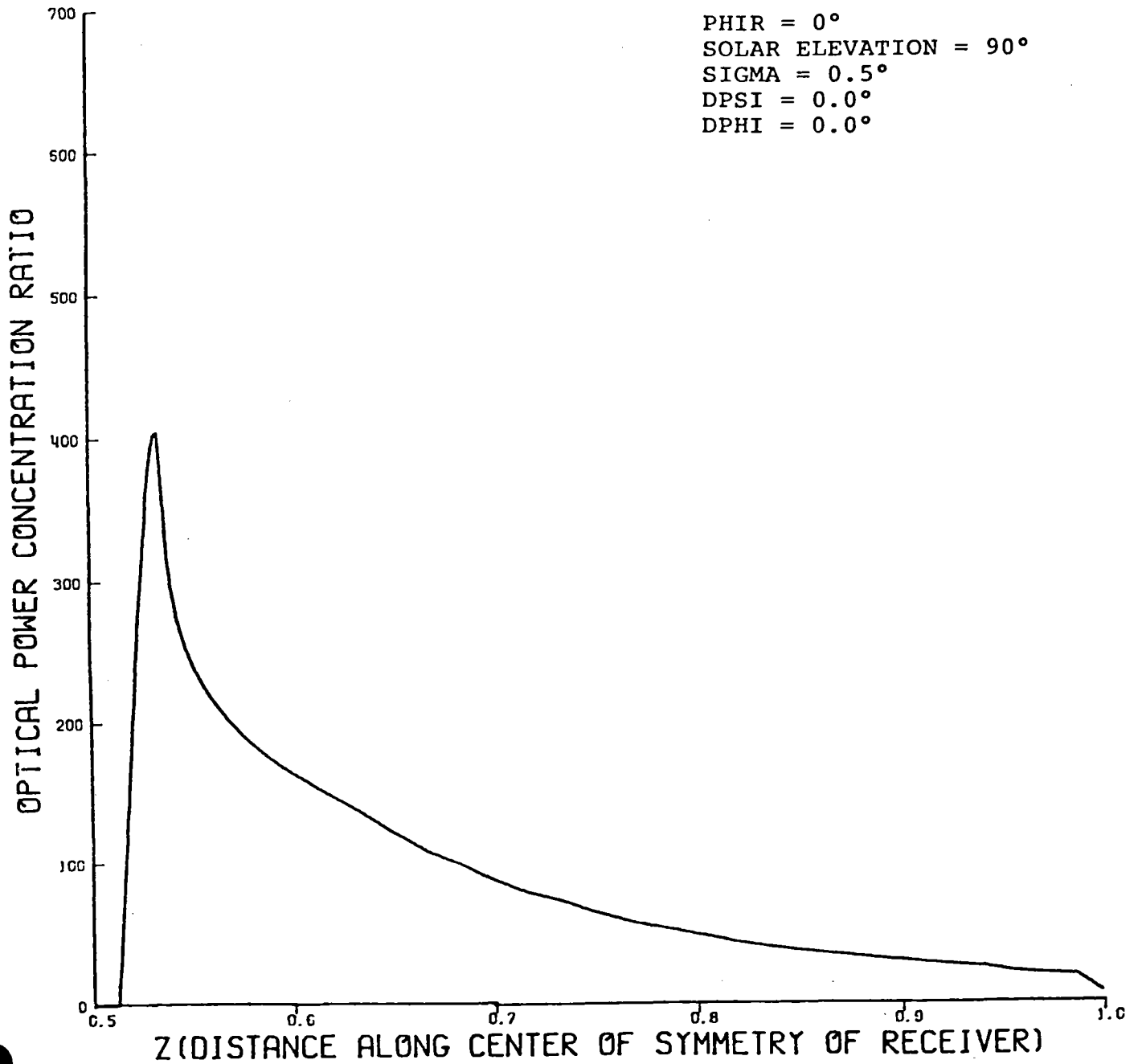


Figure VII - 1 Optical Power Concentration for a Cylindrical Receiver with an Alternate Rim Shape

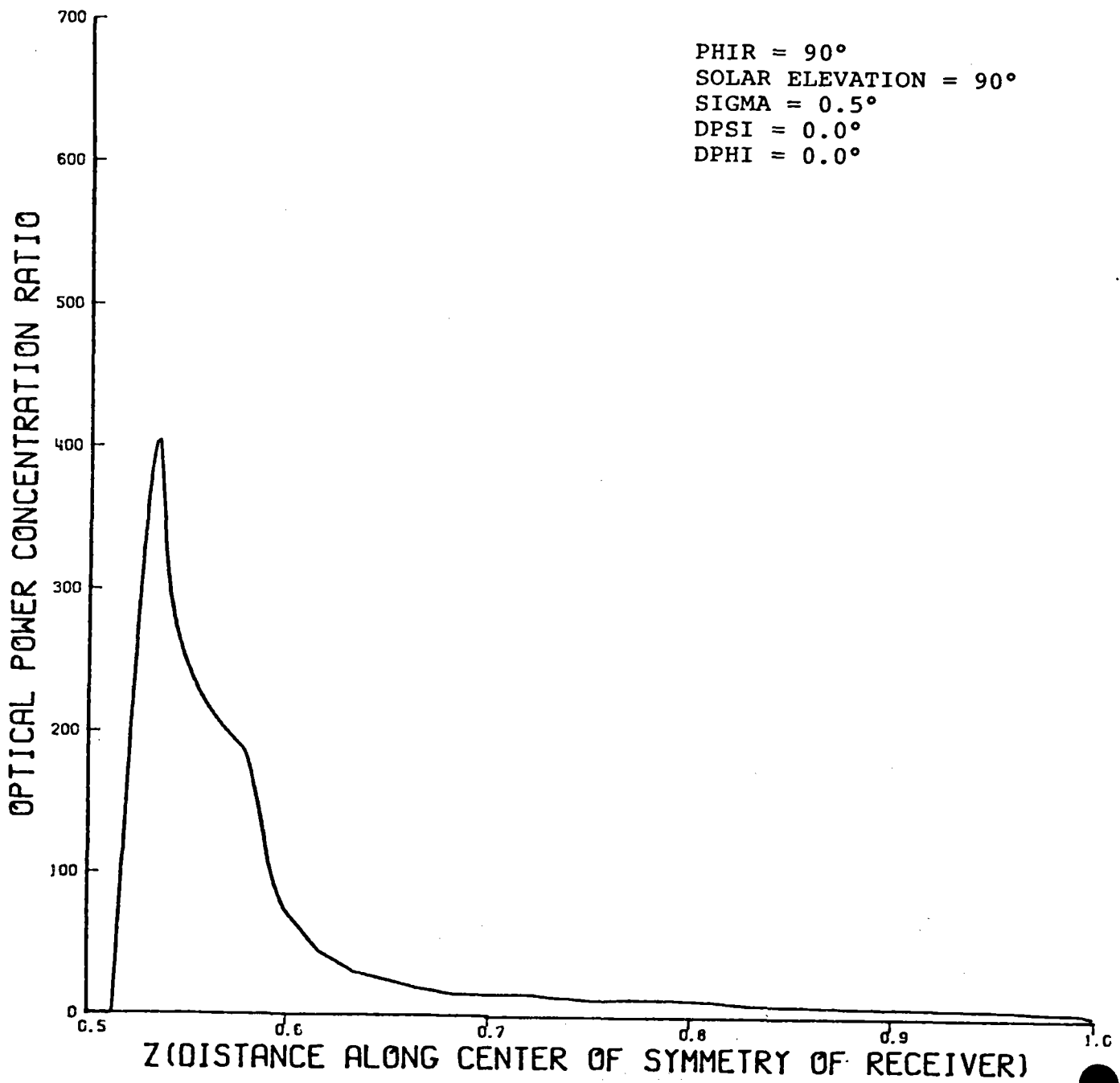


Figure VII - 2 Optical Power Concentration for a Cylindrical Receiver with an Alternate Rim Shape

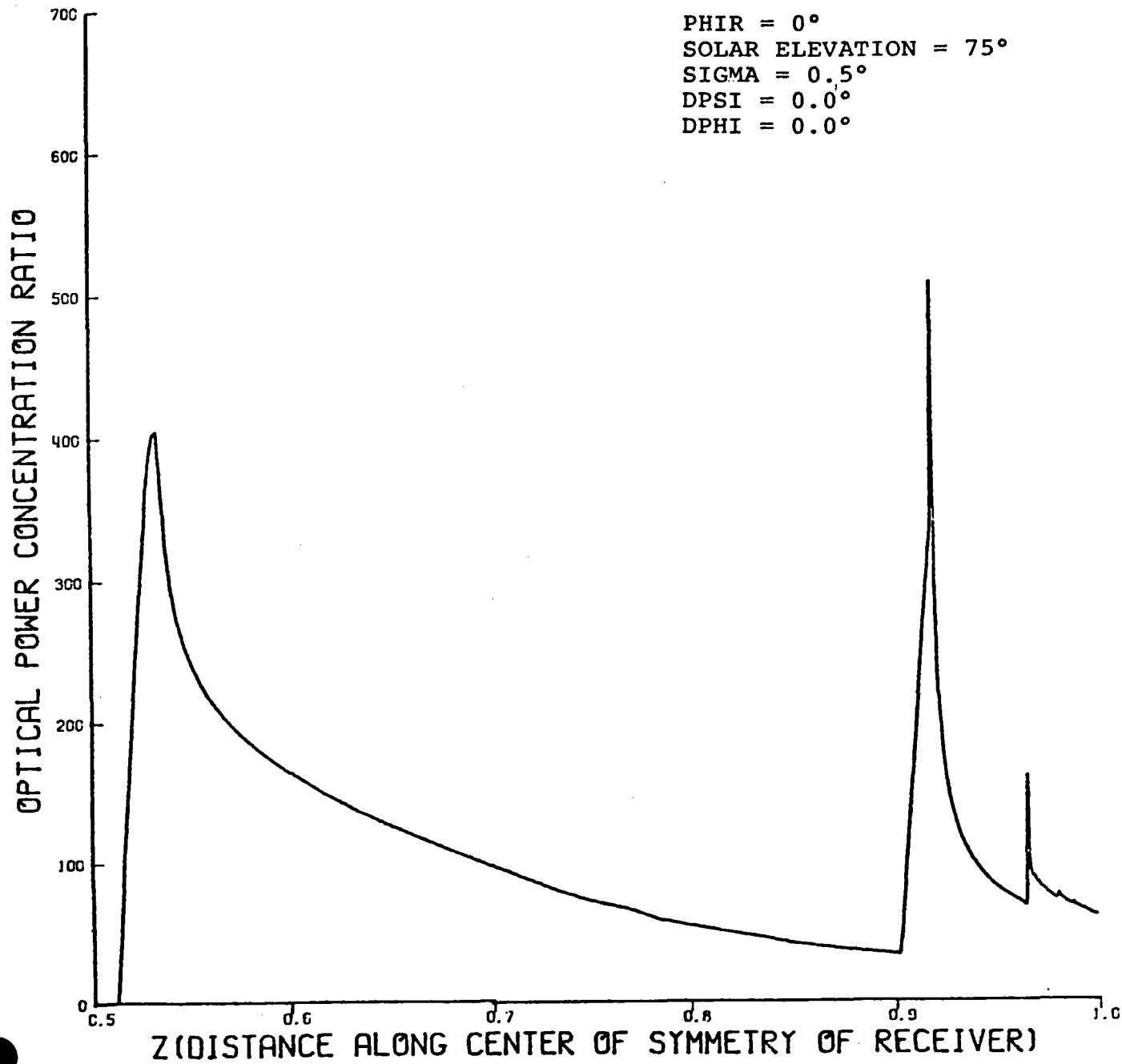


Figure VII - 3 Optical Power Concentration for a Cylindrical Receiver with an Alternate Rim Shape

## REFERENCES

1. Reichert, J. D., "A Strategy for Calculations of Optical Concentration Distributions for Fixed Mirror Systems", Proceedings of the ERDA Solar Workshop on Methods for Optical Analysis of Central Receiver Systems , August 10-11, 1977, Houston, Texas, pp. 155-174.
2. Brock, B.C., "Optical Analysis of Spherical Segment Solar Collectors", Ph.D. dissertation, Texas Tech University, Lubbock, Texas, May 1977.
3. Leung, H., "Optical Power Concentrations on Aligned and Misaligned Receivers in Solar Gridiron Power Systems", M.S. thesis, Texas Tech University, Lubbock, Texas, August, 1978.
4. Reichert, J.D., Anderson, R.M., Leung, H., et al, "Crosbyton Solar Power Project Phase 1 Interim Technical Report", The Crosbyton Solar Power Project , Vol. II, Appendix C. Texas Tech University, Lubbock, Texas, February, 1977. ERDA Contract No. E(29-2)-3737.
5. Reichert, J.D., Anderson, R.M., Ford, W.T, et al, "Analytical Optical Power Concentration Calculations For Reflection For Spherical Mirrors". Proceedings of the ASME Solar Energy Division Sixth Annual Conference. Las Vegas, Nevada, April 8-12, 1984, pp. 57-63.
6. Reichert, J.D., et al, "Performance and Cost of Solar Power Plants". The Crosbyton Solar Power Project , Vol. VII, Texas Tec University, Lubbock, Texas, November 1, 1981. United States Department of Energy Contract No. DE-AC04-76ET20255.

=====

ROSA CALCULATION CODE

=====

C \*\*\*\*\*

C ROSA IS A PROGRAM WHICH CALCULATES THE CONCENTRATION

C AT A POINT ON A RECEIVER.

C

C WRITTEN BY

C

C DR. RONALD M. ANDERSON, LEFT. OF MATHEMATICS

C

C AND

C

C DR. JOHN L. REICHERT, DEPT. OF ELECTRICAL ENGINEERING

C

C GRADUATE ASSISTANTS: C. NORWOOD, R. JOHNSTON, C. DAWSON

C

C TEXAS TECH UNIVERSITY

C

C LUBBOCK, TEXAS

C

C JULY 24, 1984

C \*\*\*\*\*

C REAL SUM(100,5),QQ(100)

C REAL ZSTART(10),ZSTOP(10)

C COMMON /BICCKA/ MOMEGA,ISTEPS,CMEGAL(2),OMEGAU(2),XYNRML,

\*ALPHA,NZ,ZNPMAL,PSIOS,PSIOC,SIGMAC,

\*RIMC4,RIMC5,RIMC6,THTARC,THTAW

COMMON /BLCKKB/ PIHALF,PI,PSIP,PSIPK,PSIM,BETAPK,Q,NEC

COMMON /CUI/ THTAR,GAMMAC,ES,A,PHID,GAMMAS,EC,PHIOC,PHIOS

REAL OMEGAL,CMEGAU,XYNRML,ZNRML,PSIC,SIGMAC,

\*RIMC4,RIMC5,RIMC6,THTARC,THTAW,PI,PSIP,PSIPK,PSIM,BETAPK,Q

INTEGER MOMEGA,ISTEPS,NZ,NBC

INTEGER NZZ(10),ITITLE(20)

C

C COORDINATE SYSTEMS USED:

C

C 1. THE S-E-V COORDINATE SYSTEM

C THIS IS THE SOUTH-EAST-VERTICAL COORDINATE SYSTEM

C WHICH IS ALIGNED WITH THE EARTH.

C

C 2. THE F-G-IS COORDINATE SYSTEM

C THIS COORDINATE SYSTEM IS ALIGNED SO THAT

C THE ES AXIS POINTS TO THE CENTER OF THE SUN.

C

C 3. THE X-Y-Z COORDINATE SYSTEM

C THIS COORDINATE SYSTEM IS ALIGNED SO THAT

C THE Z AXIS PASSES THROUGH THE CENTER OF

C THE HEMISPHERE AND THE POINT Q ON THE

C RECEIVER AND THE SUN LIES IN THE XZ PLANE.

C

C 4. THE XR-YR-ZR COORDINATE SYSTEM

C THIS COORDINATE SYSTEM IS ALIGNED SO THAT

C THE ZR AXIS IS THE RECEIVER AXIS OF SYMMETRY.

C

C 5. THE D-M-A COORDINATE SYSTEM

C THIS COORDINATE SYSTEM IS ALIGNED SO THAT

C THE A AXIS IS THE AXIS OF SYMMETRY OF THE DISH.

```

C
C      CONTINUE
C INPUT VARIABLES
C
C  A. ROTATION ANGLE VARIABLES
C      PHIRD, PSIRD = THE ROTATION ANGLES, IN DEGREES, BETWEEN THE
C                  X-Y-Z AND XP-YR-ZR COORDINATE SYSTEMS
C      DPSID, DPHID = THE ROTATION ANGLES, IN DEGREES, BETWEEN THE
C                  F-G-ES AND XR-YR-ZR COORDINATE SYSTEMS
C      ED, AD = THE ELEVATION ANGLE AND AZIMUTHAL ANGLE,
C              BETWEEN THE S-E-V AND F-G-ES COORDINATE SYSTEMS
C      GAMMAD, PHIDD = THE ROTATION ANGLES, IN DEGREES,
C                  BETWEEN THE S-E-V AND D-M-A
C                  COORDINATE SYSTEMS
C      THIRDD = ALTITUDINAL ANGLE, IN DEGREES, BETWEEN
C              THE D-M-A AND X-Y-Z COORDINATE SYSTEMS
C
C  B. OTHER INPUT VARIABLES
C      DPHIRD = THE AMOUNT PHIR IS INCREMENTED IN
C              THE PHIR-LOOP (READ IN)
C      ISTIPS = THE NUMBER OF INTERVALS USED IN
C              THE OMEGA-INTEGRATION
C              (USING SIMPSON'S RULE)
C      NZZ = NUMBER OF TIMES Z IS INCREMENTED (READ IN)
C      REFC = THE REFLECTION COEFFICIENT
C      SIGMAD = THE SUN CONE HALF-ANGLE
C      SPFHIR = THE FINAL VALUE OF PHIR (READ IN)
C      STPHIR = THE STARTING VALUE OF PHIR (READ IN)
C      ZSTART = THE INITIAL VALUE OF Z (READ IN)
C      ZSTOP = THE FINAL VALUE OF Z (READ IN)
C
C      CONTINUE
C
C INTERNAL VARIABLES
C      ALPHA = THE ANGLE BETWEEN THE X-AXIS AND THE
C              NORMAL TO THE RECEIVER
C      COEFF1, COEFF2 = USED TO CALCULATE PHIO
C      CONST = A CONSTANT USED IN THE CONCENTRATION FORMULA
C      DPSI, IPHI = IPSIC, AND DPHID IN RADIANS
C      DPSIC, DPHIC = THE COSINES OF DPSI AND DPHI
C      DPSIS, DPHIS = THE SINES OF DPSI AND DPHI
C      DZ = THE AMOUNT Z IS INCREMENTED EACH TIME THE
C          Q-LOOP IS COMPLETED
C          DZ DEPENDS ON ZSTART, ZSTOP, AND NZZ
C      CONTINUE
C      E, A = ED AND AD IN RADIANS
C      EC = THE COSINE OF E
C      ES = THE SINE OF E
C      GAMMA, PHID = GAMMAD AND PHIDD IN RADIANS
C      GAMMAC, PHIDC = THE COSINES OF GAMMA AND PHID

```

```

C GAMMAS, PHIS = THE SINES OF GAMMA AND PHID
C OMEGAL = THE LOWER BOUND ON OMEGA USED IN INTEGRATION
C OMEGAU = THE UPPER BOUND ON OMEGA USED IN INTEGRATION
C PODPC = COS(PHIC-DPHI)
C PODPS = SIN(PHIC-DPHI)
C PSIO, PHIO = THE ROTATION ANGLES BETWEEN THE SUN
C             COORDINATE SYSTEM AND THE X-Y-Z COORDINATE SYSTEM
C PSICC, PHIOC = THE COSINES OF PSIC AND PHIC
C PSICS, PHIGS = THE SINES OF PSIC AND PHIC
C             CONTINUE
C PSIRD, PHIRD = THE ROTATION ANGLES, IN DEGREES, BETWEEN THE
C             XR-YR-ZR AND THE X-Y-Z COORDINATE SYSTEMS
C PSIR, PHIR = PSIRD AND PHIRD IN RADIANS
C PSIRC, PHIRC = THE COSINES OF PSIR AND PHIR
C PSIRS, PHIRS = THE SINES OF PSIR AND PHIR
C Q = THE DISTANCE FROM THE CENTER TO THE POINT
C     WHERE THE RAY STRIKES THE RECEIVER
C RIMCI (I=1,7) = USED TO COMPUTE THTAZ
C SIGMA = SIGMA IN RADIANS
C SIGMAC, SIGMAS = THE COSINE AND THE SINE OF SIGMA
C THTAR = THTAEL IN RADIANS
C THTARC, THTAES = THE COSINE AND THE SINE OF THTAR
C XNORMAL = THE X-COMPONENT OF THE OUTWARD NORMAL
C             TO THE RECEIVER AT Q
C YNORMAL = THE Y-COMPONENT OF THE OUTWARD NORMAL
C             TO THE RECEIVER AT Q
C XYNRMI = PROJECTION OF THE NORMAL TO THE RECEIVER
C             INTO THE XY-PLANE
C XR,YR,ZR = COMPONENTS OF THE NORMAL IN TERMS OF
C             XR-YR-ZR COORDINATE SYSTEM
C Z = THE DISTANCE FROM THE CENTER TO A POINT ON THE
C     CENTRAL AXIS OF THE RECEIVER
C ZNORMAL = THE Z-COMPONENT OF THE OUTWARD NORMAL TO
C             THE RECEIVER AT Q
C
C             CONTINUE
C
C OUTPUT VARIABLES
C LI=NUMBER OF ICUNCES
C QQ = TEMPORARY VARIABLE USED TO PRINT THE VALUE OF Z
C SUM = USED TO COMPUTE THE OMEGA INTEGRAL
C SUMA = USED TO FIND THE TOTAL CONCENTRATION (N=1,5)
C
C
C PROGRAM CONSTANTS
C PI=4*ATAN(1.)
C RADIAN=PI/180.
C PIHALF=ATAN2(1.,0.)
C
C DO 14 NM=1,5

```

```

        DC 16 NN=1,100
          SUM(NN,MM)=0.
16    CCNTINUE
14    CONTINUE
C
C INPUT VARIABLES
      WRITE(6,208)
208  FORMAT(/,/,/,/,/,20X,' INPUT',/,/)
      READ(5,197) ITITLE
197  FORMAT(20A4)
      WRITE(6,198) ITITLE
      READ(5,199) DPSID,DPHID
      WRITE(6,202) DPSID,DPHID
      READ(5,299) SIGMAD,ED,AD
      READ(5,299) THTARD,GAMMAD,PHID
      WRITE(6,203) SIGMAD,ED,AD,THTARD,GAMMAD,PHID
199  FORMAT(2F10.5)
299  FORMAT(3F10.5)
202  FORMAT('
* '          BCILER-SUN ALIGNMENT PARAMETERS: ',/,/
* '          DELTA PSI (DPSID)           = ',F10.5,/,/
* '          DELTA PHI (DPHID)           = ',F10.5)
203  FORMAT(/, '
* '          SUN PARAMETERS: ',/,/
* '          SUN CONE HALF ANGLE (SIGMAD) = ',F10.5,/,/
* '          SUN POSITION: ',/,/
* '          ELEVATION (ED)              = ',F10.5,/,/
* '          DISH PARAMETERS: ',/,/
* '          DISH HALF-ANGLE (THTARD)    = ',F10.5,/,/
* '          DISH ALIGNMENT: ',/,/
* '          GAMMAD                       = ',F10.5,/,/
* '          PHID                         = ',F10.5)
      READ(5,399) REFC,ISTEPS
      WRITE(6,204) REFC,ISTEPS
399  FORMAT(F10.5,I5)
204  FORMAT(/,
* '          REFLECTION CONSTANT         = ',F10.5,/,/
* '          ISTEPS                      = ',I5,/)
      READ(5,1)  STPHIR,SPPHIR,DPHIRD
      WRITE(6,205) STPHIR,SPPHIR,DPHIRD
1    FORMAT(3F5.0)
205  FORMAT(
* '          START PHIR (STPHIR)         = ',F5.0,/,/
* '          STOP PHIR (SPPHIR)          = ',F5.0,/,/
1 '          DELTA PHIR (DPHIRD)         = ',F5.0,/,/
      READ(5,2)  NZRR
      WRITE(6,206) NZRR
2    FORMAT(I5)
206  FORMAT(
* '          NUMBER OF Z-INTERVALS (NZRR) = ',I5)
      DO 3 I=1,NZRR
        READ(5,4)  NZZ(I),ZSTART(I),ZSTOP(I)

```

```

WRITE(6,207) I, NZZ(I), ZSTART(I), ZSTOP(I)
4  FCRMAT(15,2F5.3)
207 FCRMAT('          FOR I = ',I5,/,
* '          NUMBER OF INCREMENTS' (NZZ) = ',I5,/,
1 '          ZSTART = ',F5.3,/,
* '          ZSTOP = ',F5.3)
3 CONTINUE
WRITE(6,1308)
1308 FOFMAT('1 ')
C
C CONVERSION FROM DEGREES TO RADIANS
DPSI=DPSID*RADIAN
DPHI=DPHID*RADIAN
PHI=PHID*RADIAN
GAMMA=GAMMAD*RADIAN
E=EI*RADIAN
A=AI*RADIAN
SIGMA=SIGMAD*RADIAN
C
C CALCULATION OF RIM ANGLE CONSTANTS
THIAP=THIAPD*RADIAN
THIARC=CCS(THIAP)
CONST=12.*PI*SIN(.5*SIGMA)**2
DPSIC=CCS(DPSI)
DPSIS=SIN(DPSI)
DPHIC=CCS(DPHI)
DPHIS=SIN(DPHI)
RIMC1=SIN(E)*SIN(GAMMA)*COS(A-PHID)-CCS(E)*COS(GAMMA)
RIMC2=SIN(GAMMA)*SIN(A-PHID)
RIMC3=CCS(E)*SIN(GAMMA)*COS(A-PHID)+SIN(E)*COS(GAMMA)
C
C CALCULATION OF TRIG CONSTANTS
PHIIC=CCS(PHID)
PHIIS=SIN(PHID)
SIGMAS=SIN(SIGMA)
SIGMAC=CCS(SIGMA)
EC=CCS(E)
ES=SIN(E)
GAMMAC=CCS(GAMMA)
GAMMAS=SIN(GAMMA)
C
C BEGIN LOOP FOR AZIMUTHAL ANGLE (PHIR)
PHIRD=STPHIR
JSTOP=1
IF (DPHIRE .NE. 0.) JSTOP=(SPPHIR-STPHIR)/DPHIRD+1.01
DO 250 J=1,JSTOP
PHIR=PHIRD*RADIAN
WRITE(6,5) PHIRD
5  FCRMAT('1 ','          PHIR=',F12.3)
PFIRC=CCS(PHIR)

```

```

      PHRS=SIN(PHIR)
C
C BEGINNING OF Z LOOP
      DO 600 K=1,NZRR
        Z=ZSTART(K)
        IF(NZZ(K) .LE. 1) GO TO 5000
5001      DZ=(ZSTOP(K)-ZSTART(K))/(NZZ(K)-1)
5000      NZSTCF=NZZ(K)
        DO 3000 NZ=1,NZSTOP
          CALL BCILR(Z,PHIR,PSIR,XR,YR,ZR)
          PSIRC=CCS(PSIR)
          PSIRS=SIN(PSIR)
C
C CALCULATION OF PSIO
      PSICC=DPSIC*PSIRC+DPSIS*PSIRS*PHIRC
      PSIC=ARCCS(PSICC)
      PSICS=SIN(PSIO)
      COEFF1=DPSIC*PSIRS*PHIRC-DPSIS*PSIRC
      COEFF2=PSIRS*PHIRS
C
C CALCULATION OF PHIO
      IF (AES(PSIO) .GT. 0.0) GO TO 15
10      PHIC=G.
        GC TC 20
15      PHICC=DPHIC*COEFF1-DPHIS*COEFF2
        PHICS=DPHIS*COEFF1+DPHIC*COEFF2
        PHIC=ATAN2(PHICS,PHICC)
20      PHICC=COS(PHIO)
        PHICS=SIN(PHIO)
C
C CALCULATION OF THE RECEIVER CONSTANTS
      PODFC=COS(PHIO-DPHI)
      PODPS=SIN(PHIO-DPHI)
      ZNRML=XR*(PSICS*DPSIC*PODFC+PSICC*DPSIS)
      *      + YR*PSIOS*PODPS
1      *      + ZR*(PSICS*DPSIS*PODPC-PSICC*DPSIC)
      XNRML=XR*(PSICC*DPSIC*PODFC-PSICS*DPSIS)
      *      + YR*PSIOC*PODPS
1      *      + ZR*(PSICC*DPSIS*PODPC+PSICS*DPSIC)
      YNRML=XR*DPSIC*PODPS - YR*PODPC + ZR*DPSIS*PODPS
      XYNRML=SQRT(1.-ZNRML**2)
1      IF (ABS(XYNRML) .LT. .0001 .OR. (AES(XNRML) .LT. .0001
        .AND. AES(YNRML) .LT. .0001)) GO TO 8526
      ALPHA=ATAN2(YNRML,XNRML)
      GC TC 993
8526      ALPEA = C.0
C
C CALCULATION OF ADDITIONAL RIM CONSTANTS
993      RIMC4=PSIOC*(PHIOC*RIMC1-PHIOS*RIMC2)+PSIOS*RIMC3
        RIMC5=PHIOS*RIMC1+PHICC*RIMC2

```

```

RIMC6=PSIOS*(PHIOC*RIMC1-PHIOS*RIMC2)-PSIOC*RIMC3
C
C LIMITS ARE GIVEN BY THE CMEGA(I)--
C NOMEGA IS THE NUMBER OF INTERVALS
      IF (SIGMA .LT. PSIO) GO TO 40
45      OMEGAL(1)=ALPHA-PIHALF
      OMEGAU(1)=ALPHA+PIHALF
      OMEGAL(2)=ALPHA+PIHALF
      CMEGAU(2)=ALPHA+PIHALF*3.
      NCMEGA=2
      GO TO 90
C      ELSI DO
40      CMEGA1=ACOS(SQRT((SIGMAC**2-PSIOC**2)/PSICS**2))
      OMEGAU(1)=CMEGA1
      CMEGAL(1)=-OMEGA1
      OMEGAL(2)=PI-OMEGA1
      OMEGAU(2)=PI+OMEGA1
      NCMEGA=2
C      ENDIF
C
C THE W-INTEGRATION AND THE BETA-INTEGRATION ARE PERFORMED IN
C SUBROUTINE INTGR1, SIMPSON'S RULE IS USED ON THE W-INTEGRATION
90      DO 100 NOMEGA=1,NOMEGA
      CALL INTGR1(SUM)
100     CCNTINUE
      QQ(NZ)=Z
3000    Z=Z+DZ
C END OF INTEGRATION-BEGIN PRINT OUT
      DO 500 I=1,NZSTOP
      SUMA=0.
      WRITE(6,501) QQ(L)
      DO 505 I1=1,5
      SUM(L,I1)=SUM(L,I1)/CONST*REFC**I1
      SUMA=SUMA + SUM(L,I1)
501     FORMAT('0          Z=',F8.4)
      WRITE(6,502) I1,SUM(L,I1)
502     FORMAT('          BOUNCE NUMBER='
*        ,I1,'          CONCENTRATION=',F14.4)
505     SUM(L,I1)=0.
500     WRITE(6,503) SUMA
503     FORMAT('          TOTAL CONCENTRATION=',F14.4,/,/)
600     CCNTINUE
250     PHIRD=PHIRD+DPHIRD
      WRITE(6,8343)
8343    FORMAT('1',/,/,/,/,/,'          NCRMAI TERMINATION')
      STOP
      ENI

```

```

C*DECK INTGRI
      SUBROUTINE INTGRI(SUM)
C*** INTGRI PERFORMS THE OMEGA AND BETA INTEGRATIONS
C    AND COMPUTES SUM, WHICH IS RETURNED TO THE
C    MAIN PROGRAM.
C
C***WRITTEN BY:  R.M.ANDERSON, ASSISTED BY CLINT DAWSON
C                CATHY NORWOOD, AND READ JOHNSTON
C    DATE WRITTEN: 06/01/80
C
C***EXPLANATION OF VARIABLES:
C  BETAL = LOWER LIMIT ON BETA USED IN THE INTEGRATION
C  BETAMI = MINIMUM VALUE OF BETA FOUND WHEN CONSIDERING RIM-CUTCFF
C          AND SHADOWING EFFECTS
C  BETAMX = MAXIMUM VALUE OF BETA FOUND WHEN CONSIDERING RIM-CUTCFF
C          AND SHADOWING EFFECTS
C  BETAPK = THE VALUE OF BETA CORRESPONDING TO THE
C          MAXIMUM VALUE OF PSI FOR A GIVEN VALUE OF Q
C  BETASM = BETAL + BETAU
C  BETAT = BETAU - BETAL
C  BETAU = UPPER LIMIT ON BETA USED IN THE INTEGRATION
C  BL = THE LOWER BOUND ON BETA WHEN CONSIDERING THE RELATIONSHIP
C      BETWEEN BETA, PSIP, AND PSIM
C  BU = THE UPPER BOUND ON BETA WHEN CONSIDERING THE RELATIONSHIP
C      BETWEEN BETA, PSIP, AND PSIM
C  CONSTW = A CONSTANT USED IN THE OMEGA INTEGRATION
C  DOMEGA = (OMEGAU - OMEGAL)/ISTEPS
C  ETA, EETA = USED TO COMPUTE PSIP AND PSIM
C  NBC, XN = THE NUMBER OF BOUNCES
C  OMEGA = THE AZIMUTHAL ANGLE MEASURED CLOCKWISE FROM THE X-AXIS
C  PSIM = ANGLE BETWEEN THE RECEIVER AND THE
C        LEFT EDGE OF THE SUN CONE IN THE
C        PLANE OMEGA=CONSTANT
C  PSIP = ANGLE BETWEEN THE RECEIVER AND THE
C        RIGHT EDGE OF THE SUN CONE IN THE
C        PLANE OMEGA=CONSTANT
C  PSIPK = MAXIMUM VALUE OF PSI FOR A GIVEN N AND Q
C  QSBETA = Q TIMES THE SINE OF BETAPK
C  RHO = USED TO FIND BETAMX TO ASSURE THAT THE DOT PRODUCT IS >= 0
C  SB = USED TO COMPUTE THE BETA-INTEGRAL
C  SUM1 = USED TO COMPUTE THE BETA INTEGRAL
C  THETA = USED TO COMPUTE THETAZP
C  THETAZ = USED TO FIND THETAZP AND THETAZM
C  THETAZE = THETA-EFFECTIVE, USED TO COMPUTE BETAMX
C  THETAZM = THE ANGLE BETWEEN THE RECEIVER AND THE LEFT RIM
C  THETAZP = THE ANGLE BETWEEN THE RECEIVER AND THE RIGHT RIM
C
C*****
      BIAL SUM(100,5)
C

```

```

      RIAL BL(2),EU(2)
      INTEGER NETA
      COMMON /ELCCKA/ MOMEGA, ISTEPS, CMEGAL(2), OMEGAU(2), XYNRML,
* ALPHA, NZ, ZNRML, PSIOS, PSIOC, SIGMAC,
* RIMC4, RIMC5, RIMC6, THTARC, THTAW
      COMMON /ELCCKB/ PIHALF, PI, PSIP, PSIPK, PSIM, BETAPK, Q, NBC
      COMMON /CUI/ THTAR, GAMMAC, ES, A, PHID, GAMMAS, EC, PHIOC, PHICS
C THE W-INTEGRATION--ISTEPS IS THE NUMBER OF
C INTEGRATION STEPS/INTERVAL
C SIMPSON'S RULE IS USED
      UNIT=-1.
      DCMEGA=(CMEGAU(MCMEGA)-OMEGAL(MOMEGA))/ISTEPS
      DO 101 I=2, ISTEPS
          OMEGA=CMEGAL(MCMEGA)+(I-1)*DCMEGA
          OMEGAC=CCS(OMEGA)
          CONSTW=(3.-UNIT)*DCMEGA
          CMEGAS=SIN(OMEGA)
          RHO=ATAN2(XYNRML*CCS(OMEGA-ALPHA),ZNRML)
C
C CALCULATION OF PSIM, PSIP
      ETA=ATAN2(PSIOS*CMEGAC,PSICC)
      BETA=ARCCS(SIGMAC/SQRT(PSICC**2+(PSICS*CMEGAC)**2))
      PSIP=ETA+EETA
      PSIM=ETA-EETA
C
C CALCULATION OF EFFECTIVE RIM ANGLE PARAMETERS
      RIMC7=RIMC4*OMEGAC+RIMC5*CMEGAS
      THTAW=ATAN2(-RIMC7,-RIMC6)
      THIAZ=THTARC/SQRT(RIMC6**2+RIMC7**2)
      IF (THIAZ .GT. 1.0) GO TO 101
110      THIAZ= ARCCS(THIAZ)
C**** IF YOU WANT AN ALTERNATE RIM SHAPE, REMOVE THE
C "C" IN THE NEXT LINE
C      CALL RIM(OMEGA,THTAZ,IFLAG)
      IF (IFLAG .EQ. 1) GO TO 101
      THIAZP= THIAZ+THTAW
      IF (THIAZP .LE. 0.0) GO TO 101
111      THIAZM= -THIAZ+THTAW
          THIAZM=AMAX1(0.,THIAZM)
          THIAZP=AMIN1(THIAZP,PI-THIAZP-PSIP-PSIM)
          IF (THIAZP .LE. THIAZM) GO TO 101
112      CONTINUE
C
C CALCULATION OF MINIMUM AND MAXIMUM BETA AND EFFECTIVE RIM ANGLE
C BETAMI, IETAMX AND THTAZM, RESPECTIVELY
      EETAMI=0.
      IF (THIAZM .LE. 0.0) GO TO 302
301      BETAMI=ATAN2(SIN(THIAZM),CCS(THIAZM)-Q)
302      EETAMI = AMAX1(BETAMI,-PIHALF+RHO)
C      ELSE DO

```

```

DO 370 NFC=1,5
  XN=NEC
  THTAZE=(2.*XN-1.)*THTAZP+(XN-1.)*(PSIP+PSIM-PI)
  IP ((THTAZE-THIAZM) .LE. 0.0) GO TO 300
371  BETAMX=ATAN2(SIN(THTAZE),CCS(THTAZE)-Q)
      BETAMX=AMIN1(BETAMX,PI,PIHALF+RHO)
C
C CALCULATION OF FETA-PEAK AND PSI-PEAK
      IP (Q .GT. .5) GO TO 305
380      IF (NEC .GT. 1) GO TO 305
304      BETAPK=0.0
          PSIPK=0.0
          GO TO 306
C
C      ELSE DO
305      QSBETA=SQRT(((2.*XN*Q)**2-1.)/((2.*XN)**2-1.))
          BETAPK=ARSIN(QSBETA/Q)
          PSIPK = 2.*XN*ARSIN(QSBETA) - BETAPK - (XN-1.) *PI
C
C      ENDIF
C
C CONSIDERATION OF THE RELATIONSHIP BETWEEN PSIM,PSIP,PSIPK
306      IF (PSIM .GE. PSIPK) GO TO 300
303      CALL ELIMIT(BI,EU,NBETA)
C
C TEST INTERVALS OF INTEGRATION FOR RIM EFFECTS
      SUM1=0.
      DC 360 MEETA=1,NBETA
          BETAL=AMAX1(EL(MEETA),BETAMI)
          BETAU=AMIN1(BU(MBETA),BETAMX)
          BETAT=BETAU-BETAL
          BETASM=BETAU+BETAL
          IF (BETAT .LE. 0.0) GO TO 360
352      SB=.5*(BETAT-SIN(BETAT)*COS(BETASM))*COS(OMEGA-ALPHA)
          SUM1=SUM1+.5*ZNRML*SIN(BETAT)*SIN(BETASM)+SB*XYNRML
360      CCNTINUE
370      SIM(NZ,NEC)=SUM(NZ,NBC)+SUM1*CCNSTP
300      CCNTINUE
101 UNIT=-UNIT
      RETURN
      END

```

C\*DECK SCIN

C

FUNCTION SCLN(BETA,PSI)

C\*\*\* FUNCTION SCIN COMPUTES BL AND BU USING NEWTON'S METHOD

C

C\*\*\*WRITTEN BY: R.M.ANDERSON

C\*\*\*DATE WRITTEN: 06/01/80

C

C\*\*\*EXPLANATION OF VARIABLES

C PI = ATAN2(0.,-1.)

C BETA = FIRST GUESS FOR SOIN

C PSI = BETA - (2\*NBC\*SIN(Q\*SIN(BETA))) + (NBC-1)\*PI

C Q = VECTOR FROM CENTER OF DISH TO POINT ON THE RECEIVER

C NBC = BOUNCE NUMBER

C

C\*\*\*\*\*

COMMON /ELCKB/ PIHALF,PI,PSIP,PSIPK,PSIM,BETAPK,Q,NBC

A=BETA

E=PSI

XI=NBC

E=B+(XN-1.)\*PI

LC 10 I=1,30

QIS=Q\*SIN(A)

DELA=(B-2.\*XN\*ARSIN(QAS)+A)/(1.-2.\*Q\*XN\*COS(A)/

\* SQRT(1.-QAS\*\*2))

A=A-DELA

IF (ABS(DELA) .LE. .00001) GO TO 300

11 IF (A .LT. 0.0) GO TO 200

12 IF (A .GT. PI) GO TO 200

10 CONTINUE

WRITE(6,100)

100 FORMAT(' ITERATION DID NOT CONVERGE')

GO TO 300

200 WRITE(6,201)

201 FORMAT(' ITERATION DIVERGED')

A=0.

300 SCLN=A

RETURN

END

```

C*DECK ELIMIT
      SUBROUTINE ELIMIT(EL,BU,NBETA)
C
      REAL EL(2),BU(2)
      INTEGER NBETA
      COMMON /ELCKRB/ PIHALF,PI,PSIP,PSIPK,PSIM,BETAPK,Q,NBC
C**** CONSIDERATION OF THE RELATIONSHIP BETWEEN PSIM,PSIP,PSIPK
C      IN ORDER TO DETERMINE THE BETA-LIMITS OF INTEGRATION
C
C***WRITTEN BY: R.M. ANDERSON, ASSISTED BY CLINT DAWSON,
C              CATHY NORWOOD, AND REAE JOHNSTON
C***DATE WRITTEN: 06/01/83
C
C***EXPLANATION OF VARIABLES:
C  BL(2) = ARRAY CONTAINING LOWER BETA-LIMITS
C  BU(2) = ARRAY CONTAINING UPPER BETA-LIMITS
C  NBETA = NUMBER OF BETA-REGIONS OVER WHICH TO INTEGRATE
C          NBETA=1 OR 2
C  BETA = THE FIRST GUESS FOR EL(I) OR BU(I) TO BE
C          USED IN SUBROUTINE SCIN
C
C*****
C
C      IF (PSIM .LT. C.0) GO TO 320
C
C  PSIM >= C
310      IF (PSIP .LT. PSIPK) GO TO 315
C
C  PSIM >= C AND PSIP >= PSIPK
311      G1=SQRT ((PSIPK-PSIM) / (PSIPK+ (NBC-1)*PI))
          BETA=BETAPK*(1.-G1)
          BL(1)=SCIN(BETA,PSIM)
          BETA=BETAPK*(1.+G1)
          BU(1)=SCIN(BETA,PSIM)
          NBETA=1
          GO TO 350
C
C  PSIM >= 0 AND PSIP < PSIPK
315      G1=SQRT ((PSIPK-PSIM) / (PSIPK+ (NBC-1)*PI))
          G2=SQRT ((PSIPK-PSIP) / (PSIPK+ (NBC-1)*PI))
          BETA=BETAPK*(1.-G1)
          BL(1)=SCIN(BETA,PSIM)
          BETA=BETAPK*(1.-G2)
          BU(1)=SCIN(BETA,PSIP)
          BETA=BETAPK*(1.+G2)
          EL(2)=SCIN(BETA,PSIP)
          BETA=BETAPK*(1.+G1)
          BU(2)=SCIN(BETA,PSIM)
          NBETA=2
          GO TO 350

```

```

C
C PSIM<0
320     IF (PSIF .GT. PSIPK) GO TO 325
321     IF (PSIP .GT. C.0) GO TO 323
C
C PSIM<0 AND PSIF<=C AND SINGLE BCUNCE
322     IF (NEC .GT. 1) GO TO 391
390     G1=SQRT((PSIP-PSIPK)/(-(NBC*PI+PSIPK)))
        G2=SQRT((PSIM-PSIPK)/(-(NBC*PI+PSIPK)))
        EETA=BETAPK+(PI-BETAPK)*G1
        EL(1)=SOLN(BETA,PSIP)
        EETA=BETAPK+(PI-BETAPK)*G2
        EU(1)=SOLN(BETA,PSIM)
        NEETA=1
        GO TO 350
C
C PSIM<0 AND PSIF<=0 AND MULTIPLE BCUNCE
391     EL(1)=SOLN(0.,PSIM)
        EU(1)=SOLN(EL(1),PSIF)
        G1=SQRT((PSIP-PSIPK)/(-(NBC*PI+PSIPK)))
        EETA=BETAPK+(PI-BETAPK)*G1
        EL(2)=SOLN(BETA,PSIP)
        EU(2)=SOLN(EL(2),PSIM)
        NEETA=2
        GO TO 350
C
C PSIM<0 AND 0<=PSIP<=PSIPK
323     PI(1)=0.
        IF (NEC .LE. 1) GO TO 374
373     EL(1)=SOLN(0.,PSIM)
374     G1=SQRT((PSIPK-PSIP)/(PSIPK+(NEC-1)*PI))
        EETA=BETAPK*(1.-G1)
        EU(1)=SOLN(BETA,PSIP)
        EETA=BETAPK*(1.+G1)
        EL(2)=SOLN(BETA,PSIP)
        G2=SQRT((PSIM-PSIPK)/(-(NBC*PI+PSIPK)))
        EETA=BETAPK+(PI-BETAPK)*G2
        EU(2)=SOLN(BETA,PSIM)
        NEETA=2
        GO TO 350
C
C PSIM<0 AND PSIF>PSIPK
325     EL(1)=C.
        IF (NEC .LE. 1) GO TO 376
375     EL(1)=SOLN(0.,PSIM)
376     G1=SQRT((PSIM-PSIPK)/(-(NBC*PI+PSIPK)))
        EETA=BETAPK+(PI-BETAPK)*G1
        EU(1)=SOLN(BETA,PSIM)
        NEETA=1
350     RETURN
      END

```

```

C*DECK BOILER
      SUBROUTINE BOILER(Z,PHIR,PSIR,XR,YR,ZR)
C*** BOILER SUBROUTINE FOR A CYLINDER. BOILER COMPUTES
C   XR,YI, AND ZR WHICH ARE USED TO COMPUTE
C   THE NORMAL TO THE RECEIVER
C   IN THE MAIN PROGRAM.
C
C***WRITTEN BY: R.F. ANDERSON, CLINT LAWSON,
C               CATHY NCRWOOD, AND READ JOHNSTON
C***DATE WRITTEN: 06/01/83
C
C***EXPLANATION OF VARIABLES
C   Z = POSITION OF VECTOR C PROJECTED ONTO THE AXIS OF SYMMETRY
C       OF THE RECEIVER
C   XR,YR,ZR = COMPONENTS OF THE UNIT SURFACE NORMAL
C
C*****
      COMMON /ELCCKB/ FIFALF,PI,PSIP,PSIPK,PSIM,BETAPK,Q,NBC
      RADIUS=5.938/24./37.53
      Q=SQRT(RADIUS**2+Z**2)
      PSIR=ATAN2(RADIUS,Z)
      XI=COS(PHIR)
      YI=SIN(PHIR)
      ZI=0.
      RETURN
      END

```

THE CROSBYTON SOLAR POWER PROJECT

ROSA: A COMPUTER MODEL FOR OPTICAL POWER RATIO CALCULATIONS

PART 2: Program User's Guide

TABLE OF CONTENTS

TITLE PAGE - PART II. . . . . i

LIST OF FIGURES . . . . . iii

LIST OF TABLES. . . . . iii

1. GENERAL PROGRAM OVERVIEW . . . . . 1

2. PARAMETER DATA . . . . . 6

3. PROGRAM OUTPUT . . . . . 9

4. BOILER SUBROUTINE. . . . . 15

5. RIM SUBROUTINE . . . . . 17

LIST OF FIGURES

Figure

III-3 Optical Power Profile: Cylinder (I=0,PHIR=180) . . . . . 14

LIST OF TABLES

Table

III-1 Echo Print of Input Parameters . . . . . 11

III-2 Sample Concentration Ratio Output. . . . . 12

## 1. GENERAL PROGRAM OVERVIEW

### Introduction

The Ratio of Solid Angles (ROSA) code was developed as part of the Crosbyton Solar Power Project (CSPP) for calculation of optical power concentrations due to reflection from a spherical segment mirror. It was developed primarily in support of Department of Energy Contracts DE-AC04-76ET20255 and DE-AC04-83AL21557. Detailed derivations and a technical description of the ROSA code are given in Part I of this report. The present volume is intended to provide a program users guide for the ROSA code.

The Ratio of Solid Angles formulation yields an analytical formula for the solar concentration ratio at a field point,  $Q$ , on a receiver surface. The optical power concentration,  $C$ , at a point  $Q$  on a receiver is defined as the total normally directed optical power per unit area received at that point. In the ROSA code,  $C$  is normalized by dividing by the direct normal insolation incident upon the receiver. The resulting dimensionless quantity becomes a concentration ratio expressed as "number of suns".

The ROSA method deals directly with a finite sun. The sun's size is expressed in terms of an angular radius,  $\sigma$ . Direct sunlight received at a point is viewed as a collection of rays lying inside a right circular cone with vertex at the receiver point  $Q$  and vertex angle  $2\sigma$ .

The ROSA formula for the concentration ratio,  $C$ , at a receiver point,  $Q$ , due to reflection from a mirror surface is given by

$$C(\vec{q}, \vec{b}) = \sum \frac{R^n}{\Omega_{sn}} \int \int_{\Omega_{Mn}} \vec{b} \cdot d\vec{\Omega}, \text{ for } \vec{b} \cdot d\vec{\Omega} > 0, \quad (1)$$

where,

$\vec{q}$  = the vector locating a field point Q on the receiver with respect to a convenient coordinate system;

$\vec{b}$  = the unit outward normal to the receiver at Q;

$n$  = the number of times a ray has been reflected on the mirror before striking the receiver at Q;

$\Omega_{sn}$  =  $4\pi \sin^2(\sigma_n/2)$ , the effective solid angle of the sun as viewed directly from the field point Q;

$\sigma_n$  = the effective angular radius of the sun to be used for light which reflects  $n$  times on the mirror (for a perfect mirror  $\sigma_n = \sigma$ );

$\Omega_{Mn}$  = the apparent solid angle of the sun as viewed in the mirror from the field point Q from light which has reflected exactly  $n$  times;

$R$  = the reflection coefficient of the mirror surface;  $0 \leq R \leq 1$ ;

and,

$d\vec{\Omega}$  = differential solid angle directed toward the apparent position of the sun as viewed in the mirror; i.e., the oriented element of surface area on the unit sphere, with unit outward normal.

The ROSA code evaluates this integral.

## OVERVIEW OF INPUT PARAMETER REQUIREMENTS

The optical power concentration ratio at a point on a receiver surface is dependent upon several geometrical and physical factors. These include the position of the sun, the size and orientation of the collector, the shape and alignment of the receiver and the reflection coefficient of the collector. Thus, several geometrical and physical input parameters are required for the ROSA code. They include:

### 1. Geometrical parameters of the collector (bowl).

A spherical segment is used as the standard collector in the computer model. Normalized units are employed in the model, so that the spherical segment is taken to have unit radius. The height of the spherical segment is determined by specifying the rim angle,  $\theta_R$ , of the bowl.

Bowl orientation parameters are also required. These parameters are given in terms of a SOUTH-EAST-VERTICAL (S-E-V) coordinate system. The tilt angle,  $\gamma$ , of the bowl is measured between the symmetry axis of the bowl and the VERTICAL axis. The azimuth,  $\phi$ , of the lowest point on the rim is also measured in the S-E-V coordinate system.

### 2. Sun positional parameters.

The solar elevation, ED, and the solar azimuth, AD, are specified in the S-E-V coordinate system.

### 3. Receiver orientation.

Ideally, the axis of symmetry of the receiver should point directly towards the center of the sun. Misalignment is accounted for in terms of the zenith angle,  $\Delta\psi$ , and the azimuthal angle,  $\Delta\phi$ , between the receiver axis and the vector from the center of the bowl to the sun.

#### 4. Receiver coordinates.

Actual concentration values are computed for points on the receiver surface. The receiver surface is assumed to be a surface of revolution. Points on the surface are described in terms of two input variables, a z-coordinate measured along the axis of symmetry of the receiver and an azimuthal angle  $\phi_R$ , measured about the axis of symmetry of the receiver. A user supplied subroutine, BOILER, is called to compute the radial distance from the axis of symmetry to the surface of the receiver. (A discussion of this subroutine is deferred until later). Normally, the concentration ratio is computed for several values of z and  $\phi_R$  in a given computer run

#### 5. Number of reflections.

This is the maximum number, N, of multiple reflection contributions to be included in the calculations.

#### 6. Effective sun size .

For a perfect mirror, this parameter is simply the angular radius,  $\sigma$ , of the sun cone. For imperfect mirrors, a set of effective angular radii,  $\sigma_n$ ,  $n=1, 2, \dots, N$ , can be specified to account for stochastic errors in the mirror surface.

#### 7. Reflection coefficient .

The reflection coefficient, R, of the mirror surface is also an input variable for the program.

### BOILER SUBROUTINE REQUIREMENTS

A user supplied subroutine, BOILER, is required to describe the receiver surface as a function of distance along the axis of symmetry of the receiver. The receiver is assumed to be a surface of revolution. The subroutine receives a value of the distance,  $z$ , and returns the radial distance,  $Q$ , to surface of the receiver and the components of the unit outward normal to the surface at  $z$  in the receiver coordinate system. A discussion of this subroutine, including examples for a receiver in the form of the frustrum of a right circular cone and a right circular cylindrical receiver are discussed in the section entitled SUBROUTINE BOILER.

### RIM SUBROUTINE REQUIREMENTS

A spherical segment is taken as the standard bowl shape in the model and is described by specifying the bowl rim angle,  $\theta_R$ . A user supplied routine, RIM, is used to describe more general rim shapes. The section SUBROUTINE RIM discusses an example in which the standard bowl is cut by two parallel, vertical planes. The planes are parallel to the VERTICAL-SOUTH coordinate plane and are symmetrically located on each side of this plane.

## 2. PARAMETER DATA

The parameter data cards describe the solar collector (bowl) constants, receiver alignment constants and sun parameters. The output of the program gives the solar concentration ratio at points on the surface of the receiver. These points are described in terms of an azimuthal angle,  $\phi_R$ , about the axis of the receiver and a distance,  $Z_R$ , measured along the axis of the receiver. Loops have been provided in the program for calculations at several  $(Z_R, \phi_R)$  pairs. The loop parameters are also described in the following data input summary. These cards are read only once during a concentration calculation run.

### A. Title card (40A2)

ITITLE - Describes receiver type.

### B. Boiler-sun alignment parameters (2F10.5)

DPSID -  $\Delta\psi$ , angle between the receiver axis and the line through the center of the bowl and the center of the solar disk (degrees).

DPHID -  $\Delta\phi$ , azimuthal angle measured about the bowl center, solar disk center line (degrees).

### C. Sun parameters (3F10.5)

SIGMAD - Effective sun size (degrees).

ED - Elevation angle of the sun (degrees).

AD - Azimuthal angle of the sun (degrees).

#### D. Bowl parameters (3F10.5)

THARD - Rim angle of the bowl (degrees)

GAMMAD - Tilt angle of the bowl. The angle between the symmetry axis of the bowl and vertical (degrees).

PHIDD - Angle between the lowest point on the bowl and south (degrees).

#### E. Reflection coefficient (F10.5)

REFC - Reflection coefficient of the mirror.

#### F. Omega integration parameter (I5)

ISTEPS - Number of intervals to be used in the Simpson's rule integration of the concentration ratio integral.

#### G. Loop parameters for outer calculation loop (3F10.5)

STPHIR - Azimuth of starting point for PHIR angular sweep around the receiver surface (degrees).

SPPHIR - Azimuth of stopping point for PHIR angular sweep around the receiver surface (degrees).

DPHIRD - step size for PHIR sweep (degrees).

H. Parameter for subdivision of receiver axial parameter (I5)

NZRR - Number of subdivisions of the receiver axis to be used in the concentration calculations. The concentration profile varies rapidly with  $Z_R$  over some regions and slower over other regions and this parameter permits the user to vary the distance between calculated points accordingly.

I. Loop parameters for the inner calculation loop (I5,2F5.3)  
(This data card must occur NZRR times.)

NZZ - Number of  $Z_R$  values in the Z loop.

ZSTART - Starting value of  $Z_R$ .

ZSTOP - Final value of  $Z_R$ .

### 3. PROGRAM OUTPUT

This chapter provides a brief description of the ROSA program output. A portion of the output is also shown, together with a concentration profile graph.

#### Physical and Geometrical Parameters

The ROSA program always echo prints the following input data:

- A. Boiler title card;
- B. Boiler - Sun alignment parameters;
- C. Sun Parameters;
- D. Solar bowl parameters;
- E. Reflection coefficient;

Sample output is shown in table 3.1.

#### Optical Concentration Output

Concentration ratio values are obtained at points along the receiver surface. Points on the surface are located by prescribing pairs of values  $(Z_R, \phi_R)$ , where  $Z_R$  is measured along the axis of symmetry of the receiver and  $\phi_R$  is an azimuthal angle measured about the receiver axis. The  $\phi_R$  variable is the slower varying variable in the calculations. The loop structure for the output is as follows:

```
BEGIN PHIR loop
  Print PHIR (degrees)
  Begin ZR loop
    Print ZR
    FOR J = 1 to 5
      PRINT contribution from Jth bounce
    NEXT J
```

Print the total concentration (sum of 5 bounces)

END ZR loop

END PHIR loop

(Note: we are only considering contributions from light that has reflected five times or less before striking the receiver.)  
Sample output corresponding to the input in Table 3.1 is shown in Table 3.2.

It should be noted that normalized units are used in the ROSA code. The radius of the bowl is taken to be unity, so that necessarily  $0 \leq ZR \leq 1$ . The output values are also normalized. The input solar intensity,  $I$ , at the aperture plane is an overall scale factor and all concentration results are given in "number of suns", i.e.  $I = 1$ .

Table 3.1 Echo Print of Input parameters

BOILER SHAPE: CYLINDER

BOILER-SUN ALIGNMENT PARAMETERS:

DELTA PSI (DPSID) = 0.0  
 DELTA PHI (DPHID) = 0.0

SUN PARAMETERS:

SUN CONE HALF ANGLE (SIGMAD) = 0.50000  
 SUN POSITION:  
 ELEVATION (ED) = 30.00000  
 AZIMUTH (AD) = 0.0

DISH PARAMETERS:

DISH HALF-ANGLE (THTARD) = 60.00000  
 DISH ALIGNMENT:  
 GAMMAD = 15.00000  
 PHID = 0.0

REFLECTION CONSTANT = 0.88000  
 ISTEPS = 50

START PHIR (STPHIR) = 0.  
 STOP PHIR (SPPHIR) = 0.  
 DELTA PHIR (DPHIRD) = 0.

NUMBER OF Z-INTERVALS (NZRR) = 1

NUMBER OF INCREMENTS (NZZ) = 100  
 ZSTART = 0.500  
 ZSTOP = 0.995

Table 3.2 Sample Concentration ratio output

PHIR = 0.0

Z= 0.5000

BOUNCE NUMBER=1	CONCENTRATION=	0.0
BOUNCE NUMBER=2	CONCENTRATION=	0.0
BOUNCE NUMBER=3	CONCENTRATION=	0.0
BOUNCE NUMBER=4	CONCENTRATION=	0.0
BOUNCE NUMBER=5	CONCENTRATION=	0.0
TOTAL CONCENTRATION=		0.0

Z= 0.5050

BOUNCE NUMBER=1	CONCENTRATION=	0.0
BOUNCE NUMBER=2	CONCENTRATION=	0.0
BOUNCE NUMBER=3	CONCENTRATION=	0.0
BOUNCE NUMBER=4	CONCENTRATION=	0.0
BOUNCE NUMBER=5	CONCENTRATION=	0.0
TOTAL CONCENTRATION=		0.0

Z= 0.5100

BOUNCE NUMBER=1	CONCENTRATION=	0.0
BOUNCE NUMBER=2	CONCENTRATION=	0.0
BOUNCE NUMBER=3	CONCENTRATION=	0.0
BOUNCE NUMBER=4	CONCENTRATION=	0.0
BOUNCE NUMBER=5	CONCENTRATION=	0.0
TOTAL CONCENTRATION=		0.0

Z= 0.5150

BOUNCE NUMBER=1	CONCENTRATION=	66.4747
BOUNCE NUMBER=2	CONCENTRATION=	0.0
BOUNCE NUMBER=3	CONCENTRATION=	0.0
BOUNCE NUMBER=4	CONCENTRATION=	0.0
BOUNCE NUMBER=5	CONCENTRATION=	0.0
TOTAL CONCENTRATION=		66.4747

Z= 0.5200

BOUNCE NUMBER=1	CONCENTRATION=	185.9003
BOUNCE NUMBER=2	CONCENTRATION=	0.0
BOUNCE NUMBER=3	CONCENTRATION=	0.0
BOUNCE NUMBER=4	CONCENTRATION=	0.0
BOUNCE NUMBER=5	CONCENTRATION=	0.0
TOTAL CONCENTRATION=		185.9003

Z= 0.5250

BOUNCE NUMBER=1	CONCENTRATION=	296.1956
BOUNCE NUMBER=2	CONCENTRATION=	0.0
BOUNCE NUMBER=3	CONCENTRATION=	0.0
BOUNCE NUMBER=4	CONCENTRATION=	0.0
BOUNCE NUMBER=5	CONCENTRATION=	0.0
TOTAL CONCENTRATION=		296.1956

Z= 0.5300

BOUNCE NUMBER=1	CONCENTRATION=	381.1919
BOUNCE NUMBER=2	CONCENTRATION=	0.0
BOUNCE NUMBER=3	CONCENTRATION=	0.0
BOUNCE NUMBER=4	CONCENTRATION=	0.0
BOUNCE NUMBER=5	CONCENTRATION=	0.0
TOTAL CONCENTRATION=		381.1919

Z= 0.5350

BOUNCE NUMBER=1	CONCENTRATION=	399.5920
BOUNCE NUMBER=2	CONCENTRATION=	0.0
BOUNCE NUMBER=3	CONCENTRATION=	0.0
BOUNCE NUMBER=4	CONCENTRATION=	0.0
BOUNCE NUMBER=5	CONCENTRATION=	0.0
TOTAL CONCENTRATION=		399.5920

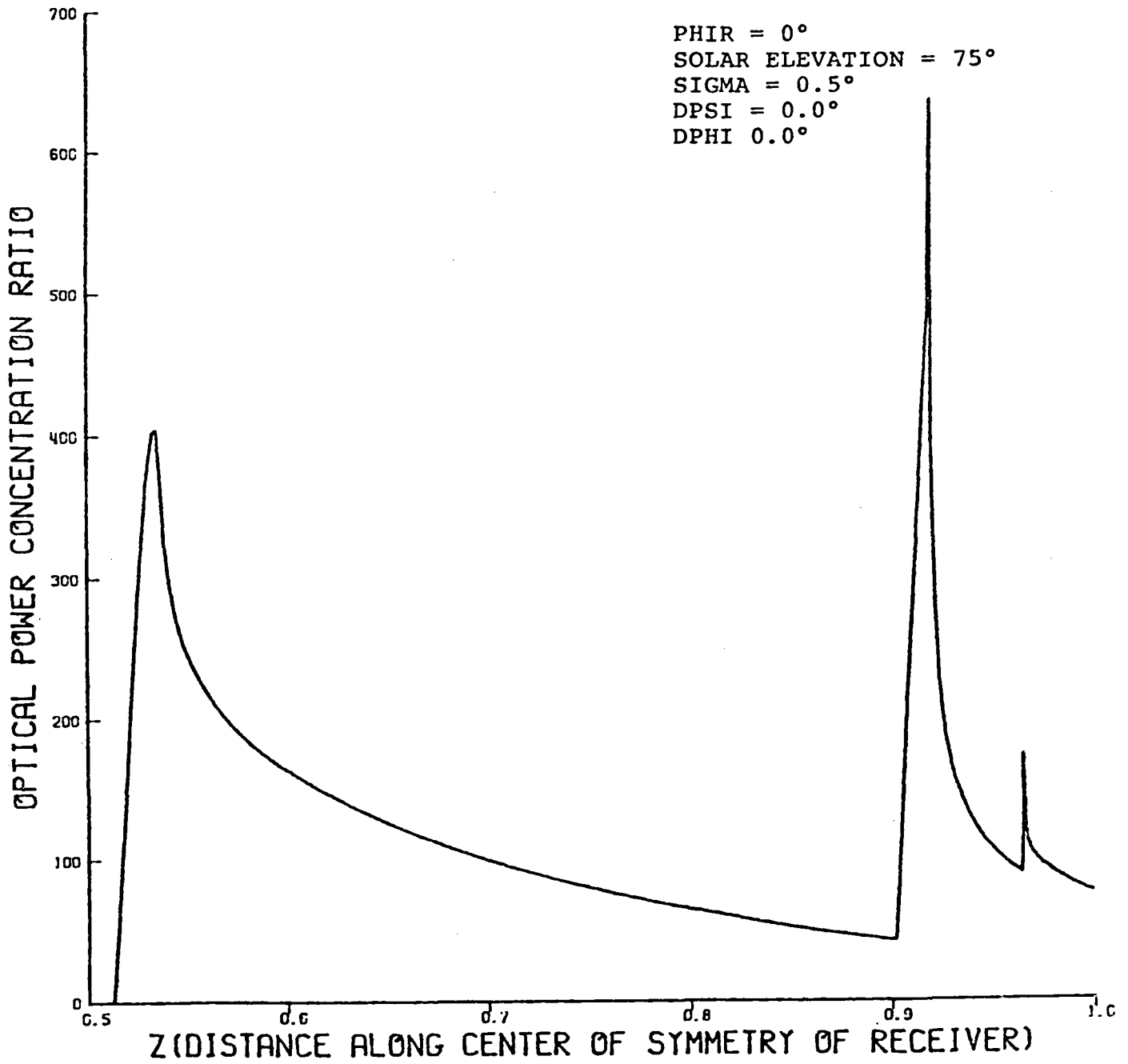


Figure III - 1 Optical Power Concentration for A Cylindrical Receiver

#### 4. BOILER SUBROUTINE

##### Introduction

The ROSA code is sufficiently general to permit any convex surface of revolution for the receiver/boiler surface. However, this requires that a BOILER subroutine be provided by the user. The formulas necessary for this routine are derived in Chapter 3, Part 1 of this report. In this chapter, we provide the ingredients for building the subroutine and give examples for a cylinder and a cone.

##### Subroutine Outline

The routine assumes that the receiver surface is described in the form

$$r = f(Z), \quad (\text{IV-1})$$

where  $Z$  is measured along the axis of the receiver (with  $Z \leq 0$ ) and  $r$  is the perpendicular distance from the axis of the receiver. Input for the routine includes the value of  $Z$  and an azimuthal angle,  $\text{PHIR}$ , measured about the axis of the receiver. These two values determine a field point on the receiver surface. The subroutine returns the distance,  $Q$ , from the origin of the receiver coordinate system to the field point, the zenith angle of the point, and the components of the unit outward normal to the surface. The routine then becomes:

```
SUBROUTINE BOILER (Z,PHIR,Q,PSIR,XR,YR,ZR)
REAL Z,PHIRD,Q,PSIR,XR,YR,ZR
F= formula for surface of revolution : r=f(Z)
FP= formula for F'(Z)
ZETA = ATAN(FP)
Q=SQRT(F**2+Z**2)
```

```

PSIR=ATAN(F/Z)
XR=COS(PHIR)*COS(ZETA)
YR=SIN(PHIR)*COS(ZETA)
ZR=-SIN(ZETA)
RETURN
END

```

For a right circular cylinder,  $f(Z) = r_0$ , a constant and  $f'(Z) = 0$ . Thus,  $ZETA = 0$ , and the above formulas can be simplified.

For the frustrum of a cone,  $f(Z) = (-\tan \Psi_R)Z$ ,  $f'(Z) = -\tan \Psi_R$ , where  $\Psi_R$  is the angular radius of the cone. Thus,  $ZETA = -\Psi_R$  for a cone.

## 5. RIM SUBROUTINE

This section presents a listing of an implementation of a RIM subroutine corresponding to the rim shape described in Chapter 7, Part 1 of this report.

=====

SUBROUTINE FIM

=====

C\*DECK RIF

SUBROUTINE RIM (OMEGA,THTAZ,IFLAG)

C\*\*\* RIM CALCULATES THTAZ FOR A DISH THAT HAS BEEN  
C PARTIALLY CUT-OFF BY TWO PLANES RUNNING PARALLEL  
C TO THE D-A PLANE (SEE D-M-A COORDINATE SYSTEM)

C\*\*\*WRITTEN BY: CLINT DAWSON AND CATHY NORWOOD

C\*\*\*DATE WRITTEN: 02/01/84

C\*\*\*EXPLANATION OF VARIABLES:

C OMEGA, THTAZ: SEE MAIN PROGRAM

C RL1-R13, RM1-RM3, RN1-RN3: ENTRIES OF THE ROTATION MATRIX  
C BETWEEN THE D-M-A AND X-Y-Z COORDINATE SYSTEMS  
C RIMC4-RIMC6, FIMC10-RIMC15: USED IN CALCULATIONS  
C OF RL1, RL2, ETC.

C CAPA: THE A-COORDINATES OF THE POINTS WHERE  
C THE PLANE CUTS THE SPHERE

C CAPD: THE D-COORDINATE OF THE LOWEST POINT  
C WHERE THE PLANE CUTS THE SPHERE

C AMIN: THE MINIMUM OF CAPA(1) AND CAPA(2)

C THTAFF: THE ARCCOS OF THE ABSOLUTE VALUE OF AMIN

C RMO: THE EQUATION OF THE PARALLEL PLANES  
C WHICH CUT THE DISH

COMMON /FICCKA/ OMEGA, ISTEPS, CMEGAL(2), OMEGAU(2), XYNRML,  
\* ALPHA, NZ, ZNRML, PSIOS, PSIOC, SIGMAC,  
\* RIMC4, RIMC5, RIMC6, THTARC, THTAW  
COMMON /CUT/ THTAR, GAMMAC, ES, A, PHID, GAMMAS, EC, PHIOC, PHIOS  
REAL OMEGA, THTAZ  
REAL RIMC10, RIMC11, RIMC12, RIMC13, RIMC14, RIMC15  
REAL A0, A1, A2, A3, AMIN, CAPA(2), RAD1, RMO, THTAPR, THTAPC, THTAPS  
REAL CAE1, EBH1, RPH1S, RPH1C, OMEGAT

IFLAG=0

RIMC10=GAMMAC\*ES\*CCS(A-PHID) + GAMMAS\*EC

RIMC11=-GAMMAC\*SIN(A-PHID)

RIMC12=GAMMAC\*EC\*CCS(A-PHID) - GAMMAS\*ES

FIMC13=ES\*SIN(A-PHID)

RIMC14=CCS(A-PHID)

RIMC15=EC\*SIN(A-PHID)

R11=PSICC\*(PHIOC\*RIMC10 + PHIOS\*RIMC11) + PSIOS\*RIMC12

R11=PHICS\*RIMC10 - PHIOC\*RIMC11

RN1=PSICS\*(PHIOC\*RIMC10 + PHIOS\*RIMC11) - PSIOC\*RIMC12

R12=PSICC\*(PHIOC\*RIMC13 + PHIOS\*RIMC14) + PSIOS\*RIMC15

R12=PHIOS\*RIMC13 - PHIOC\*RIMC14

RN2=PSICS\*(PHIOC\*RIMC13 + PHIOS\*RIMC14) - PSIOC\*RIMC15

R13=RIMC4

R13=RIMC5

R13=RIMC6

```

C
  AC=-COS (THTAR)
  RPO=.5
  CMEGAT=TAN (CMEGA)
  A1=RM1-RI1*CMEGAT
  A3=RM3-RI3*CMEGAT
  IF (A1**2+A3**2 .EQ. 0.0) GO TO 784
C ELSE CONTINUE
C
  A2=RM2-RI2*CMEGAT
  RAD1=(A1**2+A3**2)*A1**2*(1-FMC**2)
  -A1**2*A2**2*FMC**2
  IF (RAD1 .LT. 0.0) GO TO 784
C ELSE CONTINUE
C
  CAPA(1)=(-A2*A3*FMC + SQRT (RAD1))/(A1**2+A3**2)
  CAPA(2)=(-A2*A3*FMC - SQRT (RAD1))/(A1**2+A3**2)
  AMIN=AMIN1 (CAPA(1),CAPA(2))
  IF (AMAX1 (CAPA(1),CAPA(2)) .GE. A0) GO TO 785
  WRITE (6,786)
786  FCRMAT (' SEE BACK EURNER! ')
785  IF (AMIN .GE. A0) GO TO 784
C
C ELSE COMPUTE NEW THTAZ
C
  THTAPR=ARCCS (AES (AMIN))
  CIPD=- (AMIN*A3+RMO*A2)/A1
  FFHI=ATAN2 (FMO,CAP1)
  THTAPC =COS (THTAPR)
  THTAPS =SIN (THTAPR)
  FFHIC=CCS (FFHI)
  FFHIS=SIN (FFHI)
  TETAZ=RN1*FFHIC*THTAPS + RN2*FFHIS*THTAPS - RN3*THTAPC
  IF (THTAZ .GT. 1.) GO TO 794
  THTAZ=ARCCS (THTAZ)
  GO TO 784
794  IILAG=1
784  RETURN
  END

```



**United States Department of Energy**  
Office of Scientific and Technical Information  
Post Office Box 62  
Oak Ridge, Tennessee 37831

OFFICIAL BUSINESS  
PENALTY FOR PRIVATE USE, \$300

POSTAGE AND FEES PAID  
DEPARTMENT OF ENERGY  
DOE-360



10723 FR- 1  
US DEPARTMENT OF ENERGY  
ATTN S D ELLIOTT, DIR  
SOLAR ONE PROJECT OFFICE  
PO BOX 366  
SAGGETT, CA 92327